Masterthesis

Wastewater recovery at Suomen Kerta Factory

PROMOTOR :

Prof. ir. Aniceta DEXTERS

PROMOTOR :

dr. ing. Katariina PENTTILA

Siemen Steegmans

Scriptie ingediend tot het behalen van de graad van master in de industriële wetenschappen: energie, afstudeerrichting elektrotechniek

▶▶ UHASSELT   KU LEUVEN

▶▶ UHASSELT   KU LEUVEN

2018•2019
Faculteit Industriële ingenieurswetenschappen
master in de industriële wetenschappen: energie

Masterthesis
Wastewater recovery at Suomen Kerta Factory

PROMOTOR :

Prof. ir. Aniceta DEXTERS

PROMOTOR :

dr. ing. Katariina PENTTILA

Siemen Steegmans
Scriptie ingediend tot het behalen van de graad van master in de industriële wetenschappen: energie, afstudeerrichting elektrotechniek

►► UHASSELT   KU LEUVEN

Preface

This project took place from the 4th February 2019 till the 24th May 2019. I did this project at the Häme University of Applied Sciences (HAMK) in Valkeakoski, Finland. With this project, I finish my master's degree in Electromechanical Engineering - Energy: Electrotechnics Engineering at University of Hasselt in association with University of Leuven. My master's thesis contains a closed hydraulic circuit design to recover the waste water from the candle factory Suomen Kert, in Riihimäki, and a study of different ways to store this (hot) waste water seasonally.

First, I would like to thank my supervisor from the University of HAMK, dr. ing. Katariina Penttilä, and Prof. ir. Annick Dexters as my supervisor from UHasselt / KU Leuven. They both gave me good tips, interesting remarks, guided me in the right direction and gave me the motivation to successfully finish this Master's thesis. Secondly, I would like to thank Prof. dr. ir. Wim Deferme from UHasselt for his technical advice during the design of the hydraulic circuit. I would also like to thank Antti Aimo, head of the degree programme, for allowing me to do my Master's thesis at his department. The program involves electrical, automation and energy engineering, which are also my personal main interests.

During this project, I had the opportunity to broaden my knowledge in seasonal thermal energy storage and gaining more experience in designing a closed hydraulic circuit to recover waste water. I spent time in gathering information before I effectively could start designing. Since it was hard to find a solid case to discuss and I had less than four months to complete this project, I am satisfied with the results. Communication was very important during this project since this project took place at the university of HAMK in collaboration with Suomen Kerta Oy, a candle company.

As an exchange student, I also had the opportunity the widen my cultural experience with different cultures in Finland. I was also able to travel around the country and discover the beautiful and peaceful nature of Finland and the neighbouring countries. During this trip, I had the chance to improve my English language skills and learning to live on my own. I met great and inspiring people during this exchange program and I am very grateful I choose for this once-in-a-lifetime experience.

Finally, I would like to thank my parents for the endless support I receive from them. It is great to know that they are always there for me and help me where they can. The pride they show is incentive for me to go to extremes in everything I do. Without them, I would never be where I am today.

May 2019
Siemen Steegmans

Table of Contents

List of Tables

List of Figures

List of used abbreviations

ATES	Aquifer thermal energy system
BHE	Boreholes
BTES	Borehole thermal energy system
DN	Diameter nominal
HDC	High-density concrete
NPS	Nominal pipe size
NPSH	Net positive suction head
NPSHA	Net positive suction head available
NPSHR	Net positive suction head required
PB	Poly-butylene
PTES	Pit thermal energy storage
STD	Standard wall thickness
STES	Seasonal thermal energy storage
TCM	Thermochemical material
TES	Thermal energy storage
TTES	Tank thermal energy storage
UTES	Underground thermal energy storage
VFD	Variable frequency drive

Abstract

The candle factory of Suomen Kerta, located in Riihimäki, Finland, produces an enormous amount of wastewater due to the cooling of candles. The two machines handled in this master's thesis have respectively an annual water waste of 6 000 m³ and 11 000 m³. Currently, the company simply discharges its wastewater into a nearby river. The aim of this master's thesis is to reduce water consumption during the production of the candles in Suomen Kerta and to do this as energy efficiently as possible.

In the first scenario, we investigated whether STES (Seasonal Thermal Energy Storage) systems are able to reduce the wastewater from the production process by storing the hot water seasonally. A technical comparison of different STES systems is made. Also it is researched whether it is possible to use the heat from the wastewater to produce electricity and then store this in batteries (ORC systems). This is investigated on the basis of the amount of energy that can be extracted from the temperature of the wastewater.

In the second scenario, a closed hydraulic pump circuit will be designed to use the wastewater from machine A (30 °C) as cooling water in machine B (12 °C), ensuring that the pumps operate as energy efficiently as possible.

Based on the results of this master's thesis, STES will not offer a realistic solution but Suomen Kerta can invest in the construction of a closed hydraulic circuit for the reuse of their wastewater from machine A in several other machines. This results in water savings, money savings and a more environmentally friendly process.

Abstract in Dutch

In de kaarsenfabriek van Suomen Kerta, gelegen in Riihimäki, Finland, kampen ze met het probleem dat ze een enorme hoeveelheid afvalwater hebben dat ontstaat bij het koelen van kaarsen. Om een idee te krijgen van de hoeveelheden heeft een eerste machine een jaarlijks waterverspilling van 6 000 m³ en een tweede machine een jaarlijks waterverspilling van 11 000 m³. Momenteel loost het bedrijf al dit afvalwater in de rivier en kan het als pure verspilling worden beschouwd. Het doel van deze masterproef is om het waterverbruik bij de productie van de kaarsen in Suomen Kerta te verminderen en om dit zo energie-efficiënt mogelijk te doen.

In het eerste scenario wordt er onderzocht of STES (Seasonal Thermal Energy Storage) systemen in staat zijn om het afvalwater van het productieproces te verbeteren door het warme afvalwater seizoenaal op te slaan. Een technische vergelijking van verschillende STES-systemen zal worden gemaakt. Er zal ook onderzocht worden of het mogelijk is om met de warmte van het afvalwater elektriciteit te maken en deze vervolgens op te slaan in batterijen (ORC systemen). Dit zal worden onderzocht op basis van de hoeveelheid energie uit de temperatuur van het afvalwater kan worden onttrokken.

In het tweede scenario zal er een gesloten hydraulisch pompcircuit worden ontworpen om het afvalwater van machine A (30 °C) als koelwater (12 °C) in machine B te gebruiken, met in het achterhoofd dat de pompen zo energiezuinig mogelijk werken.

Op basis van de resultaten van deze masterproef kan er geconcludeerd worden dat STES systemen geen realistische oplossingen bieden. Suomen Kerta kan wel investeren in de bouw van een gesloten hydraulisch circuit voor het hergebruik van hun afvalwater van machine A in meerdere machines. Dit resulteert in waterbesparingen, geldbesparingen en een milieuvriendelijker proces.

1 Introduction

1.1 Context

Häme University of Applied Sciences

This master project takes place at Häme University of Applied Sciences (HAMK) in campus Valkeakoski, Finland, in collaboration with Suomen Kerta Oy. HAMK is a multidisciplinary higher education institution situated centrally in the most populated area of southern Finland. The Finnish higher education system comprises universities and universities of applied sciences that are authorised by the government. HAMK is situated centrally in the most populated area of the country, southern Finland, where about half of all Finns live.

Figure 1: Häme University of Applied Sciences (HAMK) logo [1]

Suomen Kerta Oy

Suomen Kerta is a Finnish family-owned company offering a wide range of consumer products for the kitchen, the table, and the home. The company manufactures sells and markets the use of consumer and specialty packaging, paper products, tissue paper and candle products. The client portfolio is wide from households to hospitality sector, as well as to different sectors in the B2B segment. In addition to its own brands, the company manufactures retailer's private label products. Suomen Kerta has three factories in Finland. The factory in Imatra manufactures products such as paper plates and cups and fast-food and storage containers. The factory in Kotka manufactures multi-coloured printed table top products under Havi, Finlayson and Nanso brand names, in addition to customer's own designs. The third factory is located in Riihimäki, where all the candle products are produced. It is in this factory where the practical case of this Master's thesis will be carried out.

Figure 2: Logo Suomen Kerta [2]

Company strategy Suomen Kerta

Suomen Kerta has a long tradition in creating success stories out of competitive products. Their long-span way of operating and expertise in local markets pave the way for excellent results. Together with Finnish and international partners, they have created strong market position. It is their aim to design the perfect atmosphere for every eating and drinking occasion.

The company's strategy is to continuously develop the product quality and offering to meet the demands of both household and professional sectors. The objective in purchasing is to strive for environmental friendly raw materials and in addition packaging materials that are biodegradable or recyclable. Suomen Kerta Ltd aims to be a flexible partner to whom service and quality are the most important values in their daily operations [2].

Figure 3: Suomen Kerta, candle machine in the factory located in Riihimäki [2]

For this master's thesis, a company visit to Suomen Kerta Oy, Finland's only remaining candle manufacturer, was planned on Wednesday 3 April 2019 to discuss the cases with the company.

Figure 4: Picture of the entrance at Suomen Kerta factory, located in Riihimaki, where the company visit took place

1.2   Cases introduction

1.2.1   Problem definition

The company has to deal with the problem that they have an enormous amount of waste water from mainly two machines that they use to produce candles. Machine A (a rotary molding machine) has an annual water waste of 6 000 m³, and machine B (cooling drums) has a water waste of 11 000 m³. This waste water is currently discharged into the river which is environmentally unfriendly and therefore a large amount of water and money is wasted. Suomen Kerta is looking for solutions to either store the hot waste water seasonally to reuse the heat in the cold winter months (case A), or to reduce the water wastage by designing a closed circuit to use the water waste from machine A (30 °C) to cool the spraying drums in machine B (12 °C) (case B). In both scenario's the company wants to save on water costs.

1.2.2   Cases description

In order to reduce the company's waste water, 2 scenarios can occur.

Case A: when the machines are not working simultaneously
While the machines are working individually and want to reduce the waste water, we can efficiently store the hot water produced in the summer, and reuse this in the cold Finnish winters. There are many TES technologies available, both commercial and emerging, and the amount of published literature on the subject is considerable. The challenging and important part of the heat recovery is not how to create or harvest it (because we have the ability to extract the heat from hot cooling water), but how to store it until needed in winter. In this case we will discuss some methods to store this heat energy seasonally when the machines are working individually and looking for possible solutions to store the waste water.
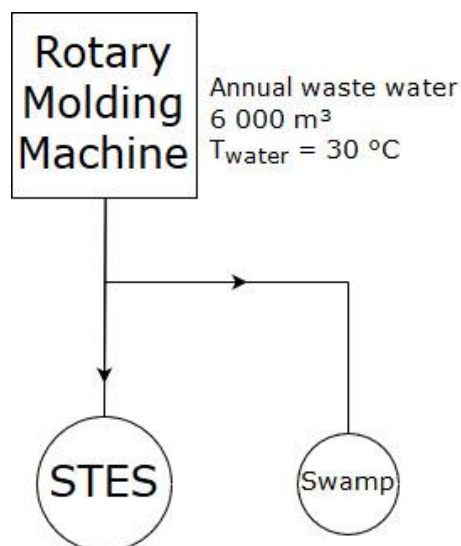
Figure 5: Principle scheme case A

Case B: when the machines are working simultaneously

The main question for this case is, is it possible to use waste water from machine A (30 °C) to cool the drums (12 °C) in machine B in a closed circuit when 1, 2 or/and 3 of the cooling drums are operating at the same time as the rotary molding machine is operating (machine A)?

If so, the amount of waste water can be reduced by using the same water twice and on a yearly base Suomen Kerta can save on water costs, money costs and have an environmental friendlier process. The centrifugal pumps must be selected in such a way that they have as little power consummation as possible and can therefore work as efficiently as possible. Depending on the installation cost, the annual energy consumption and the annual water saving, the payback time of this installation can be calculated.
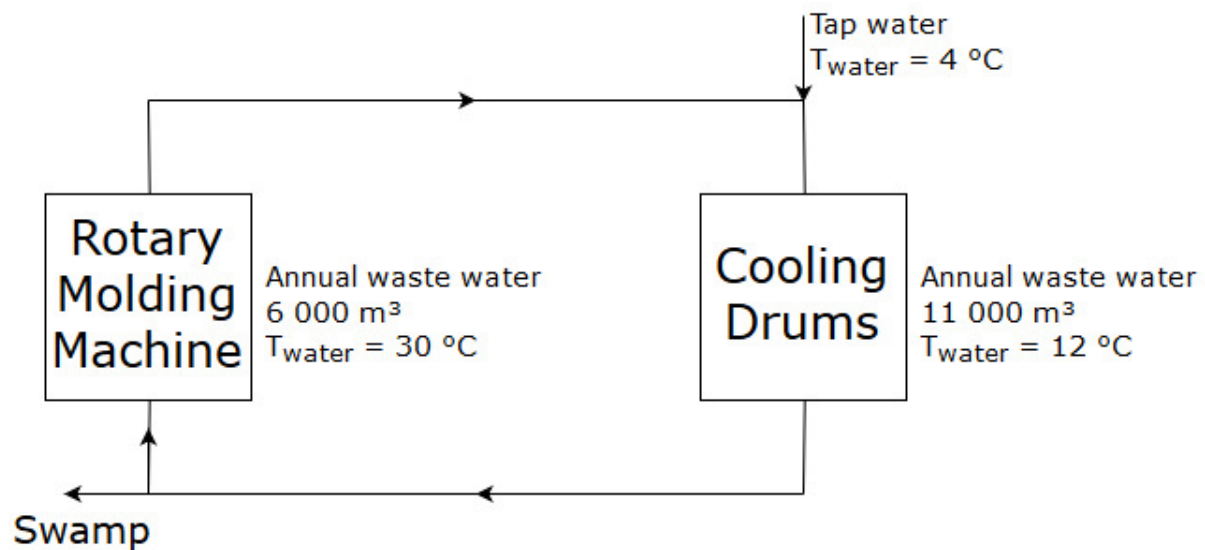
Figure 6: Principle scheme case B

1.2.3 Machines description

To better understand the cases, to do research and to be able to develop a working system, it is necessary to collect data (mainly flow rates and water flow temperatures) from the company and to clarify the operation of the individual machines on how the waste water is produced.

Machine A: rotary molding machine

The rotary molding machine RGM-1550 can fit 3 195 molds and has a capacity up to 8 500 candles per hour. It has a pre-heating and cooling system for better quality at a high capacity, even when processing stearin. Since there are several different materials available for the molds, the molds can be adapted to the corresponding candle raw material. The machine had the following options:

- fully automatic withdrawing magazine,
- candle cutting saw,
- candle base melting machine,
- colour dipping machine,
- various packing systems for putting the candles into trays, collapsible boxes or foil [3].

Figure 7 shows pictures of the rotary molding machine installed in Suomen Kerta factory.

Figure 7: Machine a: rotary molding machine used at Suomen Kerta factory

Table 1 shows the technical data collected concerning the rotary molding machine (machine A).

Table 1: Technical data rotary molding machine

Technical data machine A	
Yearly waste water	≈ 6 000 m³/year
Waste water temperature	≈ 30 °C
Waste water flow rate	10,833 l/s
Operating time per year	1060 hours
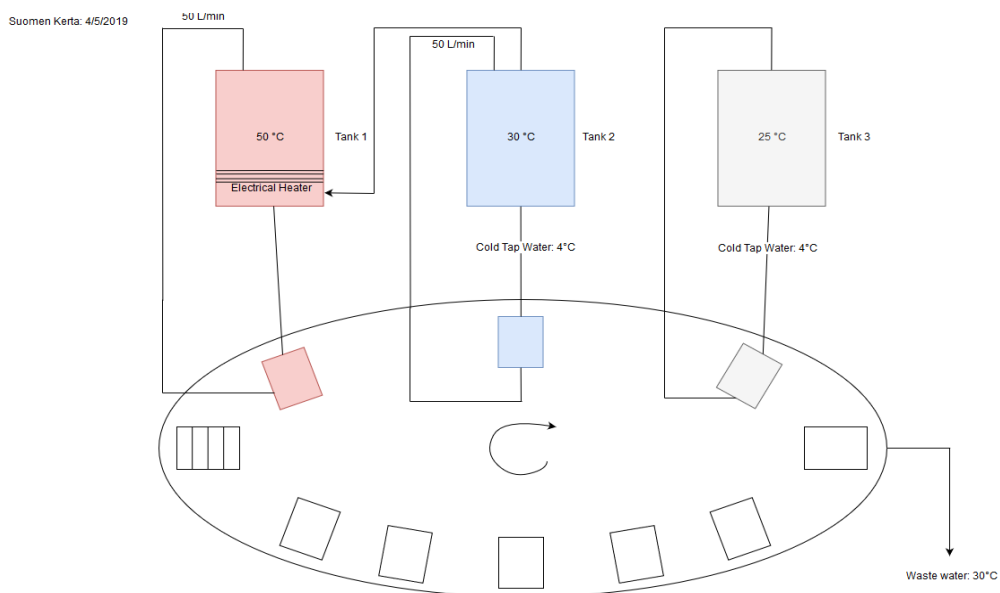
Figure 8: Sketch working principle rotary molding machine

19

Machine B: pulverization of liquid raw candle material by means of spraying drums

The water-cooled powder spray drums of the PST can produce either 400, 600, 900 or 1 200 kg paraffin powder per hour, depending on the type. The well rippling powder and its optimal quality makes it suitable for further processing in fully automated tealight presses, extruders and piston presses. This machine has the following options:

- heat exchanger for optimizing the paraffin temperature and the machine capacity,
- powder silo with conveyor unit,
- suction conveyors,
- water re-cooling units [4].

Figure 9 shows pictures of the spraying drums installed in Suomen Kerta factory.

Figure 9: Pulverization of liquid raw candle material by means of spraying drums at Suomen Kerta [4]

Table 2 shows the technical data collected concerning the spraying drums (machine B).

Technical data machine B	
Yearly waste water	≈ 11 000 m³/year
Inlet water temperature to cool the drum	12 °C
Outlet water temperature	14 °C
Water flow to cool the drum	5 l/s for each drum
Operating time per year	2000 hours
Pressure loss each drum	50 kPa

Figure 10: Raw candle material made by means of spraying drums [4]

1.3 Preparatory stage both cases
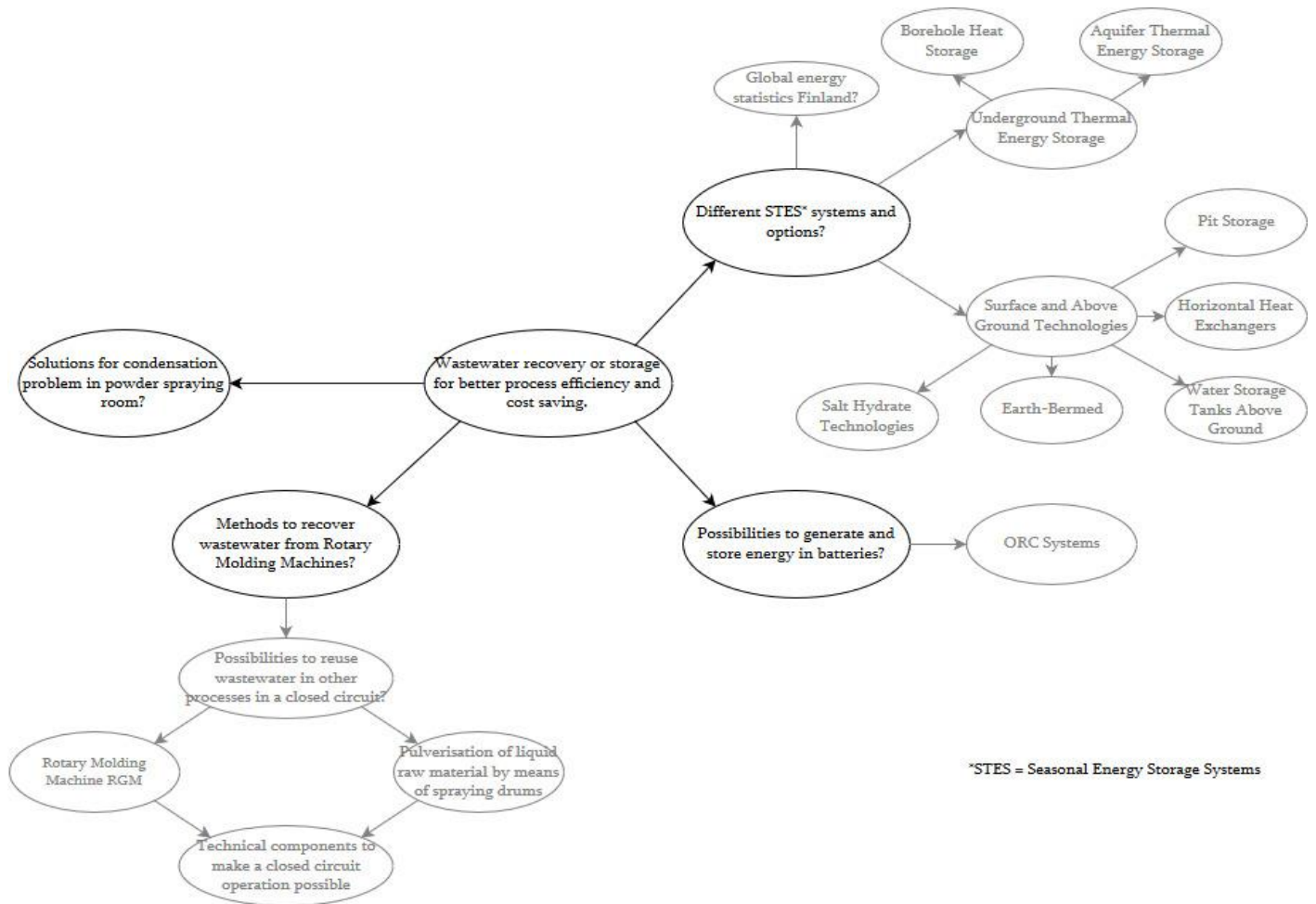
Figure 11: Preparatory scheme case study

A wide literature study in advance is necessary before going more into detail and start making a solution/design to answer the questions of Suomen Kerta. In this master's thesis we will focus on some major topics. In case A, we first give a small introduction to the global climate of Finland to get a better look when demand of heat occurs. After this, we study different systems and possibilities to store heat seasonally as initially was the focus of this thesis. We also look at the possibility to convert the heat into electricity and store it in batteries (ORC systems).

If storing for a long period of time seems not be a feasible option, we then investigate if the recovered heat can be used directly. This will be researched in case B. Here we focus on the reuse or the recovery of the wastewater in other phases of the production process, to save water and increase energy efficiency. Hereto a closed hydraulic system between different machines will be designed. All technical components to ensure flawless operation will be researched.

Case A: STES solution when the machines are not operating simultaneously

2 STES solution when the machines are not operating simultaneously: Case A

2.1 Global Finnish weather conditions

The climate of Finland is influenced most by its latitude. Finland is located between 60 and 70 N as can be seen in Figure 12. Because of Finland's northern location, winter is the longest season. Only on the south coast and the southwest summer is as long as winter. On average, winter lasts from early January to late February in the outermost islands in the archipelago and the warmest locations along the southwestern coast – notably in Hanko, and from early October to mid-May in the most elevated locations, such as north western Lapland and the lowest valleys in northeaster Lapland. This means the southern parts of the country are snow-covered about three to four months of the year, and the northern for about seven months [5]. The location of Finland in Europe can be seen in Figure 12.

Figure 12: Finland located in Europe [6]

27

The warmest annual average temperature in southwestern Finland is 6,5 °C (43,7 °F). From there the temperature decreases gradually towards north and east [6].

In table 3 we have tabulated the monthly average temperature from Tampere for the year 2007 to 2017. We notice that in the months of January, February, March, November and December the average temperature barely exceeds freezing point.

Table 3: Climate data for Tampere, South-Finland [8]

Climate data for Tampere, Finland

Observation station	Station ID	Latitude (dec.)	Longitude (dec.)	Time from…		Time to…	
Pirkkala Tampere - Pirkkala lentoasema	101118	61.41838	23.61811	2007-01-01T00:00:00.000Z		2017-12-31T23:59:59.000Z	

	Jan	Feb	Mar	Apr	May	Jun	Jul	Aug	Sep	Oct	Nov	Dec
Mean monthly T [°C]												
2007	-4	-11,8	1,9	4,3	9,9	15,1	16,2	16,3	9,9	6,1	-0,7	0,7
2008	-1,6	-1,2	-2	4,9	9,7	13,5	15,9	13,4	8,4	6,5	1	-0,6
2009	-6	-5,7	-3	3,7	10,9	13,3	16	13,8	11,4	2,1	1,4	-6,9
2010	-12,9	-10	-3,3	3,8	11,3	13,9	21,1	14	10,4	3,9	-3,5	-11,7
2011	-6,7	-12,5	-2,3	5,1	10,1	16,9	19,3	15,7	12,2	6,4	3,5	0,8
2012	-7,1	-8,9	-0,6	2,6	10,2	12,5	17,1	14,7	10,4	4,4	2,1	-8,7
2013	-6,2	-3	-7,8	2,3	12,9	16,8	16,6	15,6	10,8	5,3	2,4	0,4
2014	-9,5	-0,5	1	4,6	10,1	12,6	19,5	16,2	10,9	5,2	1,5	-2
2015	-3,4	-1,1	0,8	4,3	8,9	12,1	15,1	15,9	11,5	4,4	3,4	1,3
2016	-11,5	-1,6	-0,5	3,9	12,7	14,6	16,7	14,7	11,3	3,5	-1,6	-2
2017	-3,7	-4,5	0,2	1,5	8,4	12,7	14,9	14,5	10,1	4	1,9	-0,5
Mean monthly T 2007-2017 [°C]	-6,6	-5,53	-1,42	3,73	10,46	14	17,13	14,98	10,66	4,71	1,04	-2,65

We can therefore conclude that Finland has generally very cold months and that a solid and efficient heating system in these northern countries is more necessary than elsewhere in Europe. It is important that attention is paid to heating and that any waste of heat (or water) is reduced as much as possible. Better still is to reuse this generated and wasted heat to also improve the efficiency of other processes or to temporarily store it to use in the cold seasons.

2.2 Seasonal Thermal Energy Storage (STES) systems

If we are able to efficiently store the heat produced in the summer, and reuse this in the cold, long Finnish winters, we could be the Robin Hood of the Finnish energy provision.
There are many TES technologies available, both commercial and emerging, and the amount of published literature on the subject is considerable [7].

A challenging and important part of the heat recovery is not how to create or harvest it (because we have the ability to extract the heat from hot cooling water), but how to store it until needed in winter. In this chapter we will discuss some methods to store this heat energy. STES technologies can be divided into two major parts. Firstly, underground thermal energy storage (UTES), and secondly, surface and above ground technologies.

2.2.1 Underground Thermal Energy Storage (UTES)

An early observation was that the ground temperature was often very different from the air temperature. The ground temperature at a certain depth below ground surface, which is not influenced by the season temperature variation at the surface, is equal to the annual mean air temperature. The mean annual air temperature, at any site, is the most significant indicator for the temperature in the ground at a depth between 6 metres and 50 metres. The temperature between these depths is generally constant all year round, assumed the ground is left undisturbed, because heat moves very slowly in the ground. The temperature in the first two metres of ground fluctuates with seasonal changes in air temperature at the surface (with time lags), but these fluctuations decrease to very low level by a depth of six metres [8]. The soil temperature in Jakioinen (60°49'N 23°30'E) was measured at a depth of 50 cm below the soil surface and has an annual mean range from 5,6 – 6,4 °C [9].

There are many examples, from various regions of the world, of ancient underground buildings with comfortable temperatures around the year. Such buildings have often one outer wall or are surrounded by rock or soil. These types of storage will be less suitable for the application of this master's thesis.

A more recent underground thermal storage technology, developed during the last 40 – 50 years, means that thermal energy is actively stored for the purpose of later extraction. So, heat is either injected for later use (heat storage) or extracted from the ground (cold storage) which is later used for cooling. Such thermal energy storage is mainly for long-term storage or seasonal storage of thermal energy storage [10].

UTES systems are usually divided into two groups. In borehole thermal energy storage (BTES) systems, also called "closed" systems, a fluid (water in most cases) is pumped through heat exchangers in the ground.

In aquifer thermal energy storage (ATES) or "open" systems, groundwater is pumped out of the ground and injected into the ground by using wells to carry the thermal energy into and out of an aquifer [11]. We describe the two most common UTES systems.

Aquifer Thermal Energy Storage (ATES)

The operation of Aquifer Thermal Energy Storage (ATES) means that water is extracted from a well and is heated or cooled before it is re-injected into the same aquifer, see Figure 13. So, the thermal energy is stored in the groundwater and in the area around it. There are usually several wells, for extraction and injection, and these are separated (approximately 50m apart, see simulation model [11]) in order to keep the warm and cold water from mixing. ATES systems are large scale systems mainly for seasonal thermal energy storage both heating and cooling. In many cases the same ATES is used for both heating and cooling as can be seen in Figure 14 [10].
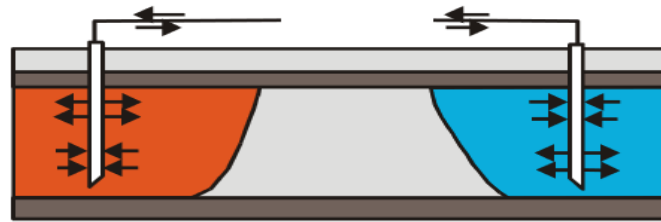
Figure 13: Aquifer heat store technology for seasonal thermal energy storage [14]
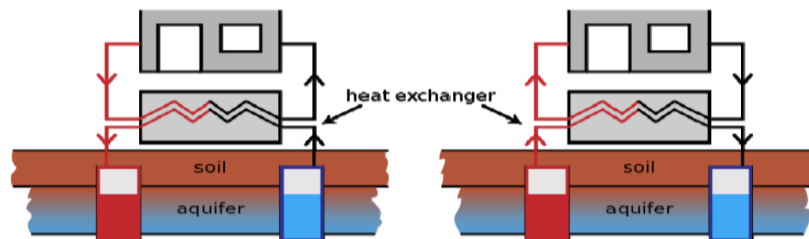
Figure 14: Outline of aquifer thermal energy storage system. Left: summer – the ATES used for cooling [14]

The thermal behaviour of the storage system depends on the direction and velocity of the groundwater flow, which is determined by the regional pressure gradient.

Some important requirements for an ATES installation are high ground porosity, medium to high hydraulic transmission rate around the boreholes, but a minimum of ground water flow through the reservoir. Another set of parameters that must be given proper attention in order to prevent scale formation to the ground water are:
- geological mapping,
- geophysical investigations,
- pumping tests in advance,
- test drillings in advance.

The test drillings will define the stratigraphic layers in the area while the geophysical investigation and geological mapping are used for extrapolation of the layers and for definition of geometry. Test drillings can be used as a part of the final system and can be considered as an early investment in the system.

Based on the results of field investigation, a conceptual model (Figure 15) is created and the hydraulic properties of the aquifer and its surrounding layers are derived. The final outcome will be a geological model that is more or less accurate and that can be used for the final design. To be able to make simulations, the loading conditions of heat and cold should be known.
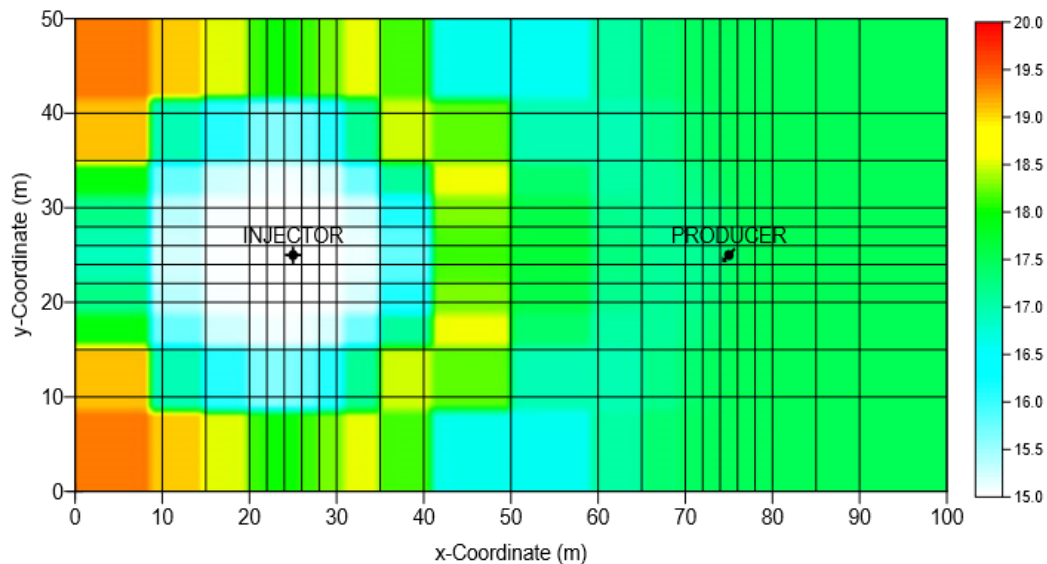
Figure 15: Example conceptual model ATES. The model shows the temperature distribution [°C] obtained with different groundwater flow after cold water injection with ground water flow from right to left (Δp = - 40 kPa) [13]

An advantage of open systems is the generally higher heat transfer capacity of a well compared to a borehole. This makes ATES usually the cheapest alternative if the subsurface is hydrogeological and hydrochemically suited for the system [11].

Operation principles

Usually, a pair of wells are pumped constantly in one direction or alternatively, from one well to the other, especially when both heating and cooling being provided. As presented in Figure 16, these two operation principles are called continuous regime and cyclic regime, respectively. Continuous regime only is feasible for plants where the load can be met with temperatures close to natural ground temperatures, and the storage part is more an enhanced recovery of natural ground temperatures. With a continuous flow, design and control of the system are much simpler and easier. Only one well or group of wells need to be equipped with pumps. A disadvantage is the limited temperature range.

Cyclic regime, or flow, will create a definite cold and heat reservoir around each well or group of wells. It is possible to maintain a ground volume above or below the natural ground temperature all the time. One disadvantage is a more complicated well design and control system with each well being able to both produce and inject groundwater [11].
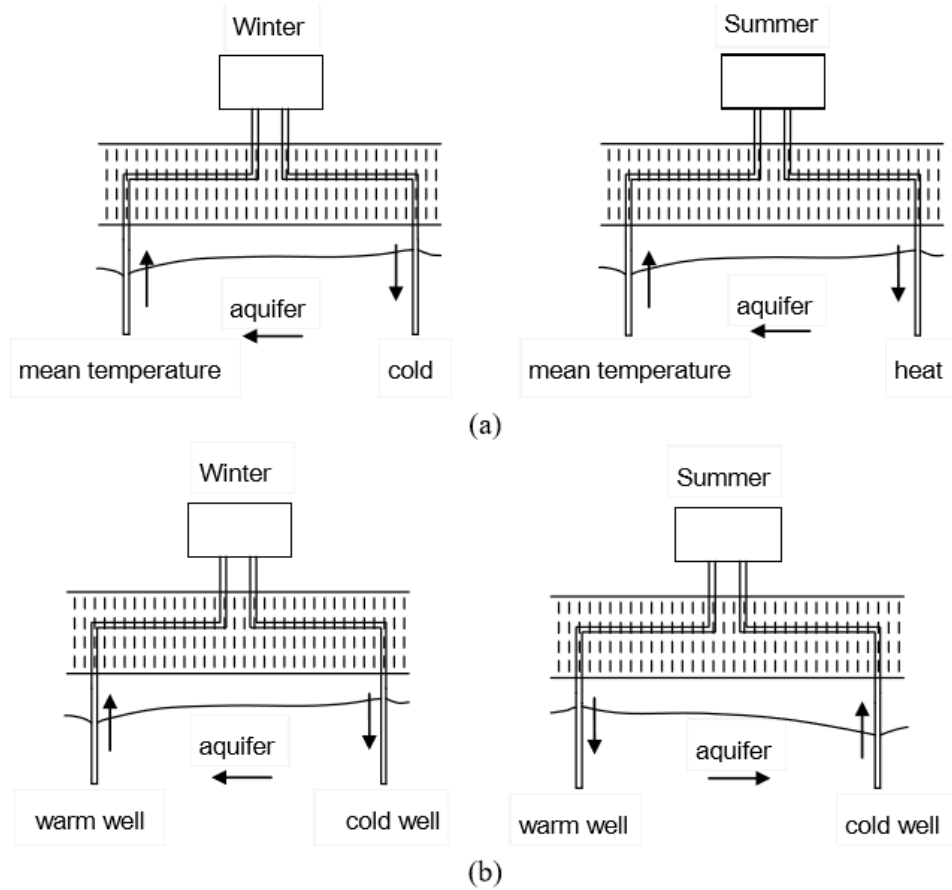
Figure 16: Basic operational regimes for aquifer thermal energy storage (a) continuous regime. (b) cyclic regime [13]

Definition of thermal recovery efficiency for ATES systems

As in other ATES studies the recovery efficiency (η_{th}) of an ATES well is defined as the amount of injected thermal energy that is recovered after the injected volume has been extracted. For this ratio between extracted and infiltrated thermal energy (E_{out}/E_{in}), the total infiltrated and extracted thermal energy is calculated as the cumulated product of the infiltrated and extracted volume with the difference of infiltration and extraction temperatures ($\Delta T = T_{in} - T_{out}$) for a given time horizon (which is usually one or multiple storage cycles), as described in formula 2.1:

$$\eta_{th} = \frac{E_{out}}{E_{in}} = \frac{\int \Delta T \ Q_{out} \ dt}{\int \Delta T \ Q_{in} \ dt} = \frac{\Delta \overline{T_{out}} \ V_{out}}{\Delta \overline{T_{in}} \ V_{in}} \tag{2.1}$$

With Q being the well discharge during time step t and ΔT the weighted average temperature difference between extraction and injection. Injected thermal energy that is lost beyond the volume to be extracted is considered lost as it will not be recovered. To allow unambiguous comparison of the results they are carried out with constant yearly storage and extraction volumes ($V_{in} = V_{out}$) [12].

Loss of heat due to displacement by ambient groundwater flow

Significant ambient groundwater flow is known to occur at ATES sites which leads to displacement of the injected volumes. This may lead to significant reduction in the thermal energy recovery efficiency of ATES systems as ambient groundwater flow (u) contributes to thermal losses by displacing the injected water during storage.

The heat transport velocity (u·) is retarded with respect to ambient groundwater flow due to heat storage in the aquifer solids. The thermal retardation (R) depends on porosity (n) and the ratio between volumetric heat capacities of water (c_w) and aquifer (c_{aq}, with $c_{aq} = n c_w + (1- n) c_s$ and c_s the solids volumetric heat capacity), as can be seen in formula 2.2:

$$u_* = \frac{1}{R} u = \frac{n \, c_w}{c_{aq}} u \approx 0,5 \, u \tag{2.2}$$

Resulting in a heat transport velocity at approximately 50% of the groundwater flow velocity (u). Under conditions of ambient groundwater flow, thermal energy stored in an aquifer will thus be displaced and can only be partly recovered [12].

Loss of heat by dispersion and conduction

Mechanical dispersion and heat conduction spread the heat over the boundary of the cold and warm water bodies around the ATES wells. As a consequence of the seasonal operation schedule, diffusion losses are negligible. Both other processes are described by the effective thermal dispersion (D_{eff}) which illustrates the relative contribution of both processes to the losses and can be calculated using formula 2.3:

$$D_{eff} = \frac{\kappa_{Taq}}{n \, c_w} + \alpha \frac{v}{n} \tag{2.3}$$

where, the first term represents the conduction, which depends on the volumetric heat capacity (c_w) of water and the thermal conductivity (κ_{Taq}) and porosity (n) of the aquifer material which are considered to remain constant at about 0.15 [m²/d] in a sandy aquifer with porosity of 0,3.

The rate at which conduction occurs can be determined by the increasing standard deviation as can be seen in formula 2.4:

$$\sigma = \sqrt{2 D_t t} \tag{2.4}$$

with D_T, the effective thermal dispersion (the left hand term and t the storage time). The second term of equation represents the mechanical dispersion, which depends on the dispersivity (α) of the subsurface, porosity and the flow velocity of the water (v), which is the sum of the force convection due to the infiltration and extraction of the well, as well as the ambient groundwater flow (u) [12].

Since losses due to mechanical dispersion and conduction occur at the boundary of the stored body of thermal energy, the thermal recovery efficiency therefore depends on the geometric shape of the thermal volume in the aquifer. The infiltrated volume is simplified as a cylinder with a hydraulic radius (R_h) defined as is formula 2.5:

$$R_h = \sqrt{\frac{V_{in}}{n\pi L}} \qquad (2.5)$$

and for which the thermal radius (R_{th}) is defined as formula 2.6:

$$R_{th} = \frac{\sqrt{c_w V_{in}}}{\sqrt{c_{aq}\pi L}} = \sqrt{\frac{nc_w}{c_{aq}}} R_h = \sqrt{\frac{1}{R}} R_h \approx 0{,}66\, R_h \qquad (2.6)$$

The size of the thermal cylinder thus depends on the storage volume (V), screen length (L, for a fully screened aquifer), porosity (n) and water and aquifer heat capacity (see Figure 17) [12].
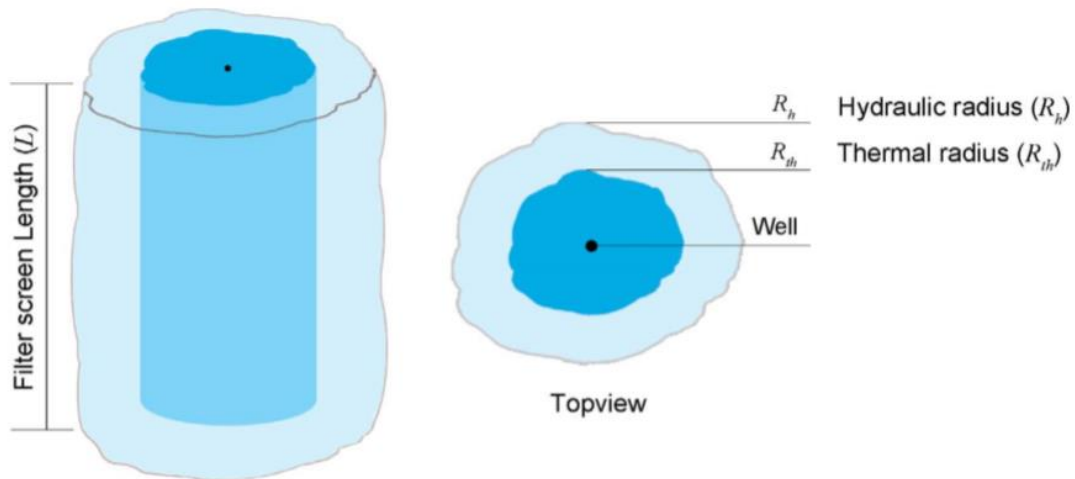
Figure 17: Simplified presentation of the resulting subsurface thermal and hydrological storage cylinder for an ATES system for homogenous aquifer conditions [12]

Borehole Thermal Energy Storage (BTES)

Today, one of the most common strategies for seasonal energy thermal storage is known as borehole heat storage. This essentially uses the heat capacity of soil to store a large amount of heat underground for months. It works by drilling an array of boreholes from about 30 – 200 m deep. During the summer the heat from the hot cooling water is transferred to water which is then stored deep in the soil and rock inside the borehole. That stored heat can later be extracted when needed and used for other applications [13]. Figure 18 shows a sketch of borehole technology.
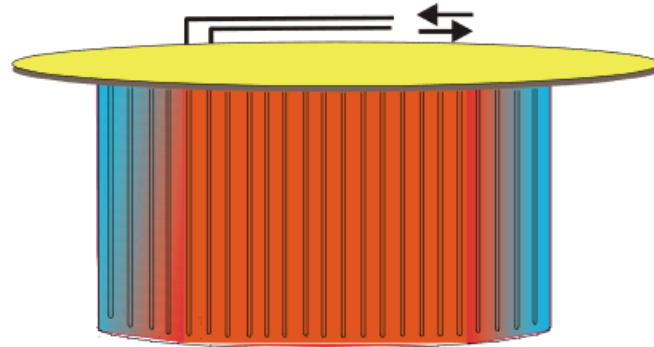
Figure 18: Borehole technology for seasonal thermal energy storage [13]
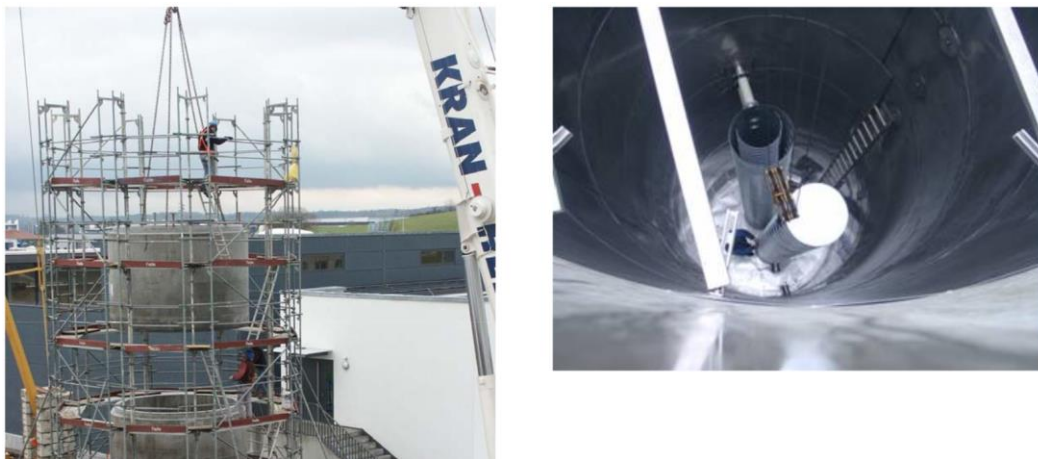
Figure 19: Crailsheim: new buffer storage with 3 bar pressure for 100 m³ water in concrete containment [14]

Such systems are "always" connected to a heat pump [10].

Even though borehole seasonal solar thermal storage is usual and preferred to aquifer storage due to its better efficiency, there are still some common barriers for its development in the world. Some of the common barriers are special geological conditions for underground water flow and the type of the subsoil, unclear heat transfer mechanism in the underground and a small heat capacity leads to a larger storage volume of the borehole installation (which raises the price of the installation). Also scientists do not fully understands the system operating characteristics and how it disturbs the underground environment [13]. Figure 19 shows a real borehole storage realised in Crailsheim.

Another challenge for borehole heat storage is that you also need access to drillable land (as in the case of ATES). Since Finland has a very low population density of 16,43 people per square kilometre (16,43/km²) [15], this should not cause any problems.

Operation

Borehole energy storage, also known as duct heat storage, do not have an exactly separated storage volume (can be a small installation for low storage volume, or bigger installations when there is need for a higher heat demand and a higher storage volume is required). BHEs can be single-or double-U-pipes or concentric pipes mostly made of synthetic materials, see Figure 20. Double-U-pipes made of poly-butylene (PB) are used for heat storage application because of the high upper temperature limit of 90 ℃. The space between the pipes and the borehole wall is usually refilled with a grouting to reduce the system's thermal borehole resistance so that the heat is better retained and the efficiency of the system can be raised (see Figure 20 below on the right). If the borehole is stable enough also water can be refilled. Distances between boreholes vary between 1,5 and 3 m, depending on size and depth of the store. Heat insulation can only be installed on top. Duct heat stores do not only have a vertical temperature stratification but also a horizontal stratification from the centre to the borders.

Water-saturated clay, claystones as well as rocks are suitable ground conditions because of the high heat capacity.

Advantages of BTES are the extendibility and the low effort for construction (compared to pit storages what will be discussed next). On the other hand, the size of a duct heat store has to be ± 1,5 higher compared to other storages of the same amount of heat (see the table below). This because of the reduced heat capacity of the storage material and the smaller power rates for charging and discharging due to the heat transfer in the BHEs.
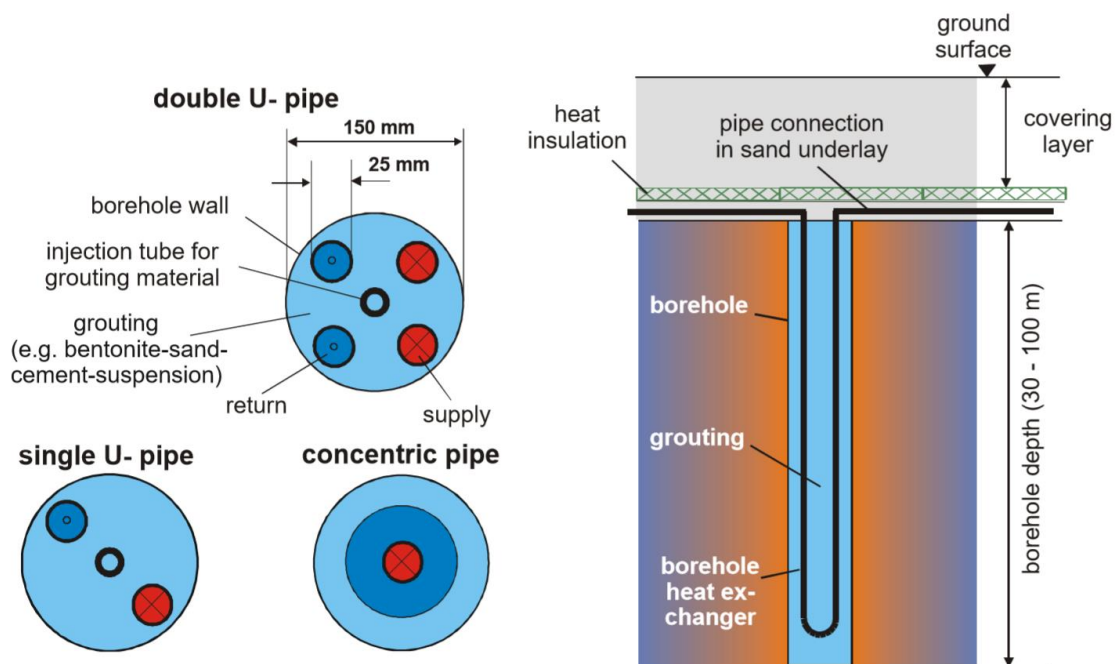
Figure 20: Types of borehole heat exchangers and sample installation [16]

BTES Performance

Measuring the performance of BTES systems can be done in many ways. A common measure of system efficiency remains the BTES efficiency, which is a measure of the total heat extracted ($Q_{extracted}$) divided by the total heat injected into the storage ($Q_{injected}$), as shown in equation 2.7 [17]:

$$\eta_{BTES} = \frac{Q_{extraced}}{Q_{injected}} \qquad (2.7)$$

2.2.2 Comparison ATES – BTES

In this section there is an overview of a comparison of the storage types discussed above.

Table 4: Comparison of Underground Storage Concepts (ATES vs BTES) [14]

Comparison of Storage Concepts		
	ATES	BTES
Storage medium	Ground material (sand/gravel…–water)	Ground material (soil, rock…)
Heat capacity in kWh/m³	30 – 40	15 - 30
Storage volume for 1m³ water equivalent	2 - 3 m³	3 - 5 m³
Geological requirements	• Natural aquifer layer with high hydraulic conductivity [I] • Confining layers on top and below • No or low natural groundwater flow • Suitable water chemistry at high temperatures (40 – 70 ℃) [18], [19] • Aquifer thickness 20 – 50 m	• Drillable ground • Groundwater favourable • High heat capacity • High thermal conductivity • Low hydraulic conductivity for long heat storage • Natural ground-water flow < 1 m/a • 30 – 100 m deep
Installation cost	Lower installation cost then BTES, but higher operation cost because heat pumps are involved	Higher installation cost then ATES, but lower operation cost
Water temperature	± 15 ℃ from groundwater to keep groundwater quality [20]	From 70 ℃ up to 110 ℃ (inlet temperatures) [21]

[I] *Hydraulic conductivity: hydraulic conductivity is a measure of how easily water can pass through soil or rock. High values indicate permeable material through which water can pass easily. Low values indicate that the material is less permeable* [63].

2.2.3 Surface and Above Ground Technologies

In addition to storing the water from the process underground, there are also options for storing the water above ground. We will investigate whether some of these applications are eligible for the application in this master's thesis.

Pit Storage (PTES)

Pit thermal energy storages are made of an artificial pool filled with storage material as water, gravel-water mixture, or gravel and closed by a lid. The usually naturally tilted walls of a pit can be heat insulated and then lined with watertight plastic foil. The storage is filled and a heat insulated roof closes the pit as can be seen in the concept in Figure 21.
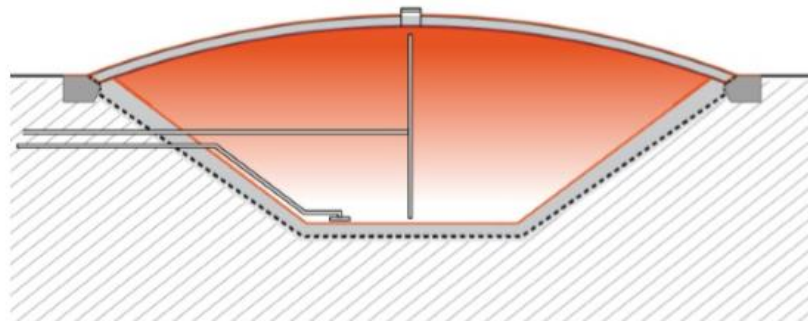
Figure 21: Pit thermal energy storage concept [22]

Pit thermal energy storage filled with gravel-mixture have heat storage capacities between 30 and 50 kWh/m³ (water: 60 to 80 kWh/m³), equivalent to $1,3 - 2m^3$ of water. This means that a pit storage filled with a gravel-water mixture must be 1,3 times to twice the size of a pit- or tank storage filled with water to reach the same storage capacity. An advantage is that the space over the storage can be more easily used for example a parking lot. The maximal temperature of all realised pit storages is about 80 °C [22]. Figure 22 shows a realised pit storage in Eggenstein.

Figure 22: Pit storage in Eggenstein, 4 500 m³, 2008 [14]

Large-scale pit thermal storage with water

To achieve a high heat storage capacity per unit volume the heat storage material should have a high specific heat and a high density. Water scores highly in this respect and has the further advantages of being cheap, safe and easy to handle, so today it is almost always the storage material of choice for sensible heat storage systems operating at temperatures in the range 0 – 100°C [23]. Large scale STES water storage tanks can be built above ground, insulated, and then covered with soil, Figure 23 [14].

Figure 23: Left: schematic sketch of a water pond heat storage. Right: a 75 000 m³ water pond under construction at Marstal solar heating plant [23]

2.2.4   Comparison of hot water and gravel water PTES

In this section we made a small overview of a comparison of the pit thermal energy storage types discussed above and shown in table 5.

Table 5: Comparison of hot water and gravel water PTES [24]

Pit Thermal Energy Storage	
Hot water	Gravel/sand/soil water
+ thermal capacity + operation characteristic + thermal stratification + maintenance / repair	+ low static requirements + simple cover
- sophisticated and expensive cover - low static cover load - costs for landfill of excavated soil (if applicable)	- thermal capacity - charging system - additional buffer storage (if applicable) - maintenance / repair - gravel cost

Tank Thermal Energy Storage

There are some examples of tank storages being used as seasonal storage. Seasonal tank storage is made of reinforced concrete and partially buried in the ground. This type of storage can be built almost independently of geological conditions. It is thermally insulated on the top and on the vertical walls (see Figure 24). The shape of the store is mostly cylindrical and half of it is buried into the ground. Stainless steel liners and insulation are used on the top and on the sides. Moreover, 4 500 m³ store in Hamburg and the 12 000 m³ store in Friedrichshafen are other examples of large scale tank storage. Inside of these storages, stainless-steel liners are used to ensure water tightness and to reduce heat losses caused by steam diffusion via the concrete wall. In addition, polyethylene or polyvinylchloride film was applied as the thermal insulation to the storage. Inner steel liner can be avoided if high-density concrete (HDC) material with lower vapour permeability is used [24]
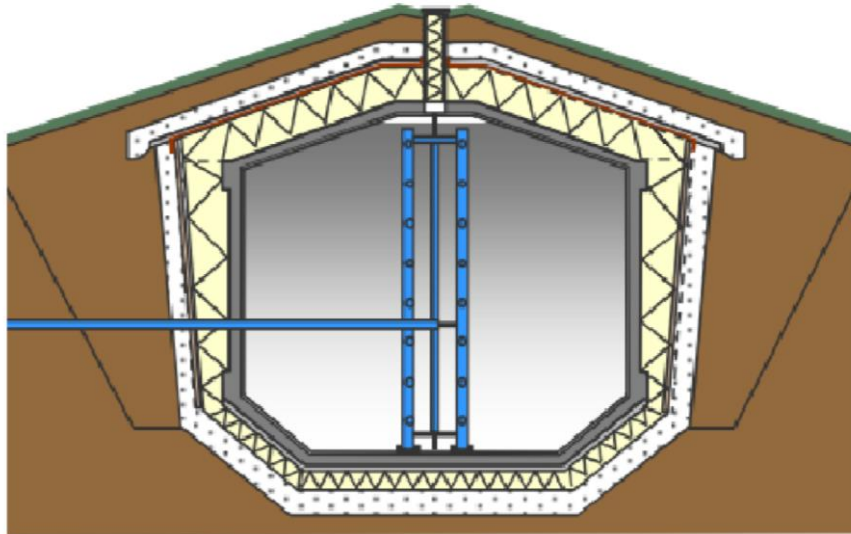
Figure 24: Tank thermal energy storage [24]

Earth-bermed storages

Earth-bermed buildings stores heat passively in surrounding soil. Seeking refuge in the heart of earth and benefitting from soil's thermal property, based on experience, is a strategy employed in the past across some regions. The passive systems are amongst the cheapest methods of providing heating and cooling demands of the buildings. These systems experience the lowest impact of environmental degradation while increasing the energy efficiency of the building through decreasing heat gain and loss. The idea of the earth-sheltered buildings is amongst the passive construction that has been embraced by the architects. An earth-sheltered building, as a passive idea, can guarantee, extensively, the reduction of energy consumption and provides the required conditions for thermal comfort. Considering to the results, by increasing the depth of sheltering in amount of soil, its energy consumption saving will increase. In this situation annual temperature fluctuation decreases 50% and it saves about 67% of energy consumption [25].

Figure 25: House in Tempe, Arizona, uses earth-sheltered construction methods to help decrease cooling costs. Photo by Pamm McFadden [26]

Another example is a large rock cavern heat storage established by Helen, a Finnish producer of city energy, planned in Helsinki. Helen is planning to build a new energy storage facility in disused underground oil caverns located deep in the bedrock of Helsinki. Two of the rock caverns are identical and they now can be converted for heat storage use. During the heat load of the coldest days of the winter, the start-up of separate natural gas and oil-fired heating plants can be avoided by using the storage facility. The storage facility would accommodate over 40 times as much hot water as the amount of water in the pools at the Helsinki Swimming Stadium. Three large oil caverns used for the storage of heavy fuel oil before are located underground in Mustikkamaa. The logic of using the heat storage facilities currently in use in Helsinki is based on the balancing of daily consumption peaks. Due to the large energy capacity of the rock cavern heat storage, production can be optimised for a longer period, at a weekly level.

Facts:
- disused oil caverns are designed to be used as an energy storage facility;
- hot water is used for the storage of energy;
- the effective volume of the rock cavern storage facility is about 260 000 m³;
- the amount of energy stored is 11,6 GWh;
- the charging/discharging capacity of the storage facility is 120 MW (sufficient for about four days);
- the use of the rock caverns as a heat storage facility will have no impact on other activities in Mustikkama [27].

Unfortunately there are no possible earth-sheltering storages near the candle factory to benefit from soil's thermal property to eventually store the waste water, this in turn will not offer a possible, cheap solution.

Salt hydrate technology

Salt hydrates are used as thermochemical materials (TCMs) for seasonal heat storage in the built environment. With the current concept of seasonal heat storage, including closed and open systems, whereby only one dehydration cycle per year is performed under a system energy density of 1 GJ/m³, it is not realistic for large scale implementation to use pure salt hydrates as heat storage material. By adjusting the constraints, such as multiple cycles per year or higher water vapor pressures, salt hydrates can still be used as TCMs [28].
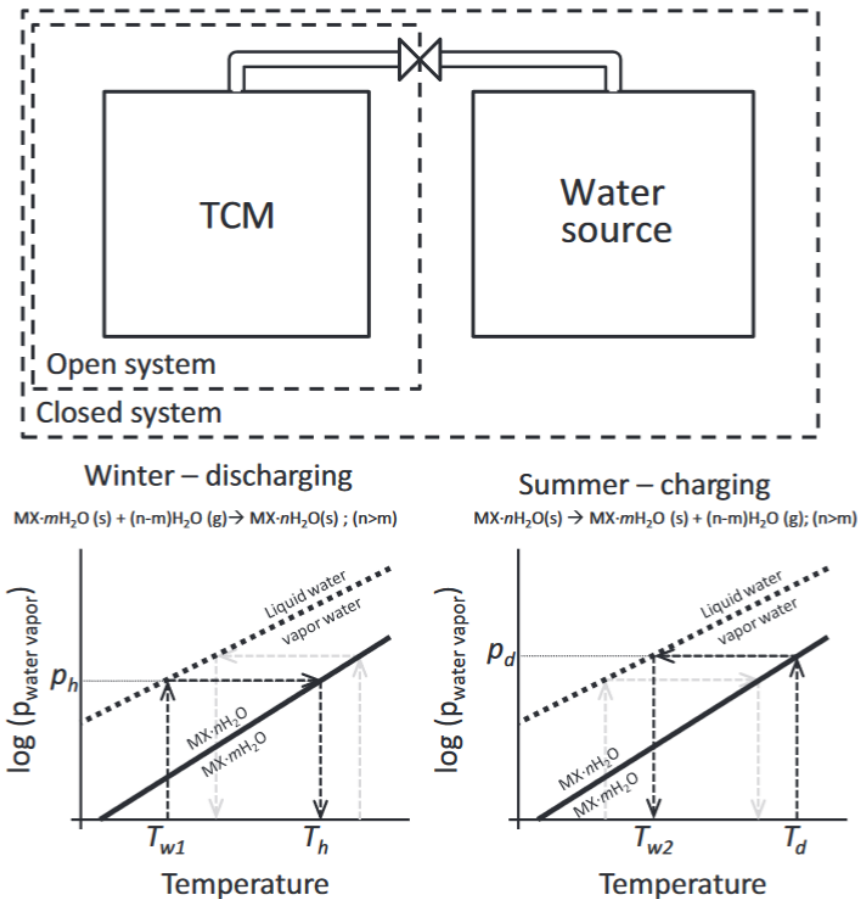
Figure 26: The concept of a heat storage system with help of a TCM is schematically given. On the top, the reactor system is shown, where two compartments are drawn, one filled with a TCM and the other with water, in between these compartments a valve is located [28]

For heat storage, two main concepts are considered, closed and open systems. In the case of a closed system both compartments are part of the system and all water necessary for the hydration/dehydration reactions is stored within the system. In the case of an open system, the water is not stored in the system itself, but externally released/supplied to the system dependent on TCM dehydration/hydration. The working conditions of TCM systems are determined by the phase diagram of the TCM in question. A phase diagram indicates the conditions under which a certain TCM undergoes hydration or dehydration [28].

Salt hydrates systems stores the thermal energy by drying the salt hydrate and storing the dry salt and the water separately. The reversible reaction of hydration and dehydration of a salt hydrate is shown in equation 2.8:

$$salt + xH_2O \leftrightarrow salt.xH_2O + heat \qquad (2.8)$$
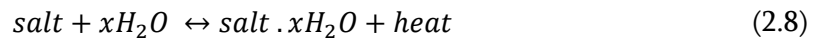
Salt hydrates for thermal energy storage have a minimum storage density of 1 GJ/m³ (depending on operating conditions) and no loss of heat occurs during storage. Using salt hydrates, a storage volume of 4 – 8 m³ would be sufficient for the storage of the energy needed for an average household for one year. The energy density of the TCM will determine the precise volume of the storage system, the cost and the storage capacity [29].

Operation salt hydrate technology

If you pour water into a beaker containing solid or concentrated sodium hydroxide (NaOH), the mixture heats up. The dilution is exothermic: chemical energy is released in the form of heat. Moreover, sodium hydroxide solution is highly hygroscopic and able to absorb water vapor. The condensation heat obtained as a result warms up the sodium hydroxide solution even more. The other way round is also possible: if we feed energy into a dilute sodium hydroxide solution in the form of heat, the water evaporates; the sodium hydroxide solution will get more concentrated and thus stores the supplied energy. This solution can be kept for months and even years, or transported in tanks. If it comes into contact with water (vapor) again, the stored heat is rereleased. A safety precaution as concentrated sodium hydroxide solution is highly corrosive. If the system springs a leak, it would be preferable for the aggressive liquid to slosh through the environment. This method also enables solar energy to be stored in the form of chemical energy from the summer until the wintertime. The stored heat can also be transported elsewhere in the form of concentrated sodium hydroxide solution, which makes it flexible to use [30].
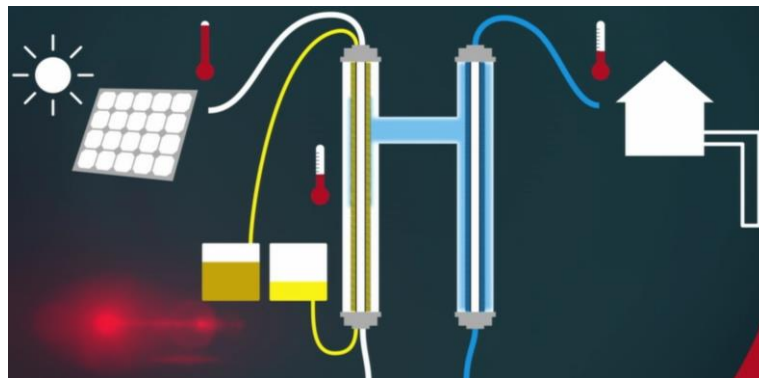
Figure 27: Working principle heat storage with a TMC [30]

Salt hydrate technology used for domestic seasonal heat storage?

Salt hydrate materials can store and release heat with a high energy storage density four times higher than the energy storage density of water (over a temperature range of 60 °C) with the additional benefits of low heat losses over the storage time and allowing for low cost and safe systems. Although some salt hydrate materials have interesting properties for domestic application of seasonal heat storage, pure salt hydrates are currently not suitable for a multiple cycle application, due to the breakdown of the material structure over cycles. For future research, this work indicates the need of using structurally stable sorption materials for developing a long term concept of seasonal heat storage [31].

2.3 Conclusion different STES systems

In this section a conclusion is made from the literature study above about thermal energy storage technologies, especially, large-scale thermal storages such as aquifer and borehole thermal storages, tank and pit thermal energy storages. Each storage has its own advantages and disadvantages as well. ATES systems are highly dependent on the geological structure of the subsurface layers, especially on an aquifer type, while BTES systems do not need special geological conditions, except there should not be emptied caverns or high pressure geysers in the subsurface. Moreover, TTES (Tank Thermal Energy Storage) system can be built independently of geological conditions and it is reliable and efficient if it was constructed properly, otherwise leakage problems might arise. Special liners are used in TTES system to hinder thermal energy loses from the storage. Another large scale storage is PTES (Pit Thermal Energy Storage) system. Some PTES systems include gravel with water as the storage media. TTES storage is usually covered by a lid and construction of a lid requires most of the effort and is the most expensive part of the storage.

In order to achieve a good efficiency with these systems, the minimum possible water temperature is required (+50 ℃). If this is not the case, the payback period of these installations will be too long. In the practical case of the problem in this Master's thesis, we have a water temperature of 30 ℃ and mainly high flow rates (5 l/s) which are both detrimental factors for thermal energy storage in pits, tanks, boreholes...

Unfortunately, also earth-bermed systems are not a possible solution because there are no earth-sheltering storages near the candle factory to benefit from soil's thermal property to eventually store the waste water, this in turn will not offer a possible, cheap solution.

A system working on salt hydrate technology is currently still too fierce in the research phase, not yet user-friendly enough, requires too high a water temperature (52 ℃ for salt [29]) and is still too expensive to be able to develop such a system applicable at Suomen Kerta factory .

Additional aim of the review was to gather necessary knowledge in the area of thermal energy storage and apply the knowledge to develop a thermal energy storage for our application, which is able to store thermal energy for short term as well as long term purposes.

We can conclude that, unfortunately, none of the above techniques can be used and we will have to continue to look for other solutions to reduce the water wastage of the Suomen Kerta factory.

2.4 ORC Systems

Since most of the wasted energy in Suomen Kerta factory is discharged in form of hot water with a low temperature, it makes storing this heat a very difficult task. We thus will take a closer look on the existing technologies dedicated to recover low to medium waste heat and if there are possibilities to generate electricity from it [32].

ORC is the abbreviation of Organic Ranking Cyclus. The working principle of an Organic Rankine Cycle power plant is similar to the most widely used process for power generation, the Clausius-Rankine Cycle. The main difference is the use of organic substances instead of water (steam) as working fluid. The organic working fluid has a lower boiling point and a higher vapour pressure than water and is therefore able to use low temperature heat sources to produce electricity. The organic fluid is chosen to best fit the heat source according to their differing thermodynamic properties, thus obtaining higher efficiencies of both cycle and expander. The main components of an Organic Rankine Cycle power plant design are the turbine, the heat exchangers, the condenser, the feed pump [33].
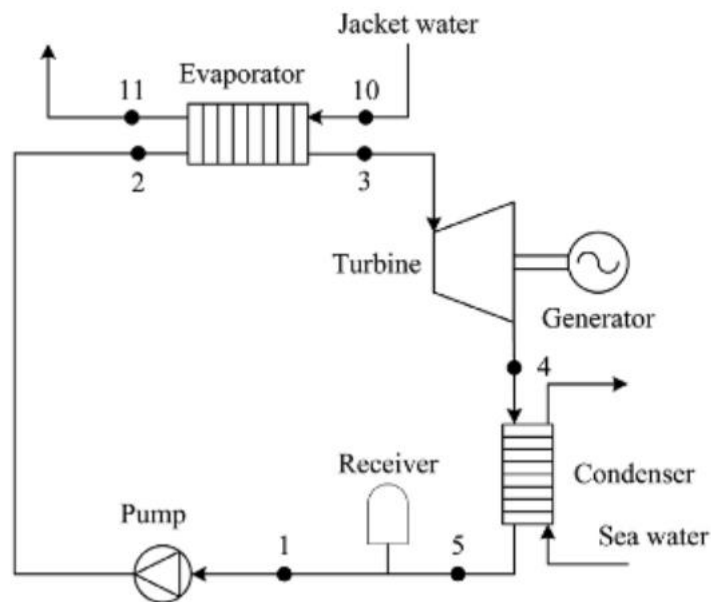
Figure 28: Block diagram of an Organic Rankine Cycle Power System recovering the heat from hot jacket water [33]

Organic Rankine Cycle (ORC) systems are used for power production from low to medium temperature heat sources in the range of 80 to 350 °C and for other small-medium applications at any temperature level. This technology allows for exploitation of low-grade heat that otherwise would be wasted. Performance and economy of an ORC mainly depend on the selection of the working fluid.

Since this technology produces power at temperature heat sources in the range of 80 to 350 °C, this technology will again not be usable for the waste water (30 °C) problem of Suomen Kerta.

2.5   Domestic Heat Recovery Systems

Drain Water Recovery

Since the use of thermal energy storage and ORC systems are not suitable for the application of this Master's thesis, it may be possible to develop a circuit to use the waste water in the factory's domestic appliances.

Drain water recovery from utilities, such as dish washers and laundry machines, don't have applications like shower drain heat exchangers and there are good reasons for that. One difficulty for recovering drain water from such utilities is that they don't use hot water from the accumulator, but heat the needed cold water to washing temperature, as these machines don't have a constant need for hot water. Furthermore, the machines may also use cold water in their operations and the drain water can be expected to be dirtier than shower drain water, making it difficult to implement an efficient heat exchanger. Furthermore, especially in the dish washer case there is a possible clotting risk.

The drain water heat recovery systems can be categorized by how the preheated cold water is used. The best performance, but with the highest cost, is achieved with a balanced flow system, illustrated in the Figure 29, in which the preheated water is fed both into the shower water mixer as well as the hot water accumulator. In this case the flow of the cold water is equal to the flow of the drain water, thus giving the best performance energy savings wise [34].
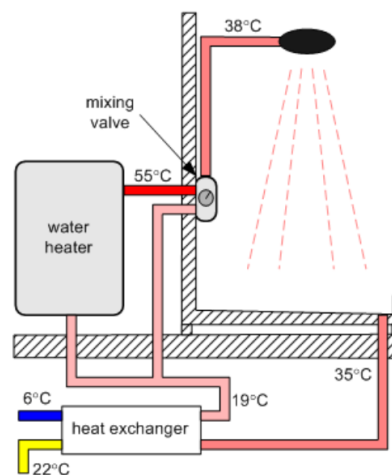
Figure 29: Shower with a drain water heat exchanger installed (balanced flower) [34]

Conclusion ORC and domestic heat recovery systems

ORC is a very interesting but still new and young technique that can be very useful for certain applications with high water temperatures. Before this technique will be widely applicable it must be economically advantageous. Since this technology produces power at temperature heat sources in the range of 80 to 350 °C, ORC systems will unfortunately not be usable for the waste water (30 °C) problem of Suomen Kerta.

Also, the waste water from the machine will not be useful enough to use for domestic applications. The wastewater will contain too many impurities to be used to wash your clothes in a washing machine or to wash your dished in a dishwasher, for example. The installation cost with the necessary control systems will also be too high implementation cost and too complicated to make a decent design.

2.6 Summary case A

Table 6: Conclusion different STES systems

Underground thermal energy storage systems	Aquifer thermal energy storage	• Water at high temperatures (40 – 70 °C) [18], [19] required; • high installation costs.
	Borehole thermal energy storage	• Water at high temperatures (70 – 110 °C) required; • high installation costs.
Above ground thermal energy storage systems	Pit thermal energy storage	• Too complex and cost intensive structure for our low temperature application.
	Tank thermal energy storage	• Too complex and cost intensive structure for our low temperature application.
	Horizontal heat exchangers	• Too complex and cost intensive structure for our low temperature application.
	Earth-bermed systems	• No earth-sheltering storages near the candle factory to benefit from soil's thermal property to eventually store the waste water.
	Salt hydrate technology	• Currently still too fierce in the research phase; • not yet user-friendly enough to use in a factory; • requires high water temperature (52 °C for salt [29]); • still too expensive; • not possible for multiple cycle application, due to the breakdown of the material structure over cycles.
ORC (Organic Rankine Cycle)		• Used for power production from low to medium temperature heat sources in the range of 80 to 350 °C.
Domestic heat recovery		• Wastewater will contain too many impurities; • installation cost with the necessary control systems will be too high; • implementation too complicated to add to current domestic water circuit.

Case B: Closed hydraulic circuit design when the machines are operating simultaneously

3 Closed hydraulic circuit design when the machines are operating simultaneously: Case B

3.1 Introduction

The main question for this case is: is it possible to use waste water from machine a (30 ℃) to cool the drums (12 ℃) in machine b in a closed circuit when 1, 2 or/and 3 of the drums are operating?

Consider the cooling water network shown schematically in the diagram/design below. The main components are the rotary molding machine, pumps, a filter, the cooling drums with control valves, back pressure valves and connecting pipes. Water is drawn from the rotary molding machine basin by a series of parallel pumps (P_i, i=1…nP) via horizontal suction lines of length L_a without a foot valve. The pumps can be closed by the ball valves for possible maintenance. On the pressure side, the parallel flows are merged and guided by a filter F_1. After this, the water is transported over a length of L_b, after which it is divided over three parallel branches (j = 1…3). Each branch has a supply line of length L_c and a return line of length $L_{c'}$. Each branch also has a cooling drum with a control valve K and a back pressure valve K_{bp}. After collecting the three flows from the different branches, the water is transported back through a pipe of length $L_{b'}$ that is connected with a three-way valve to reheat and re-use the water in the rotary molding machine, or if there is no need for it to empty it into the river. This includes the dimensioning of the pipes, valves and pumps to deliver the desired flow rates.

The water level in the rotary molding machine basin is at $z_1 = 0,5$ m height, the pumps are at $z_2 = z_3 = 0,5$ m height, and the drums are at a height of $z_d = 2,5$ m. The pipes have a roughness of e = 0,35 mm. The pipes between pumps and filter have a negligible pressure loss. Also, the effects of kinetic energy are negligible if the pipe sections are correctly dimensioned. The water in the circuit has a maximum temperature of 30 ℃.

The drums have a pressure loss at their design flow rate of Δp_{ld}. The filter has a pressure loss at design flow rate of Δp_{F1} and the counter pressure valve K_{bp} is set for a pressure loss at design flow rate of Δp_{kbp}. The rotary molding machine has a total pressure loss of Δp_{lRMM}.

For stable valve control, a valve pressure drop can be assumed at design flow rate equal to approx. 80% of the pressure drop over the remaining part of the branch (supply distribution + cooling drum + return distribution). The valve is then dimensioned so that it is open to a maximum of 90% in the event of the pressure drop. Note that the control valves are not dimensioned by matching the connection diameter to the connected pipe!

The tap water that is mixed with has a temperature of 4 ℃ and a flow rate of 15 m³/h

All the data used in the case description are also shown in the design scheme.

3.1.1 First global design sketch
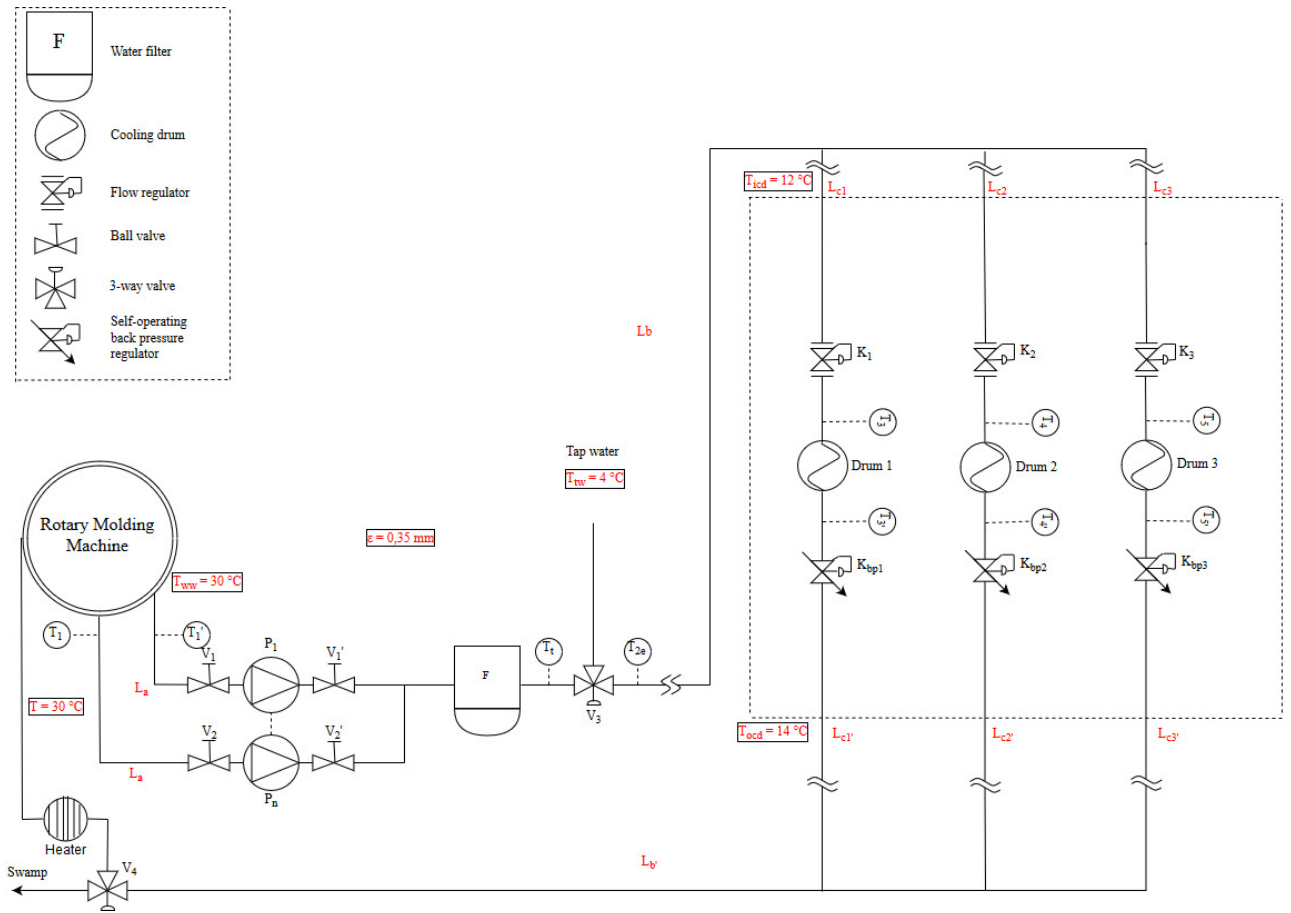
Figure 30: First hydraulic design scheme, case B

3.2 Balancing hydraulic circuit

3.2.1 Intro

Today's control systems have to meet a number of fundamental requirements, i.e. to guarantee a high level of thermal comfort and to control energy costs. In order to achieve this, the correct amount of cooling water should be delivered to the cooling drums of the installation. Only in this way is it possible to cool according to the design requirements. In other words, it must be ensured that the hydraulic circuit is always perfectly balanced. Due to the hydraulic imbalance between the different cooling drums, pressure drops can occur. This results in temperature fluctuations of the water which effects the pulverization of liquid raw candle material and reducing its operation. As can been seen in Figure 31 below, an example of a central heating system, which can be related to the cooling drums, where non-uniform temperature zones occurs because of bad balancing.
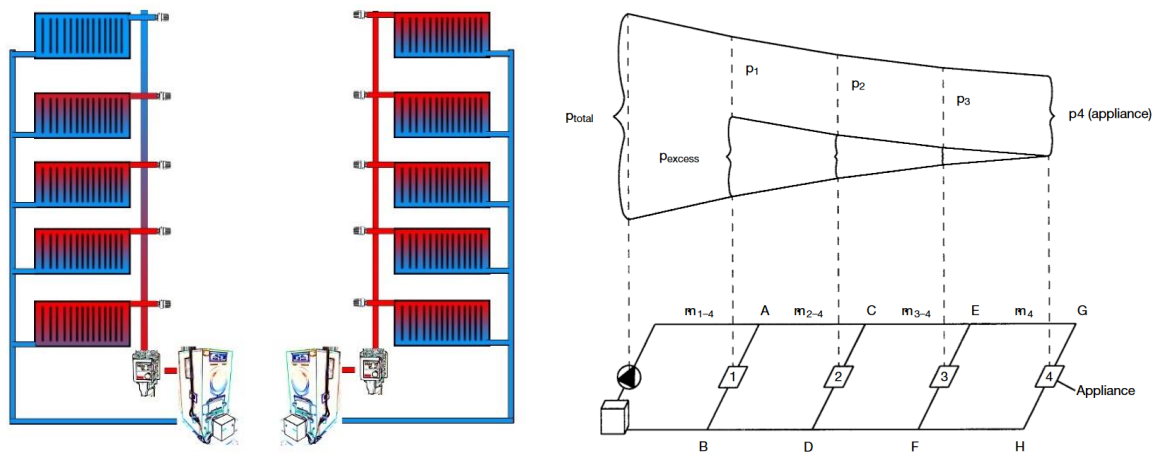
Figure 31: Example, left: unbalance vs balanced central heating system [35], *right: course of pressure in a circuit* [36]

Energy saving

Wrong flow rates in the various circuits lead to an increased energy consumption. On the one hand, a higher pump capacity must be provided to guarantee a sufficient supply of each appliance and on the other hand appliances being installed at a favourable hydronic position are then oversupplied. This will result in varying water temperatures.

In cooling systems, temperatures being 1 °C too low will result in an increase in energy consumption of about 15 %. Installations, in which the hydronic balancing was not carried out, have to start the heating operation earlier in order to achieve the desired temperature in time [36].

3.2.2 Balancing components

Pressure regulator vs. Backpressure regulator

It is important to know the similarities and differences between a pressure regulator and a backpressure regulator. Both are automatic, mechanical control valves that sense and respond to changes in process pressure. In most pressure control valves, the process fluid acts upon a piston that opens and closes the valve. An adjustable control element in the valve, such as a spring or compressed air, offsets the process pressure. When the process pressure exceeds the force of the control element, it moves the piston up. When pressure drops, the spring or compressed air moves the piston down. It is the function of that movement that determines whether the valve is a "pressure regulator" or a "backpressure regulator".

Backpressure regulator

When the spring force exceeds the pressure of the process fluid, the downward movement of the piston causes the valve to close. The backpressure regulator is designed to sense inlet pressure. The backpressure regulator is a normally-closed valve installed at the end of a piping system to provide an obstruction to flow and thereby regulate upstream (back) pressure. The backpressure regulator is called upon to provide pressure in order to draw fluid off the system.
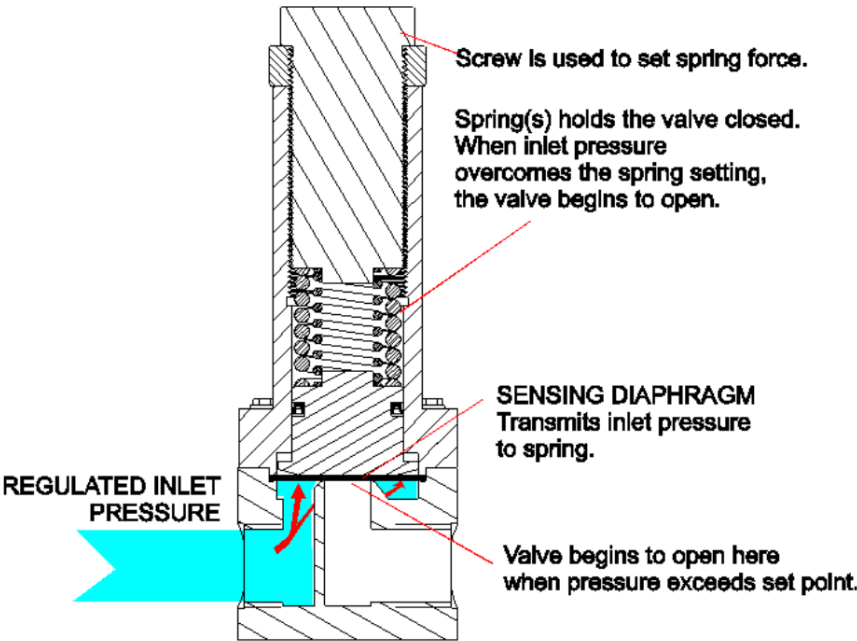
Figure 32: Function of backpressure regulator [37]

Pressure regulator

When the spring force exceeds the fluid pressure, downward movement of the piston causes the valve to open. The pressure regulator is designed to sense pressure at the valve outlet.

The pressure regulator is a normally-open valve and is installed at the start of a system or before pressure sensitive equipment to regulate or reduce undesirable higher upstream pressure.
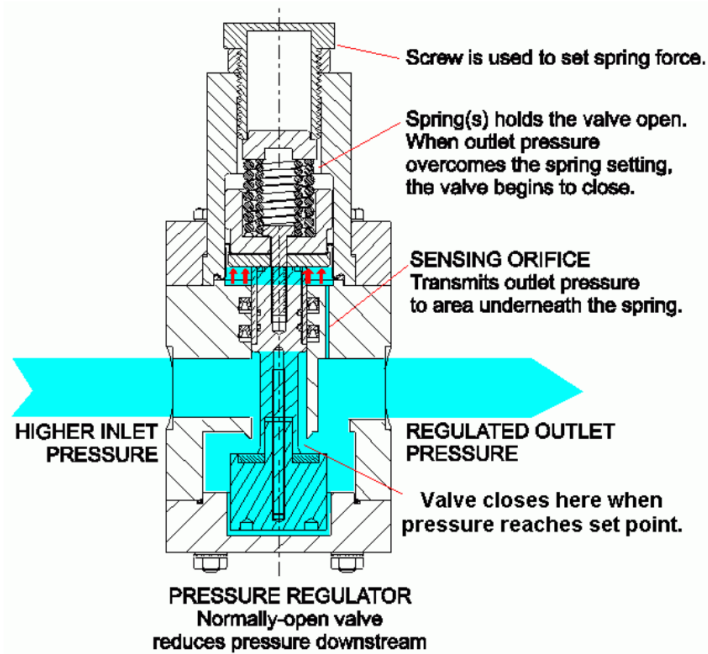
Figure 33: Function of pressure regulator [37]

Balancing a system

The combination of a pressure regulator at the beginning of a system, and a backpressure regulator at the end of a system will ensure balanced pressure throughout our system.
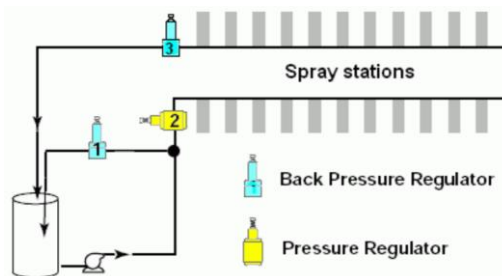
Figure 34: Back pressure regulator vs pressure regulator [37]

First pressure control in the line (#1): backpressure regulator, teed off the main line. This valve ensures proper backpressure on the pump, so that it will operate properly. It provides the additional benefit of relieving pressure if the line should become blocked, thus preventing the pump from deadheading.

The second control is a pressure regulator, (#2) which ensures that the downstream pressure does not exceed the maximum pressure rating of the spray heads.

Finally, another backpressure regulator (#3) is used at the end of the line, to provide an obstruction and ensure that all of the spray heads have sufficient pressure to function properly [37].

Self-operating back pressure regulator
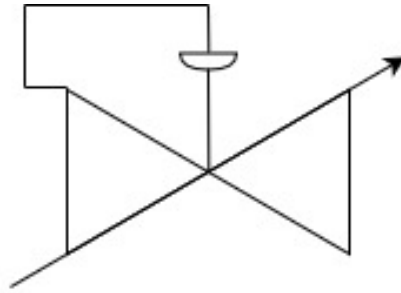
Figure 35: Symbol self-operating back pressure control valve

As mentioned before, the back pressure valve opens when upstream pressure rises. It regulates the fluid pressure upstream of the valve to a pre-adjusted set point value. It are these back pressure regulators that will be used in this design.

The medium flows through the valve (1) as indicated by the arrow. The position of the valve plug (3) and hence the free area between the plug and seat (2) determine the flow rate. The plug stem (5) with the plug is connected to the stem (11) of the actuator (10). To control the pressure, the operating diaphragm (12) is tensioned by the positioning springs (7) and the set point adjustment nut (6) so that the valve is opened by the force of the positioning spring when both pressures are balanced ($p_1=p_2$). The upstream pressure p_1 to be controlled is tapped upstream of the valve and transmitted via the control line (14) to the operating diaphragm (12) where it is converted into a positioning force. This force is used to adjust the valve plug (3) according to the force of the positioning springs (7) which is adjustable at the set point adjustment nut(6). When the force resulting from the upstream pressure p_1 rises above the adjusted set point, the valve opens proportionally to the change in pressure. The fully balanced valves are equipped with a balancing bellows (4). The downstream pressure p_2 acts on the inner bellows surface, whereas the upstream pressure p_1 acts on the outer surface of the bellows. In this way, the forces produced by the upstream and down-stream pressures acting on the plug are balanced. The valve seat must be exchanged if the flow divider is retro-fitted [38].
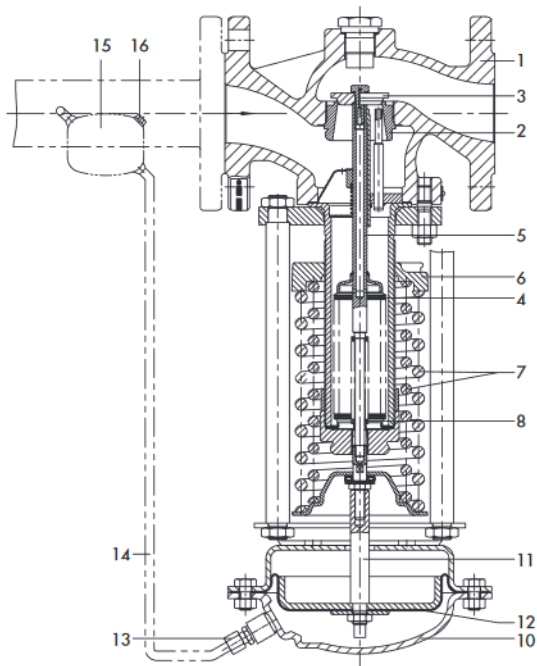
Fig. 2.1 · Type 41-73 Back Pressure Valve, principle of operation

Actuator with two diaphragms and diaphragm rupture indicator
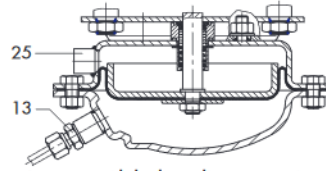
Actuator with leakage line connection

For 290 to 400 psi   For 145 to 320 psi   For 75 to 145 psi
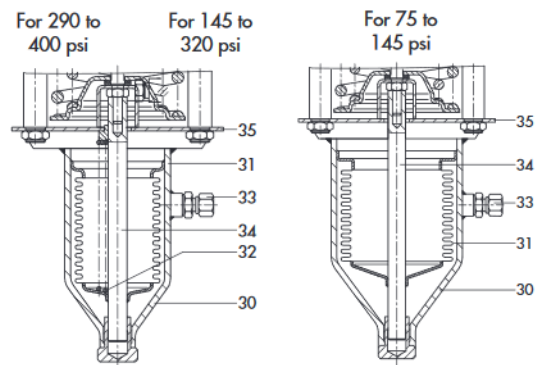
Metal bellows actuator (only for valves up to 2")

Fig. 2.2 · Type 2413 Actuators, different versions

1	Valve body Type 2417	10	Type 2413 Actuator	20	Two diaphragms
2	Seat (exchangeable)	11	Actuator stem	21	Diaphragm rupture indicator
3	Plug (with metal sealing)	12	Operating diaphragm with diaphragm plate	25	Leakage line connection ½"
4	Balancing bellows			30	Metal bellows actuator
5	Plug stem	13	Control line connection ⅜" (screw joint with restriction)	31	Bellows with lower part of body
6	Set point adjustment nut			32	Additional springs
7	Positioning springs	14	Control line	33	Control line connection ⅜"
8	Bellows seal	15	Condensation chamber	34	Bellows stem
		16	Filler plug	35	Bracket

Figure 36: Type 41 – 73 back pressure valve [38]

61
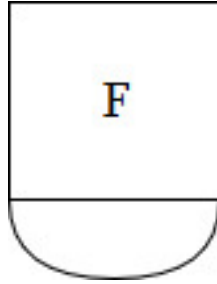
Water filter

Figure 37: Symbol filter

Because the process water flows through candles in order to cool them down (machine A), there will be impurities in the wastewater (mainly candle wax), which is detrimental to the cooling water of the drums (machine B). A good water filter is a critical component of the industrial water purification process.

Industrial filters are able to remove suspended solids, oils, and other contaminants from water. Water is pumped through various types of filtration products, these filters then trap and remove the contaminants (candle wax) as water passes through them [39].

Control valves
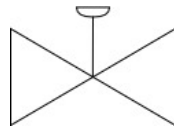
Figure 38: Symbol control valve

A control forms a continuously variable restriction for the flowing medium, in our case the wastewater. The control valve can be manual, self-regulating or sensor-controlled by a process automation system. In the first phase of the design, we will operate the control valves manually, in a later phase the choice will be made to control the control valves automatically via sensors.

K_{vs}-value control valves

In the case of control valves, the flow coefficient K_v is used to calculate the flow as a function of the differential pressure across the valve as can be seen in equation 3.1.

$$Q = K_v \sqrt{\frac{\Delta p/bar}{RD}} \ m^3/h \qquad (3.1)$$

RD = relative density of the liquid in relation to density of water 1 000 kg/m³.
K_v varies between 0 (fully open) and K_{vs} (fully open). K_{vs} is determined by the size of the valve and therefore varies for different sizes (see table below).
The flow coefficient is then expressed as in formula 3.2:

$$K_v = f_v \cdot K_{vs} \qquad (3.2)$$

F_v varies between 0 (valve fully closed) and 1 (valve fully open) as can be seen in Figure 39.

C_v	0.12	0.2	0.3	0.5	0.75	1.2	2	3	5	7.5	12	20	30	47	70	95	75	120	190	300	290	420	735	1150	1730
K_{vs}	0.1	0.16	0.25	0.4	0.63	1.0	1.6	2.5	4.0	6.3	10	16	25	40	60	80	63	100	160	260	250	360	630	1000	1500
NPS / DN																									
½ / 15	•	•	•	•	•	•	•	•	•																
¾ / 20	•	•	•	•	•	•	•	•	•	•															
1 / 25	•	•	•	•	•	•	•	•	•	•	•														
1½ / 40			•	•	•	•	•	•	•	•	•	•	•												
2 / 50			•	•	•	•	•	•	•	•	•	•	•	•											
2½ / 65													•	•	•										
3 / 80													•	•	•	•		•1)							
4 / 100																	•	•	•						
6 / 150																	•	•	•	•					
8 / 200																		•	•		•	•	•		
10 / 250																		•	•		•	•	•	•	
12 / 300																			•		•	•	•	•	•

1) With 19 mm overtravel (not with bellows seal)

Figure 39: K_{vs} values of control valves: Samson Type 3241 Globe Valve [40]

For simplicity for stable valve control, a valve pressure drop can be assumed at design flow rate equal to approx. 80% of the pressure drop over the remaining part of the branch (supply distribution + drum + return distribution). The valve is then dimensioned so that it is open to a maximum of 90% in the event of the pressure drop [41].

Three-way valve
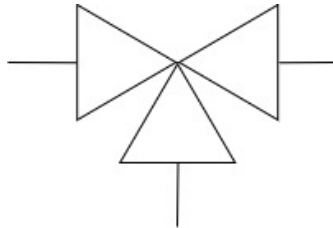
Figure 40: Symbol three-way valve

A three-way tap makes it possible to connect different water flows. In our installation there will be a mixture of waste water coming from machine A (30 °C) with tap water (4 °C) to arrive at cooling water (12 °C) in order to cool the drums of machine B.

3.3 Selecting hydraulic balancing components

For a good balancing of this system, control valves, flow regulators, and self-operating back pressure regulators will be used and selected for the design (as can be seen in the design scheme).

3.3.1 Selecting flow regulator – Hydromat QTR

Function:

They are designed for use in heating or cooling systems to maintain a constant flow within a necessary proportional band. To achieve the set nominal flow, a minimum differential pressure of about 200 mbar is required. The required flow is set at the scale. The diaphragm will hold the differential pressure at a constant rate by moving the valve disc; therefore the mass flow will not exceed the nominal value.

Specification:

The flow regulator "Hydromat QTR" for a constant control of the set flow rate is a proportional regulator which works without auxiliary energy. The nominal value which is visible from outside can be infinitely adjusted, locked and secured with a lead seal. With isolating facility and ball valve for draining and filling, installation in the supply or return pipe, oblique pattern.

Figure 41: Left: Hydromat QTR, right: Hydromat QTR illustrated section [42]

Installation:

As already mentioned above, the flow regulator can be installed in either the supply or the return pipe. Installation is possible in any position provided the direction of flow conforms to the direction of the arrow on the valve body. The pipework has to be flushed thoroughly before installation of the flow regulator [42].
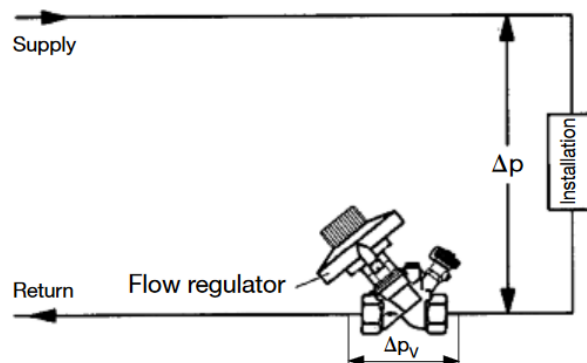
Figure 42: Example installation Hydromat QTR [42]

The characteristic of a circuit with and without flow regulator are illustrated here. In case of overload, the flow rate only slightly exceeds the design value ($q_{mDesign} = q_{mmax}$).
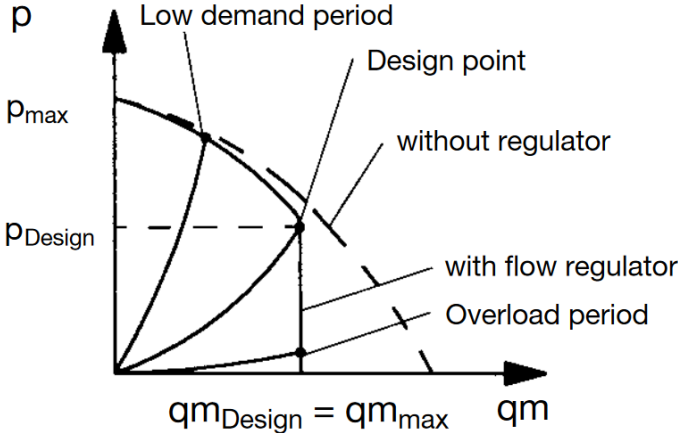
Figure 43: Circuit flow with and without flow regulator [42]

Technical data:

Table 7: Technical data Hydromat QTR [42]

Max. operating pressure ps	10 bar (PN 16)
Max. differential pressure Δpv	2 bar
Operating temperature ts	-10 °C up to +120 °C
Flow ranges	DN 15: 100 – 800 kg/h
	DN 20: 100 – 1200 kg/h
	DN 25: 200 – 1900 kg/h
	DN 32: 300 – 3000 kg/h
	DN 40: 400 – 4000 kg/h

K_{vs} value flow regulator:
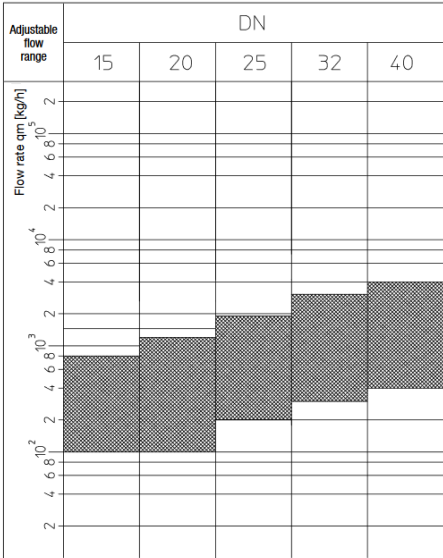
Figure 44: Adjustable flow values at "Hydromat QTR", flow regulation for application range between 40 kg/h and 400 kg/h [36]

Example flow regulator

Required: Size "Hydromat QTR" + differential pressure of regulator p_q

Given:
Flow rate circuit: q_m = 1 000 kg/h
Existing differential pressure of circuit: p_0 = 300 mbar
Differential pressure of system: p = 100 mbar

Solution:
Size "Hydromat QTR" = DN 20 (taken from pressure loss charts [42])
Accordioning to the charts, the minimum regulator size is chosen for q_m = 1 000 kg/h.
The flow regulator has to be set to 1 000 kg/h.
The differential pressure of the regulator, see equation 3.3:

$$p_q = p_0 - p \tag{3.3}$$

$$p_q = 300 - 100$$
$$p_q = 200 \ mbar$$
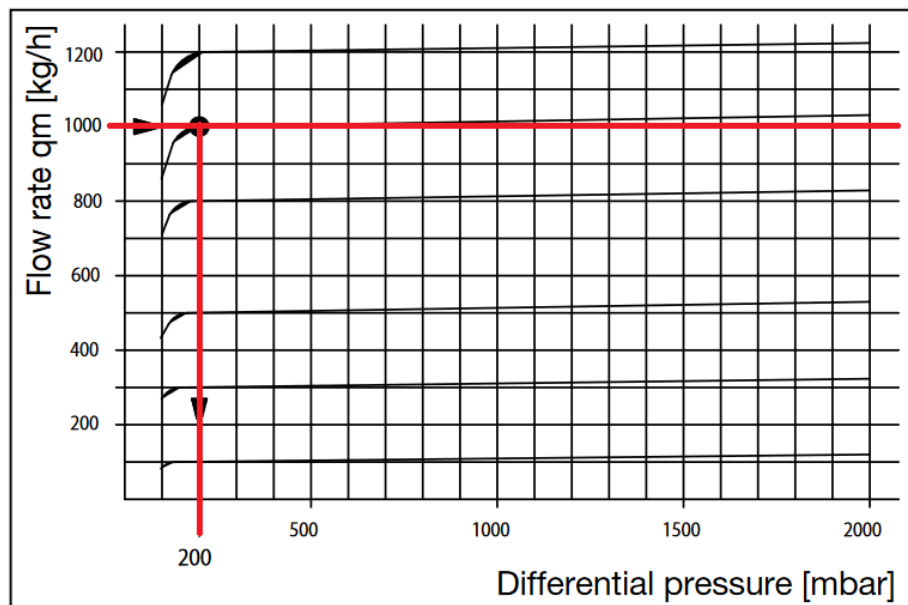
Figure 45: Chart example flow regulator [42]

3.3.2 Selecting back pressure regulator – Hydrocontrol VTR

As already mentioned before, a back pressure regulator is a device that maintains a defined pressure upstream of itself (at its own inlet). When fluid pressure exceeds the set point the valve opens more to relieve the excess pressure. Back pressure regulators work similarly to relief valves, but the emphasis is on steady state pressure control instead of on/off actuation [43].

Function:
Regulating and commissioning valves are installed in the pipework of hot water central heating and cooling systems and serve to achieve a hydronic balance between the different circuits of the system. The balance is achieved by a presetting with memory lock. The required presetting values can be obtained from flow charts in technical datasheets. All intermediate values are infinitely adjustable. The selected presetting can be read off two scales (basic and fine setting scale). The double regulating and commissioning valves have two threaded ports which can be fitted with fill and drain ball valves or pressure test points for differential pressure measurement. The double regulating and commissioning valves may be installed in either the supply or the return pipe. When installing the valve it must be ensured that the direction of flow conforms to the direction of the arrow on the valve body and that the valve is installed with a minimum of L = 3 x Ø of straight pipe at the valve inlet and of L = 2 x Ø of straight pipe at the pipe outlet. The flow charts from the technical datasheets are valid for both, installation in the supply or the return pipe, provided the direction of flow conforms to the arrow on the valve body. Note that in cooling systems using mixtures of water and glycol, the correction factors related to the indicated chart values have to be taken into consideration (which will not apply to us).

Specification:
The selected double regulating and commissioning valve, both ports female thread according to EN 10226, are not suitable for steam. It has colour rings for marking of supply and return pipe. The oblique pattern with secured, infinitely adjustable fine presetting is controllable at any time. Optical display of the presetting depending on the position of the handwheel. The valve body and bonnet is made of bronze, disc and stem are made of brass resistant to dezincification (DZR), disc with PTFE seal, maintenance-free stem seal due to double O-ring. All the functional components in one plane. Pressure test point and fill and drain ball valve interchangeable [44].

Figure 46: Double regulating and commissioning valve "Hydrocontrol VT" [44]

Installation:
It can be installed either in the supply or return pipe.
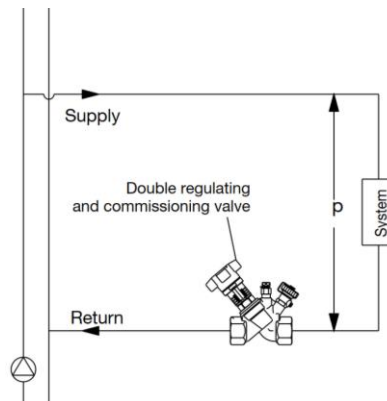
Figure 47: Installation double regulating and commissioning valve [44]

The characteristic lines of a circuit with and without double regulating and commissioning valve as well as the shifting of the characteristic lines caused by the influence of a differential pressure regulated pump are illustrated in the figure below. It can be seen that in the design the flow in the circuit is reduced by using double regulating and commissioning valves, i.e. the flow in each circuit can be regulated by carrying out presetting. If the installation is overloaded, e.g. by completely opened radiator valves, the differential pressure in the circuit is only increased slightly. The supply of the other circuits is still guaranteed. Periods of low demand, i.e. with ip increasing via the installation, the double regulating and commissioning valve only has a slight effect on the characteristic line of the circuit.
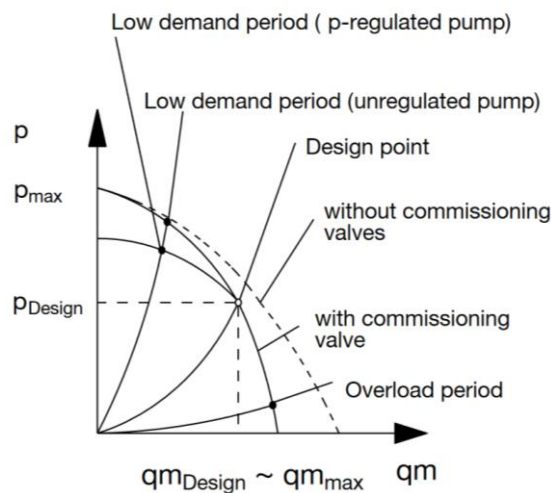
Figure 48: The design flow in the circuit, reduced by using double regulating and commissioning valves [44]

Technical data:

Table 8: Technical data Hydrocontrol VTR [44]

Max. operating temperature t_s	150 °C (press connection: 120 °C)
Min. operating temperature t_s	-20 °C
Max. operating pressure p_s	25 bar (PN 25)
	16 bar (PN 16)

K_v value back pressure regulator:
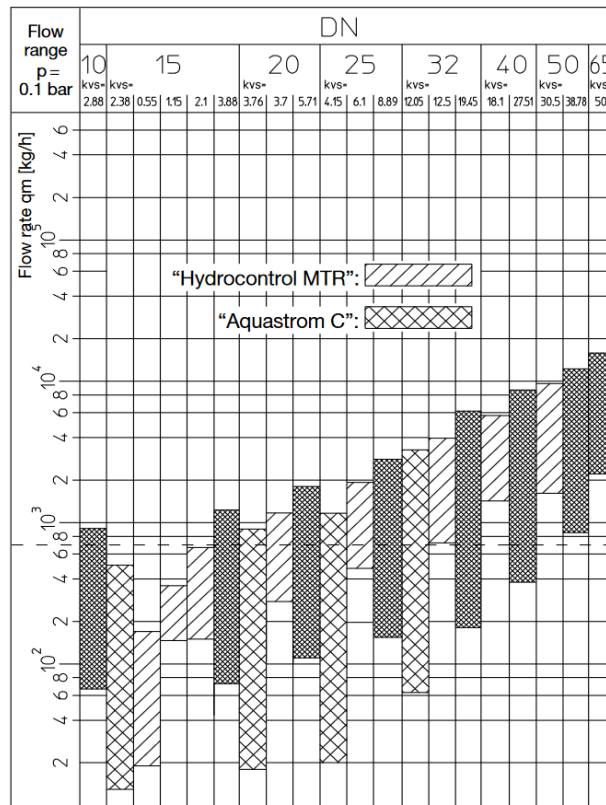
Figure 49: Flow balancing via double regulating and commissioning valves. Regulation according to pipework calculation or by using an ip measuring gauge [36]

Example back pressure regulator
Required:
Presetting "hydrocontrol VTR"

Given:
Flow rate circuit: Q_m = 2 000 kg/h ≈ 0,56 l/s
Differential pressure valve: p_v = 100 mbar
Valve size: DN 25

Solution:
Presetting 5.0 (taken from figure below)
K_v – value = 6,72
Zeta value = 20

DN 25
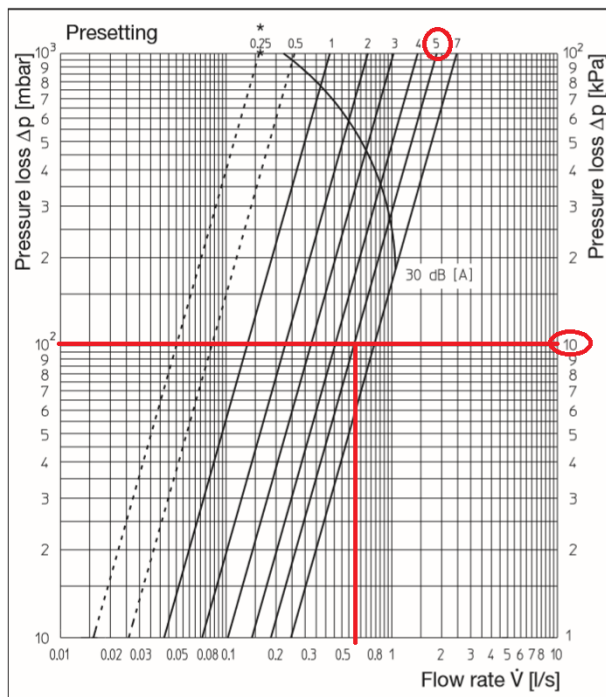
Turns	k_v value	Zeta value	Turns	k_v value	Zeta value	Turns	k_v value	Zeta value
0.25	0.57	2774						
0.5	0.93	1042						
0.75	1.22	605						
1.	1.52	390	5.	6.72	20			
1.1	1.64	335	5.1	6.84	19			
1.2	1.76	291	5.2	6.96	19			
1.3	1.87	258	5.3	7.08	18			
1.4	1.98	230	5.4	7.20	17			
1.5	2.08	208	5.5	7.32	17			
1.6	2.18	190	5.6	7.44	16			
1.7	2.28	173	5.7	7.56	16			
1.8	2.38	159	5.8	7.68	15			
1.9	2.48	147	5.9	7.80	15			
2.	2.58	135	6.	7.91	14			
2.1	2.67	126	6.1	8.02	14			
2.2	2.77	117	6.2	8.12	14			
2.3	2.87	109	6.3	8.22	13			
2.4	2.98	101	6.4	8.31	13			
2.5	3.09	94	6.5	8.41	13			
2.6	3.20	88	6.6	8.51	12			
2.7	3.31	82	6.7	8.61	12			
2.8	3.43	77	6.8	8.71	12			
2.9	3.56	71	6.9	8.80	12			
3.	3.69	66	7.	8.89	11			
3.1	3.82	62						
3.2	3.96	57						
3.3	4.11	53						
3.4	4.26	50						
3.5	4.42	46						
3.6	4.57	43						
3.7	4.72	40						
3.8	4.87	38						
3.9	5.02	36						
4.	5.16	34						
4.1	5.32	32						
4.2	5.47	30						
4.3	5.63	28						
4.4	5.79	27						
4.5	5.95	25						
4.6	6.10	24						
4.7	6.26	23						
4.8	6.42	22						

Figure 50: Presetting and solution example "Hydrocontrol VTR" [36]

3.3.3 Selecting filter

Function:

The dirt separator separates off the impurities circulating within the system closed circuits. The impurities are collected in a large collection chamber, that requires low frequency cleaning procedures, from which they can be removed even while the system is in operation. Versions fitted with a magnet are designed for the separation of ferrous impurities [45]. Filter type 5466 is selected because we assume the size of the pipes in an industrial application will have a range from DN 50 - DN 300.

Figure 51: Water filter type 5466 [45]

Operating principle:

The dirt separator operating principle is based on the combined action of a number of physical phenomena. The internal element (1) consists of a set of radial reticular surfaces. The impurities in the water, on striking these surfaces, get separated, dropping into the bottom of the body (2) where they are collected. In addition, the large internal volume slows down the flow speed of the medium thus helping, by gravity, to separate the particles it contains. The collected impurities are discharged, even with the system running, by opening the drain cock (3); this procedure can even be performed while the system is in operation. The dirt separator is designed in such a way that the direction in which the medium is flowing inside makes no difference [45].
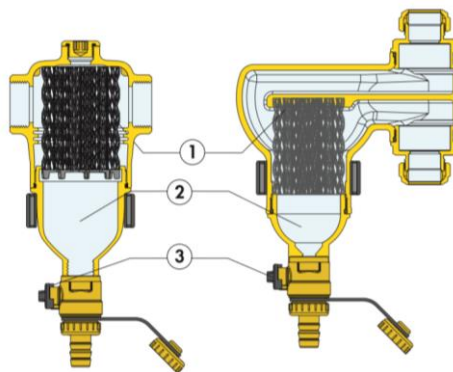
Figure 52: Operating principle water filter [45]
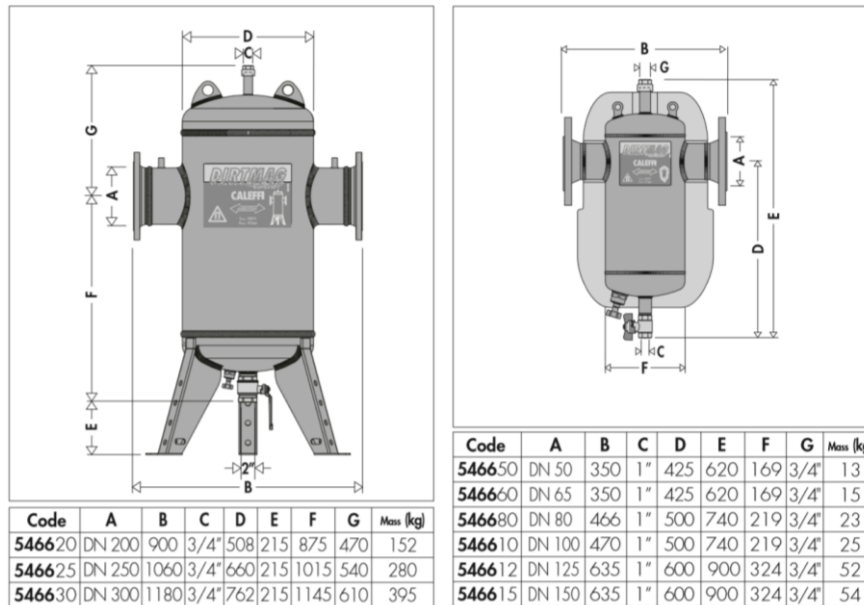
Figure 53: Technical sketch filter type 5466 flanged (DN 50 – DN 300) [45]

Filter volume:

Table 9: Volumes filter type 5466 [45]

Size	DN 50	DN 65	DN 80	DN 100	DN 125	DN 150	DN 200	DN 250	DN 300
Volume (l)	7	7	18	18	52	52	211	415	639

Technical performance specifications:

Table 10: Technical performance specifications filter type 5466 [45]

Medium	Water, non-hazardous glycol solutions
Max. working pressure	10 bar
Working temperature range	0 – 100 ℃
Particle separating rating	Down to 5 μm
Magnetic induction of magnet	DN 50 – 65: 7 x 0,475 T
	DN 80 – 150: 12 x 0,475 T
	DN 200 – 300: 3 x 17 x 0,475 T

Pressure losses:

When the pipe diameters are dimensioned, the pressure losses of the filter can be determined by using the following scheme:
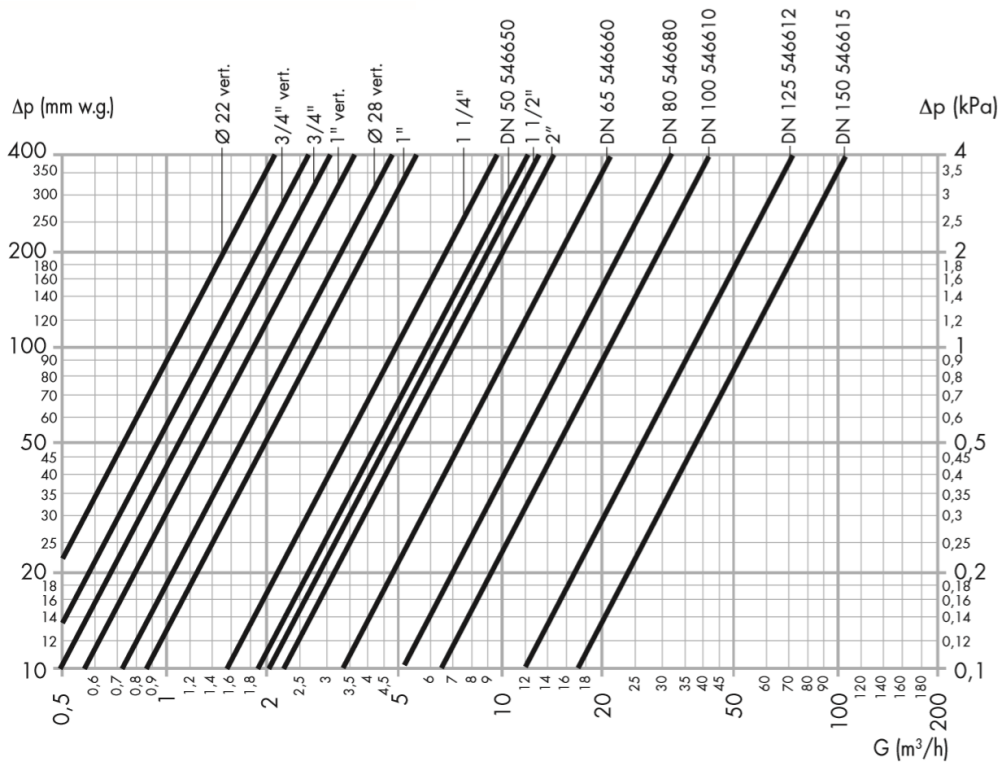
Figure 54: Hydraulic characteristics water filter [45]

Kv value filter:

Table 11: Kv value water filter [45]

DN	DN 50	DN 65	DN 80	DN 100	DN 125	DN 150	DN 200	DN 250	DN 300
Kv (m³/h)	60,5	110	160	216	365	535	900	1200	1500

Installation:

The filter can be easily installed after the centrifugal pumps as can be seen in the design scheme.

3.3.4 Selecting control valve

Function:

The brass ball valve is opened/closed by turning the lever/handle by 90°. The position of the ball is indicated by the position of the lever or handle which moves parallel to the ball. If the lever or handle is removed, the stem with two flats still indicates the position of the ball [46].

Figure 55: Brass ball valves with full flow [46]

Specification:

The selected brass ball valves "Optibal" with full flow can be used in industrial, commercial and domestic installations for the isolation of pipes transporting fluids. Depending on the model, they may be used for the following fluids: water, mineral, heating, hydraulic and diesel oil and air [46].

Installation:

The ball valves (or valves) are mainly placed around pumps and collectors, in order to be able to close them and, if necessary, carry out maintenance on them. Some smaller pumps are equipped with valves as standard [46].

Technical data:

Table 12: Technical data brass ball valve "Optibal" [46]

Max. operating pressure p_s	16 bar at 70 °C
	12 bar at 85 °C
	8 bar at 100 °C
Operating temperature t_s	-10 °C up to +100 °C

K$_{vs}$ value:

Once we dimensioned the distribution pipes we can use the table below to find the K$_{vs}$ value. The flow values may vary due to the different screw-in depths of the threaded pipes into the ball valve and a not fully opened switching ball.

Table 13: Flow values ball valves [46]

DN	K$_{vs}$
8	5,6
10	8,8
15	22
20	43
25	67
32	99
40	143
50	254
65	470
80	720
100	1120

3.3.5 Selecting three-way valve

Function:

For use as mixing valve, the three-way diverting and mixing valve "Tri-CTR" has two inlet ports (A and B) and one outlet port (AB). Depending on the position of the regulating sleeve, the cold (the tap water) and hot water (our waste water) is mixed. For use as diverting valve, the three-way valve has one inlet port (AB) and two outlet ports (A and B). Depending on the position of the regulating sleeve, the direction of flow is diverted from one to the other outlet port [47].
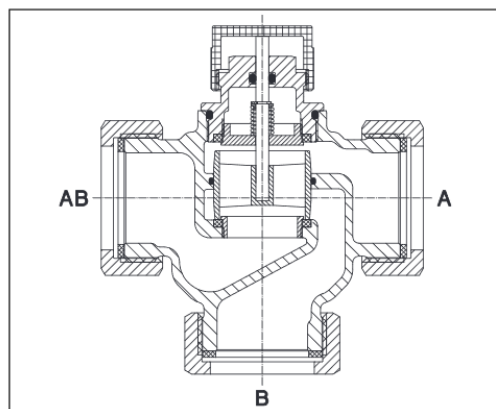
Figure 56: Illustrated section three-way valve [47]

Technical data:

Table 14: Technical data three-way valve [47]

Max. operating temperature t$_s$	120 °C
Min. operating temperature t$_s$	-10 °C
Max. operating pressure p$_s$	16 bar

K_{vs} value:

Size	DN 15	DN 20	DN 25	DN 32	DN 40	DN 50
K_{vs} value	2.5	4.4	5.7	7.2	8.5	10.0
Max. differential pressure [bar]	3	2	1	1	1	0.75

Installation:
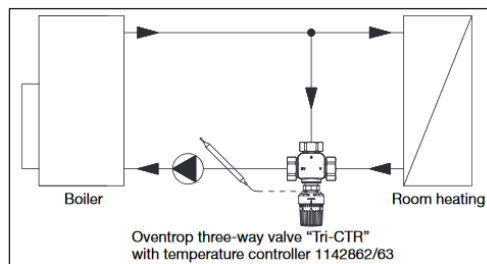
Figure 57: System illustration of the three-way valve as mixing valve [47]

Pressure loss:

The pressure losses of the three-way valve can be calculated used the following diagram.
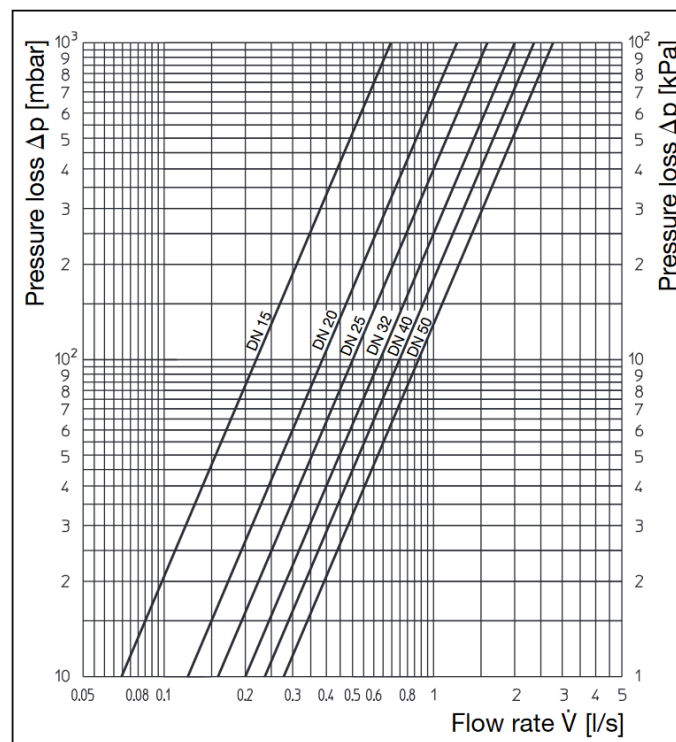
Figure 58: Pressure loss diagram three-way valve [47]

3.4 Other engineering components

Through a pumping system (closed system) we will use the waste water from machine a to cool the drums in machine b. In this section of the master's thesis we will discuss the other technical components besides the hydraulic ones we use to design the installation that ensures that we have less wastewater. The closed system will be designed in the most (energy) efficient way possible (important when selecting the pumps).

Circulation pumps
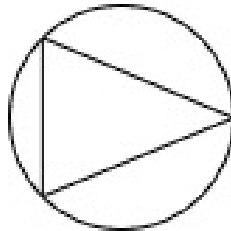
Figure 59: Symbol circulation pump

A circulation pump is a specific type of pump used to circulate gases, liquids, or slurries in a closed circuit. These pumps are commonly found circulating water in a hydronic heating or cooling system. Because they only circulate liquid within a closed circuit, they only need to overcome the friction of a piping system (this is the reason we need to calculate the friction of our piping system).
In industrial applications they range in size up to many horsepower and the electric motor is usually separated from the pump body by some form of mechanical coupling. In this application we will use electrically powered centrifugal pumps for transporting the water.

As from 1 January 2013, circulators must comply with European regulation 641/2009. This regulation is part of the ecodesign policy of the European Union [48]. So keep in mind when selecting the circulator, it will have to comply with the proposed standards.

Efficiency circulation pumps

The efficiency for conversion from electrical power to mechanical drive power can be calculated by equation 3.4:

$$\eta_{el \to mech} = \eta_{mot,N} \; x \; \alpha_{load\%} \; x \; \alpha_{VFD} \tag{3.4}$$

η_{motn} is the motor efficiency at nominal speed and nominal load (100%), $\alpha_{load\%}$ is a correction factor for partial load operation and α_{VFD} is a correction factor due to variable frequency drive (VFD). The nominal efficiency of electric motors depends on the type of construction, number of pole pairs, mains frequency and power.

The minimum value is defined by the efficiency class (IEC 6003430-1:2014). The table below shows the minimum efficiency values for 2-pole and 4-pole induction motors at 50Hz from IE3 efficiency category ("Premium efficiency"). We will assume the correction factor for partial load operation $\alpha_{load\%}$ on one.

$\dfrac{\dot{W}_{mech,N}}{kW}$	1,1	1,5	2,2	3,0	4,0	5,5	7,5	11,0	15,0	18,5	22,0	30,0
$\dfrac{\eta_{mot,N}^{2-pole}}{\%}$	82,7	84,2	85,9	87,1	88,1	89,2	90,1	91,2	91,9	92,4	92,7	93,3
$\dfrac{\eta_{mot,N}^{4-pole}}{\%}$	84,1	85,3	86,7	87,7	88,6	89,6	90,4	91,4	92,1	92,6	93,0	93,6

The correction factor for variable speed control α_{VFD} can be approximated according to the values in the table below. Efficiency correction factors for variable speed controllers without VFD has an $\alpha_{VFD} = 1$.

Table 17: Idealized VDF Efficiency Factor (Motor Plus VFD Controller) that ignores motor duty-point movement [52]
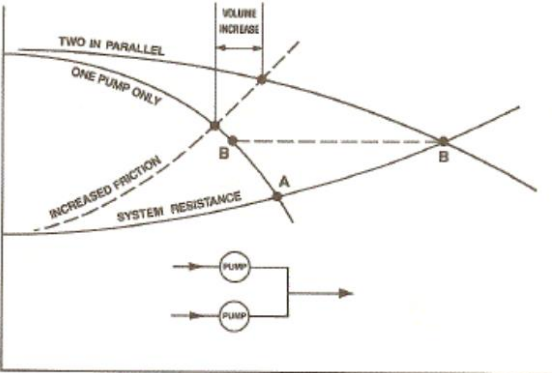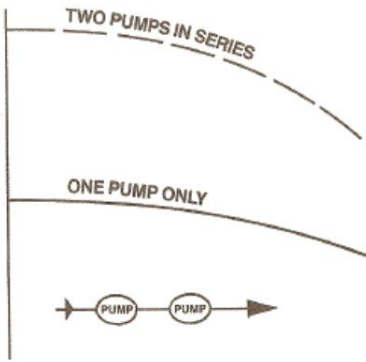
α_{VFD}	
Rated motor frequency (%)	VFD efficiency factor
100	0,97
90	0,945
80	0,92
70	0,9
60	0,875
50	0,85
40	0,825

Parallel operation of centrifugal pumps

In order to increase the volumetric flow rate in a system, to compensate losses or to have more flexibility, centrifugal pumps can be installed parallel or in series.

Parallel operation of centrifugal pumps is used to increase flow rate through the system. Pumps operating in parallel take their suction from a common header and discharge into a common discharge. While head changes only slightly, flow is almost doubled at any given point. The table below shows some things that must be taken into account when installing a centrifugal pump in parallel or series.

Table 18: Things to consider when you connect pumps in parallel or series [53]

Parallel operation	Series operation
Figure 60: Parallel operation centrifugal pumps [49]	Figure 61: Series operation centrifugal pumps [49]
Centrifugal pumps in parallel are used to overcome larger volume flows than one pump can handle alone [50].	Centrifugal pumps in series are used to overcome larger system head loss than one pump can handle alone [50].
- Both pumps must produce the same head this usually means they must be running at the same speed, with the same diameter impeller. - Two pumps in parallel will deliver less than twice the flow rate of a single pump in the system because of the increased friction in the piping. - The shape of the system curve determines the actual increase in capacity. If there is additional friction in the system from throttling (see dotted line in the following diagram), two pumps in parallel may deliver only slightly more than a single pump operating by its self. - If you run a single pump only, it will operate at a higher flow rate (A) than if it were working in parallel with another pump (B) because it will be operating further out on the curve requiring increased power. The rule is that if a pump is selected to run in parallel, be sure it has a driver rated for single operation.	- Both pumps must have the same width impeller or the difference in capacities could cause a cavitation problem if the first pump cannot supply enough liquid to the second pump. - Both pumps must run at the same speed. - Be sure the casing of the second pump is strong enough to resist the higher pressure. Higher strength material, ribbing, or extra bolting may be required. - The stuffing box of the second pump will see the discharge pressure of the first pump. You may need a high-pressure mechanical seal. - Be sure both pumps are filled with liquid during start-up and operation. - Start the second pump after the first pump is running.

It can be concluded that parallel pumps are notorious for operating at different flows. In this case the pumps will be used to overcome larger volume flows and have more flexibility than one pump can handle alone or than pumps connected in series. It must be noted the volumetric flow rate is actually less than twice the flow rate achieved by using a single pump. This is caused by a larger system head loss resulting from higher flow rate [51].
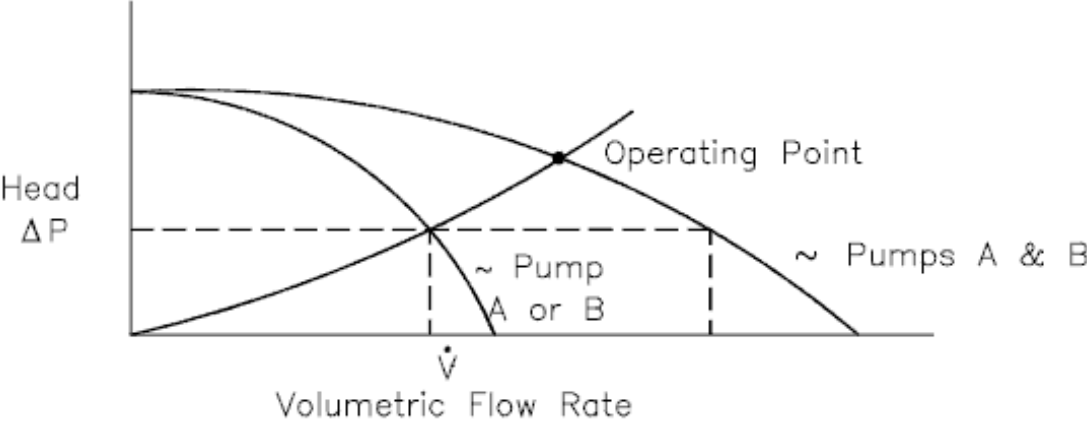
Figure 62: Parallel operation centrifugal pump [49]

Cavitation

Cavitation is something that must always be taken into account when dimensioning/selecting a circulation pump, especially using centrifugal pumps. Cavitation occurs when air bubbles are generated inside a pump because of the partial pressure drop of the flowing liquid, resulting in a cavity at the relevant part. Changes in pressure inside the pump turn the liquid into vapor and, as the pump's impellers spin, back to liquid again. The air bubbles move, pressure is increased and the air bubbles instantaneously implode. The collapse of vapor bubbles erodes the impeller surface, and if strong cavitation occurs at the impeller inlet, pump performance decreases, which can lead to pumping failure/damage, loud noises and loss of capacity.

Figure 63: Damage by cavitation in centrifugal pump [52]

When problems with suction cavitation occurs in the system, it can be solved by [52]:
- lowering the temperature;
- reduction of motor RPM if possible;
- increase of the diameter of the eye of the impeller;
- use of an impeller inducer;
- use of two parallel pumps with lower capacity;
- use of a booster pump to feed the principal pump.

To ensure that cavitation does not occur in the pumps in this Master's thesis, the NPSH will be calculated. The net positive suction head (NPSH) is a characteristic value that expresses a pump's suction condition. There are two types of NPSH. NPSHA (net positive suction head available) and NPSHR (net positive suction head required). NPSHA must be equal to or greater than the NPSHR and NPSHR is mostly given by the manufacturer.

The net positive suction head available can be calculated by using equation 3.5:

$$NPSH_a = \frac{p_{atm}}{\rho\, g} - h_s + \frac{c_{1'}^2}{2\,g} - \Delta h_p - \Delta h_m - \frac{p_{vap}}{\rho\, g} \qquad (3.5)$$

P_{atm} is the atmospheric pressure, divided by ρ and g (water density and gravity). $C_{1'}$ is the acceleration we have by the pump. H_p are the losses along the way from the entry of the pipe to the suction of the pump and hm are any minor losses that we have along that distance. P_{vap} is the vapor pressure of the fluid at the current temperature of that liquid.
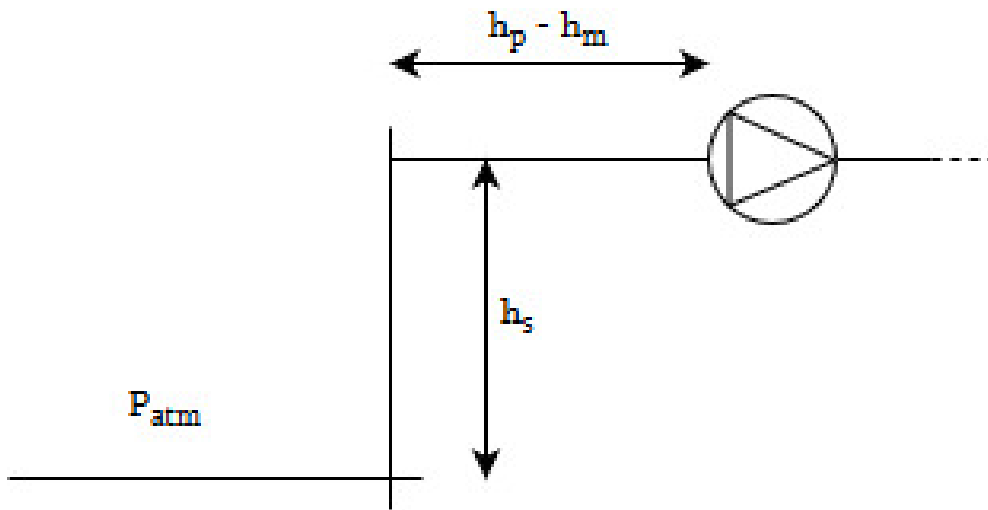
Figure 64: Sketch of NPSH of pumps

After this the value of NPSH$_a$ is compared with the value of NPSH$_r$ given by the manufacturer and one can decide whether cavitation will occur or not, see equation 3.6.

$$NPSH_a > NPSH_r \qquad (3.6)$$

3.4.1 Distribution pipes

Pipes are used to transport the water from machine a to machine b in a closed circuit.
For metal pipes standard sizes are used (diameter nominal (DN), nominal pipe size (NPS)) which define the outer dimensions. For standard wall thicknesses (STD schedule), the corresponding internal diameters are given in the following table.

Table 19: Standard diameters for metal pipes with standard thickness [41]

DN	15	20	25	32	40	50	65	80	100	125	150	200	250	300
NPS	0,5"	0,75"	1"	1,25"	1,5"	2"	2,5"	3"	4"	5"	6"	8"	10"	12"
D_{out}/mm	21,3	26,7	33,4	42,2	48,3	60,3	73,0	88,9	114,3	141,3	168,3	219,1	273,1	323,9
t/mm	2,8	2,9	3,4	3,6	3,7	3,9	5,2	5,5	6,0	6,5	7,1	8,2	9,3	9,5
D_{in}/mm	15,7	20,9	26,6	35,0	40,9	52,5	62,6	77,9	102,3	128,1	154,1	202,7	254,5	304,9

The pipe diameters can be calculated more easily by assuming some statements. For larger conveying lines, the speed is kept below 3.5 m/s. For smaller distribution lines, the speed is kept below 3 m/s. For suction lines of centrifugal pumps, the speed shall be kept below 2 m/s [41].

Insulation

We can isolate the circulation pipe and the tap water pipes of the installation, thereby reducing external temperature influences. The heat loss to the environment is limited and there is a more constant temperature of the cooling water. It will be necessary to check whether the cost of insulation outweighs the energy gain and how closely a temperature deviation is permitted in order to improve the quality of the insulation.

Legionella

The risk of legionella increases in summer. During the holiday period, or in the event of machine downtime, water stays in the pipes for longer so that the installation can become an ideal breeding ground for the dangerous bacteria. In our application we have water between 10℃ and 30℃. With water from 20 to 50 °C it is able to grow, below 25 °C (ideally below 20 °C) and above 60℃, there is almost no growth anymore, as can be seen in the table below. Legionella does not necessarily have to be taken into account in this project.

Table 20: Temperature affects the survival of Legionella [53]

Temperature affects the survival of Legionella as follows	
Above 70 °C	Legionella dies almost instantly
At 60 °C	90% die in 2 minutes (Decimal reduction time (D) = 2 minutes)
At 50 °C	90% die in 80 – 124 minutes, depending on strain (D = 80 – 124 minutes)
48 to 50 °C	Can survive but do not multiply
32 to 42 °C	Ideal growth range
25 to 45 °C	Growth range
Below 20 °C	Can survive, even below freezing, but are dormant

3.4.2 Hydraulic losses

Also hydraulic losses must be taken into account when dimensioning an closed pumping circuit. The length losses are called hydraulic losses and can be calculated from formula 3.7:

$$\Delta p = f \frac{L}{D} \frac{1}{2} \rho C^2 \qquad (3.1)$$

In this formula, f is the Darcy-Weisback friction factor (/), L (m) is the length and D (m) is the diameter of the pipes. The density of water is represented by the symbol ρ (kg/m³) and C is the mean flow rate of the fluid (m/s). Darcy-Weisbach friction factor f is in function of the Reynolds number Re and the relative roughness ε/D. This function can be calculated according to the Colebrook equation 3.8.

$$R_e = \frac{\rho . C . D}{\mu} \qquad (3.2)$$

This formula is best transformed into an expression with the flow rate. The dynamic viscosity (pa.s) is represented by the symbol μ. Once this calculation has been done for the design flow, f may be considered constant at variable flow [41].

The Darcy coefficient of friction can be found in graphs, the so-called Moody diagrams. For laminar flow conditions, where the Reynolds number Re is less than ± 2000, f can be approximated by equation 3.9:

$$f = \frac{64}{Re} \qquad (3.3)$$

For turbulent flow conditions, where the Reynolds number is greater than ± 4000, f can be searched in Moody Diagrams or approximately calculated using the Colebrook equation, also called Colebrook-White equation 3.10:

$$\frac{1}{\sqrt{f}} = -2 . \log_{10}(\frac{2.51}{Re . \sqrt{f}} + \frac{\varepsilon}{3.7 \, D}) \qquad (3.4)$$

In this equation, ε is the roughness of the pipe. This is an implicit function in f, which means it must be solved using an iterative method, assuming an estimated value of f. This is a difficult and time-consuming calculation, unless it is done with a computer program. We will choose to use the Moody diagram as it is a graphical representation of this equation. For very turbulent flow, with great value of the Reynolds number, the first term of the right section can be neglected and f calculated as a function of the ratio ε/D. This is the area in the Moody diagram where the lines run horizontally.

Moody Diagram:
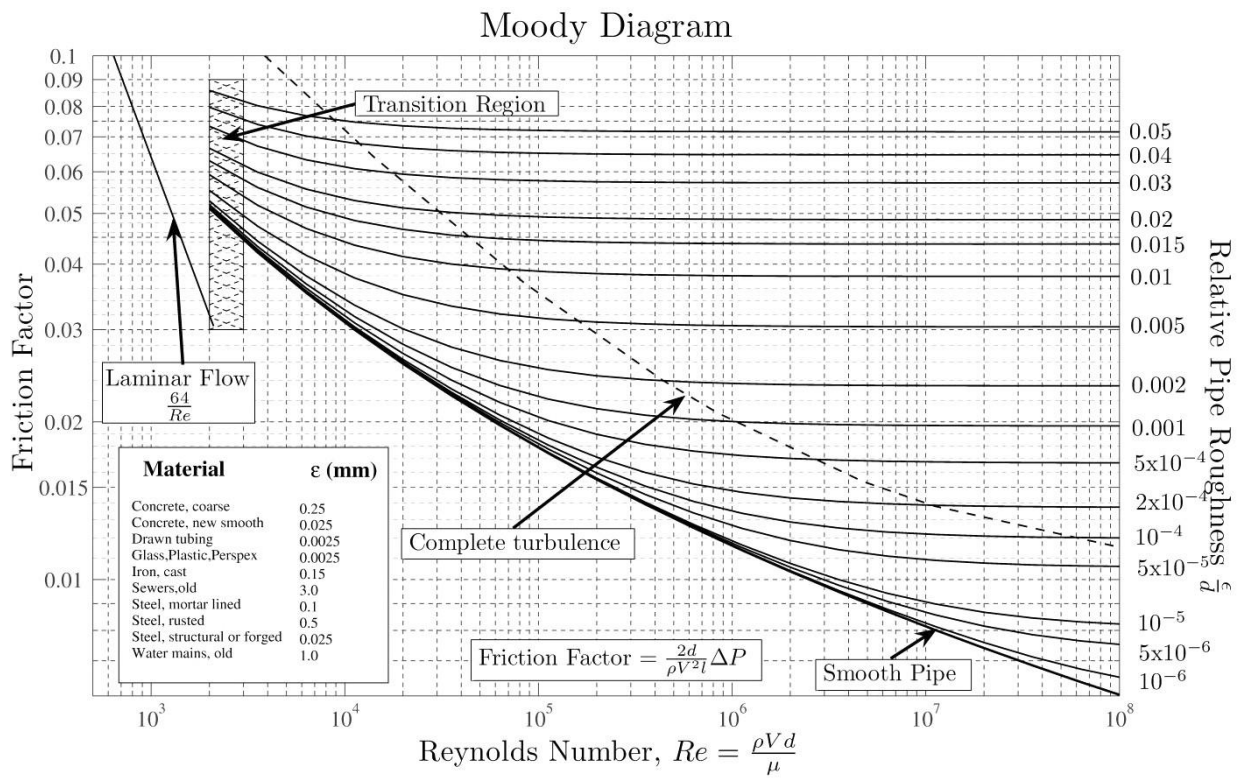
Figure 65: Moody diagram [54]

4   Calculation of case B

4.1   Design data

First we will start by giving a clear overview of our design data. Some data is given by Suomen Kerta itself. If the data is unknown, a realistic estimation is made by us.

Flow rate cooling drums, rotary molding machine and tap water:

Table 21: Flow rate cooling drum, rot. mol. mach. and tap water

Description	Symbol	Flow rate (m³/h)	Flow rate (m³/s)
Cooling drum 1	Q_{cd1}	18	0,005
Cooling drum 2	Q_{cd2}	18	0,005
Cooling drum 3	Q_{cd3}	18	0,005
Rot. Mol. Machine	Q_{RMM}	20	0,005 556
Tap water	Q_{tapw}	37 [55] (for DN 100)	0,010 278

Length of the distribution pipes:

Table 22: Length of the pipes

Description	Symbol	Length (m)	Total length (+ retour) (m)
Suction pipe	L_a	4	Depending on x pumps
Transport pipe	L_b	30	60
Distribution pipe CD1	L_{c1}	10	20
Distribution pipe CD2	L_{c2}	15	30
Distribution pipe CD3	L_{c3}	20	40

Losses occurring in the machines:

Table 23: Losses occurring in the machines

Description	Symbol	Losses (kPa)	Losses (Pa)
Cooling drum 1	p_{ld1}	50	50 000
Cooling drum 1	p_{ld2}	50	50 000
Cooling drum 1	p_{ld3}	50	50 000
Rot. Mol. Mach	p_{lrmm}	30	30 000
Heater	p_{lh}	5	5 000

The other occurring losses in the filter, valves, flow regulators… can be calculated later once the nominal pipe diameters are known.

Other data:

Table 24: Other design data

Description	Symbol	Roughness (mm)	Roughness (m)
Roughness of pipes	ε	0,35	0,000 35

		Temperature (°C)	
Temperature waste water	T_{ww}	30	
Temperature tap water	T_{tw}	4	
Temperature inlet cooling drums	T_{icd}	12	
Temperature outlet cooling drums	T_{ocd}	14	
Temperature after heater	T_h	30	

		Dyn. viscosity (mPa.s) [56]	Dyn. viscosity (Pa.s)
Dynamic viscosity water (30°C)	μ_{30}	0,798	0,000 798
Dynamic viscosity water (12°C)	μ_{12}	0,961	0,000 961
Dynamic viscosity water (14°C)	μ_{14}	0,920	0,000 920
Dynamic viscosity water (4°C)	μ_4	1,573	0,001 573

		Mass density (g/cm³) [56]	Mass density (kg/m³)
Mass density water (30°C)	ρ_{30}	0,995	995
Mass density water (14°C)	ρ_{14}	0,999	999
Mass density water (12°C)	ρ_{12}	0,999	999
Mass density water (4°C)	ρ_4	1	1 000

Assumptions:

Permitted velocities in the pipes		
Description	Symbol	Velocity (m/s)
Larger transmission pipes	C_t	3,5
Smaller distribution lines	C_d	3
Suction lines	C_s	2

Valves	
Loss of valve	80 %
Pressure drop	90 %

4.2 Calculation of pipe diameters

With the above data we can already calculate the pipe diameters, take a standard size for this and therefore also calculate the flow velocities in the pipe.

Flow rates pipes:

Description	Symbol	Flow rate (m³/h)	Flow rate (m³/s)
Flow rate suction pipe La	Q_a	Negligible at first calculations since the pumps and numbers of L_a's are not yet known.	
Flow rate transportation pipe Lb	Q_b	54	0,015
Flow rate distribution pipe Lc1	Q_{LC1}	18	0,005
Flow rate distribution pipe Lc2	Q_{LC2}	18	0,005
Flow rate distribution pipe Lc3	Q_{LC3}	18	0,005
Flow rate tap pipe	Q_{tw}	37	0,010 278

Calculation and standardization nominal pipe diameters:

For the calculation of the nominal pipe diameters, the following formulas (4.1, 4.2 and 4,3) are used:

$$Q = A \cdot c \tag{4.1}$$

$$A = \frac{\pi \cdot D^2}{4} \tag{4.2}$$

$$D = \sqrt{\frac{Q_v \cdot 4}{c \cdot \pi}} \tag{4.3}$$

A is the surface that we use to calculate the diameter D. We know the needed flow rates and the velocities are assumed to be 3,5 m/s for the large transmission pipes and 2 for the distribution smaller pipes.

Description	Symbol	Diameter (m)	Diameter (mm)
Diameter pipe L_a	D_{la}	Negligible at first calculations since the pumps and numbers of L_a's are not yet known.	
Diameter pipe L_b	D_{lb}	0,073 870	74
Diameter pipe L_{c1}	D_{lc1}	0,046 066	46
Diameter pipe L_{c2}	D_{lc2}	0,046 066	46
Diameter pipe L_{c3}	D_{lc3}	0,046 066	46
Diameter pipe L_{tw}	D_{tw}	0,080 889	80,889

For the selection of the standard sizes of pipes, table 17 can be used.
We choose the same diameter for the distribution lines, we will adjust the flow by means of the valves. These data are then taken from table 1 page 4 (appendices). This avoids more constrictions,

which is more practical in terms of installation and therefore practically takes less time and is simpler in terms of ordering.

Description	Symbol	Name pipe	Inner D (mm)	Inner D (m)
Diameter pipe L_a	D_{la}	Negligible at first calculations since the pumps and numbers of L_a's are not yet known.		
Diameter pipe L_b	D_{lb}	DN 100	102,3	0,1023
Diameter pipe L_{c1}	D_{lc1}	DN 50	52,5	0,0525
Diameter pipe L_{c2}	D_{lc2}	DN 50	52,5	0,0525
Diameter pipe L_{c3}	D_{lc3}	DN 50	52,5	0,0525
Diameter pipe L_{tw}	D_{tw}	DN 100	102,3	0,1023

Calculation actual flow rates:

Now that the broad, permitted estimate of the pipe diameters is made, the actual speeds in the pipes can be calculated using formula 4.4.

$$c = \frac{Q}{\frac{\pi \cdot D^2}{4}} \tag{4.4}$$

Table 29: Actual flow rates pipes

Description	Symbol	Velocity pipe (m/s)
Water velocity pipe L_a	C_{La}	L_a not yet invoiced
Water velocity L_b	C_{Lb}	1,825
Water velocity L_{c1}	C_{Lc1}	2,4
Water velocity L_{c1}	C_{Lc2}	2,4
Water velocity L_{c1}	C_{Lc3}	2,4
Water velocity L_{tw}	C_{tw}	1,250

4.3 Calculation hydraulic losses

4.3.1 Hydraulic pressure losses in the pipes

As now the flow rates, water velocities and nominal diameter of the pipes are known, a calculation of the hydraulic losses in the pipes can be made and the hydraulic losses in the used components can be extracted from the graphs. The hydraulic losses of the tap water pipe will not be calculated as there is no idea at all where the factory has the possibility to take tap water and use it to mix it with the waste water.

The Reynolds number and the relative roughness can be calculated. With these 2 data we can then determine the friction factor using the Moody diagram. When we have the friction factor we can calculate the hydraulic losses. It is also possible to calculate the friction factor using Colebrooks formula.

Colebrooks equation can be described as follows, the same formula as in 3.8:

$$Re = \frac{\rho \cdot C \cdot D}{\mu} \tag{4.5}$$

C is the velocity in the relevant pipe, D is the diameter of that pipe. Table 24 is used to know the mass density (ρ) and the dynamic viscosity (μ) of the water at that particular temperature.

Table 30: Reynolds number in the pipes

Description	Symbol	Reynolds number (/)
Reynolds number pipe L_a (30 °C)	Re_{La}	L_a not yet invoiced
Reynolds number pipe L_b (30 °C)	Re_{Lb}	233 013,742
Reynolds number pipe L_{c1} (12 °C)	Re_{Lc1}	126 055,825
Reynolds number pipe L_{c1} (12 °C)	Re_{Lc2}	126 055,825
Reynolds number pipe L_{c1} (12 °C)	Re_{Lc3}	126 055,825

Remember that for laminar flow conditions, where the Reynolds number Re is less than ± 2000, f (Darcy coefficient of friction) can be approximated by formula 7.8. For turbulent flow conditions, where the Reynolds number is greater than ± 4000, f can be searched in Moody Diagrams or approximately calculated using the Colebrook equation, also called Colebrook-White equation formulated in formula 7.10. In this case the Moody diagram is used and gives us the following results given in table 31. First ε/D is calculated (ε is given (0,0035) and D is calculated before:

Table 31: Calculation relative pipe roughness ε/D

Description	Symbol	Relative pipe roughness $\frac{\varepsilon}{D}$
Relative pipe roughness L_a (30 °C)	$(\varepsilon/D)_{La}$	L_a not yet invoiced
Relative pipe roughness L_b (30 °C)	$(\varepsilon/D)_{Lb}$	0,003 421
Relative pipe roughness L_{c1} (12 °C)	$(\varepsilon/D)_{Lc1}$	0,006 667
Relative pipe roughness L_{c2} (12 °C)	$(\varepsilon/D)_{Lc2}$	0,006 667
Relative pipe roughness L_{c3} (12 °C)	$(\varepsilon/D)_{Lc3}$	0,006 667

With the use of the Moody diagram, f can be extracted:

Table 32: F extracted from Moody diagram

Description	Symbol	Friction factor
Friction factor pipe L_a (30 °C)	f_{La}	L_a not yet invoiced
Friction factor pipe L_b (30 °C)	f_{Lb}	0,027
Friction factor pipe L_{c1} (12 °C)	f_{Lc1}	0,0323
Friction factor pipe L_{c2} (12 °C)	f_{Lc2}	0,0323
Friction factor pipe L_{c3} (12 °C)	f_{Lc3}	0,0323

Finally, the hydraulic losses in the pipes can be calculated using equation 3.7.

Table 33: Hydraulic losses pipes

Description	Symbol	Pressure loss (Pa)	Pressure loss (kPa)
Pressure loss L_a (30 °C)	Δp_{ILa}	L_a not yet invoiced	
Pressure loss L_b (30 °C)	Δp_{ILb}	274,589	0,274 589
Pressure loss L_{c1} (12 °C)	Δp_{ILc1}	90,375	0,090 375
Pressure loss L_{c2} (12 °C)	Δp_{ILc2}	135,563	0,135 563
Pressure loss L_{c3} (12 °C)	Δp_{ILc3}	180,751	0,180 751

4.3.2   Pressure losses in the components

Pressure loss filter
The pressure loss of the filter can be extracted from the graph shown in Figure 56.
DN 100 and Q_b = 39 m³/h
Kv value filter = 216

Pressure loss filter Δp_{lf} = 4,5 kPa.

Pressure loss back pressure regulators – Hydrocontrol VTR
Pressure loss back pressure regulator Δp_{lkbp} = 20 kPa.

Pressure loss three-way valves
The pressure loss of the three-way valves can be calculated using figure 63.
Pressure loss three-way valve Δp_{l3wv} = 100 kPa

Pressure loss cooling drums:
Because Suomen Kerta don't know the pressure loss of the cooling drums, we assume it to be 50 kPa as an realistic value.

Table 34: Pressure loss cooling drums

Description	Symbol	Pressure loss (Pa)	Pressure loss (kPa)
Pressure loss Cooling Drum 1	Δp_{ld1}	50 000	50
Pressure loss Cooling Drum 2	Δp_{ld2}	50 000	50
Pressure loss Cooling Drum 3	Δp_{ld3}	50 000	50

4.3.3   Determining the position of the valves

As we don't know the pressure loss of the flow regulators, we mentioned before that for simplicity a valve pressure drop can be assumed at design flow rate equal to approx. 80% of the pressure drop over the remaining part of the branch (supply distribution + drum + return distribution). The valve is then dimensioned so that it is open to a maximum of 90% in the event of the pressure drop [41]. If we apply this theory, we need the hydraulic losses in the supply and return distribution and in the drums. Those losses are calculated before.

The hydraulic losses in the pipes are calculated and can be found in table 33. The losses occurring in the cooling drums are given and can be found in table 34. Following formula 4.6 can be used to calculate the hydraulic losses from the valves.

$$\Delta p_{lk1...3} = \Delta p_{lc1...3} + \Delta p_{ld1...3} \tag{4.6}$$

The results are given in table below:

Table 35: Pressure loss flow regulator valves

Description	Symbol	Pressure loss (Pa)	Pressure loss (kPa)
Pressure loss valve 1	Δp_{lk1}	40 072,300	40,072
Pressure loss valve 1	Δp_{lk2}	40 108,451	40,108
Pressure loss valve 1	Δp_{lk3}	40 144,600	40,145

Once the hydraulic pressure losses in the valves are known, the K_v value of the valves can be calculated using formula 3.1 where $Q_{cd1...3}$ = 18 m³/h, RD_{H2O} = 1 000 kg/m³ and the pressure losses from the flow regulators are given in table 35.

Table 36: K_v value flow regulator valve

Description	Symbol	K_v [/]
K_v valve 1	K_{v1}	28,435
K_v valve 2	K_{v2}	28,422
K_v valve 3	K_{v3}	28,409

Next the Kvs value can be calculated assuming that the valve is open to a maximum of 90% in the event of the pressure drop, as can be seen in formula 4.7.

$$K_{vs1...3} = \frac{K_{v1...3}}{0,9} \tag{4.7}$$

Table 37: K_{vs} value flow regulator valve

Description	Symbol	K_{vs} [/]	Real K_{vs} taken from figure 39
K_{vs} valve 1	K_{vs1}	31,594	40
K_{vs} valve 2	K_{vs2}	31,580	40
K_{vs} valve 3	K_{vs3}	31,566	40

As can be seen in the datasheet from the Hydromat QTR on page 2 [42], the K_{vs} value can also be calculated using formula 4.8:

$$K_{vs} = 0,002 \text{ x set value} \qquad (4.8)$$

The set value is 18 m³/h or 18 000 kg/h (mass density water 1 000 kg/m³).
This results in $K_{vs} = 36 \approx 40$ which also corresponds to the values calculated above.

Using figure 39 the nominal diameter of the valves can be found.

Table 38: DN valves

Description	Symbol	DN using figure 39 (mm)
Diameter valve 1 (K_{vs} = 40)	D_{K1}	DN 50
Diameter valve 2 (K_{vs} = 40)	D_{K2}	DN 50
Diameter valve 3 (K_{vs} = 40)	D_{K3}	DN 50

And finally the position of the valves can be calculated using formula 3.2 where F_v varies between 0 (valve fully closed) and 1 (valve fully open).

Description	Symbol	Fv
Position valve 1 (K_{vs} = 40)	f_{VK1}	0,711
Position valve 2 (K_{vs} = 40)	f_{VK2}	0,711
Position valve 3 (K_{vs} = 40)	f_{VK3}	0,710

4.3.4 Pump selection

First the total manometric pressure needs to be calculated. Manometric head, or manometric pressure, is defined by British Standards as the sum of the actual lift + the friction losses in the pipes + the discharge velocity head. Manometric head is the actual total head that could be achieved by the pump. It is smaller than the Euler head by an extent of *h* representing the energy loss in the impeller and casing. These losses are known as hydraulic losses and include fluid frictional losses in the blade passage, circulatory flow between the blades due to finite number of blades in the impeller and shock losses at the entrance to the impeller [57].

The heights from table 39 will be used:

Table 39: Heights components

Description	Symbol	Height (m)
Height RMM basin	$H_{RMMbasin}$	0,5
Height pumps	$H_{pump1...n}$	0,5
Height cooling drums	$H_{cd1...3}$	2,5
Height others	H_{others}	3

The total pressure drop in the distribution line with the highest pressure drop (L_{c3}) is selected and calculated using formula 4.9 where h_{geo} is the height between $H_{RMMbasin}$ and H_{others}:

$$p_{geo} = \rho \cdot g \cdot h_{geo} \qquad (4.9)$$

96

Table 40: manometric head pressure

Description	Symbol	Head pressure (Pa)	Head pressure (kPa)
Geodetic head pressure	h_{geo}	24 402,375	24,402
Pressure loss over distribution line L_{c3}	Δp_{lLc3}	90 325	90,325
Pressure loss filter	Δp_{lf}	4 500	4,5
Pressure loss back pressure valve	Δp_{lkbp}	20 000	20
Pressure loss RMM	Δp_{lRMM}	30 000	30
Pressure loss Lb	Δp_{lLb}	274,589	0,274 589
Pressure loss La	Δp_{lLa}	Unknown	Unknown
Pressure loss three-way valve	Δp_{l3wv}	100 000	100
			+
Manometric head pressure	p_{man}	269 502,316	269,502
			Manometric head (m)
Manometric head	h_{man}	27,61	

The manometric head (m) can be calculated by equation 4.9 but using manometric pressure instead of geodetic pressure.

On/off control at fixed rated speed

To select the pumps, a scenario will be worked out in which the pumps can be controlled on/off and in which each pump always runs at a fixed nominal speed. For each scenario, 3 operating points must be met, the specifications of which can be seen in the following table 41. These scenarios correspond approximately to when 1, 2 or/and 3 cooling drums are working.

Table 41: Flow rates different scenarios

Flow rate	Symbol	Percentage (%)	Absolut flow rate (m³/h)	Absolute flow rate (m³/s)
Design flow rate (3 drums are operating)	DQ (%)	100	54	0,015
Average flow rate (2 drums are operating)	AQ (%)	66	35,64	0,0099
Low flow rate (1 drum is operating)	LQ (%)	33	17,82	0,00495

The rotary molding machine has a total operating time of 1060 hours each year. Only when machine A is operating, the waste water be recycled and used in the cooling drums, machine B. We will assume that there is 1 drum working 700 hours, 2 drums are working or 300 hours and 60 hours every 3 drums are working. See table 42.

Table 42: Operating times different scenarios

Description	Symbol	Time (h)	Percentual time (%)
Design operating time (3 drums)	Td (h)	60	0,06
Average operating time (2 drums)	Ta (h)	300	0,283
Low operating time (1 drum)	Tl (h)	700	0,66

Now a selection of the pumps can be made in such a way that you get a cost-efficient installation. We don't do this by selecting a pump for each flow, but by selecting e.g. 2 pumps for 3 operating points where it is possible to switch 2 pumps in parallel at the largest flow rate. So it is possible to divide the design flow over 2 pumps and then connect them in parallel. Parallel connection of pumps will ensure that we can add up the flow rates while the head remains the same. The calculated head for this installation is 27,61 m (see manometric head pressure).

Selection pump 1

First we will select only one pump that can covers the average flow (35,64 m³/h). After this a smaller second pump is selected which can cover the low flow rate individual, and the design flow rate in cooperation with pump 1.

For selecting the pumps we use the pump curves from SIHI Supernova [58]. The motor is also selected from a datasheet from SIHI Supernova [59]. Using the average flow rate (m³/h), manometric head (m) and the pump curve we can select pump 1. All the data selected of the pump can be found in the appendix. In table 43 a summary can be found.

Table 43: Data summary pump and motor 1 [58], [59]

Pump Type 1	SIHI Supernova - 050315
Average flow rate (m³/h)	35,64
Manometric head (m)	27,61
Operating time (h)	300
Impeller diameter (mm)	⌀ 300
η_{pump}	56 %
Q_{min} factor	0,3
Q_{max} factor	1,2
$Q_{optimum}$ (m³/h)	38
Q_{min} (m³/h)	11,4
Q_{max} (m³/h)	45,6
NPSHr (m)	1,3

Motor Type 1	SIHI Supernova – 132 M
Speed (min^{-1})	1450
kW needed	5
kW selected	7,5
η_{motor1}	90,4
Electrical power (kW)	7,5 / 0,904 = 8,3
Consumption kWh/year	8,3 . 300 = 2490

Selection pump 2

A smaller second pump is selected which can cover the low flow rate individual, and the design flow rate in cooperation with pump 1. This will result in an flow rate of 18 m³/h and a minimum manometric head pressure of 27,61 m.

For selecting the pumps we use the pump curves from SIHI Supernova [58]. The motor is also selected from a datasheet from SIHI Supernova [59]. All the data selected of the pump can be found in the appendix. In table 44 a summary can be found.

Table 44: Data summary pump and motor 2 [58], [59]

Pump Type 2	SIHI Supernova - 040315
Average flow rate (m³/h)	18
Manometric head (m)	27,61
Operating time (h)	700
Impeller diameter (mm)	⌀ 325
η_{pump}	43,5%
Q_{min} factor	0,3
Q_{max} factor	1,1
$Q_{optimum}$ (m³/h)	17
Q_{min} (m³/h)	5,1
Q_{max} (m³/h)	18,7
NPSHr (m)	1,2

Motor Type 2	SIHI Supernova – 112 M
Speed (min⁻¹)	1450
kW needed	3,5
kW selected	4
η_{motor2}	88,6
Electrical power (kW)	4 / 0,886 = 4,515
Consumption kWh/year	4,515 . 700 = 3160,5

Yearly electricity consumption pumps

The yearly electrical consumption of the motors can be calculated using formula 4.10:

$$P_{elec/year} = \frac{P_{selected}}{\eta_{motor}} \cdot T_{operating} \qquad (4.10)$$

Table 45: Yearly electricity consumption motors

Description	Time (h)	Operating motors	Consumption (kWh/year)
Consumption design operating time (3 drums)	60	Motor 1 + 2	768,9
Consumption average operating time (2 drums)	300	Motor 1	2 490
Consumption low operating time (1 drum)	700	Motor 2	3 160,5
			+
Total yearly consumption motors			6 419,4

If the price for 1 kWh is 6,43 cents/kWh (basic electricity for companies) in Finland [60], the centrifugal pumps connected in parallel will have an annual electrical cost of € 412,77.

Pressure losses pipe L_a

Now the pumps are selected, we can determine the diameters and losses in the La pipes. For these calculations we refer to the table 46 below.

Table 46: Calculation pressure loss pipe L_a

	Pump 1	Pump 2
Flow rate (m³/h)	36	18
Diameter (mm)	79,788	56,42
DN pipe	DN 80	DN 65
Inner diameter pipe (mm)	77,9	62,6
Real velocity (m/s)	2,098	1,625
Reynoldsnumber	203 999,19	126 929,211
ε/D	0,004 493	0,005 591
Frictionfactor f	0,028	0,032
Pressure loss (Pa)	3 148,79	2 684,67
Head L_a (m)	0,323	0,275

Now the total losses (m) is the losses (m) from pipe L_a, and the total losses in the circuit.
$$27,6 + 0,323 = 27,933 \text{ m}$$

Now the losses in La pipes are known, we can see if the selected pumps can operate with this actual head. If not, we must select a stronger pump.

Since the total delivery height only increases slightly, we can consider that these pumps are still ok.

4.3.5 NPSH check / cavitation check

The concept cavitation is already explained in section 3.4: other engineering components –
circulation pumps.

So cavitation is caused where the static pressure of a liquid drops below a critical value that is close
to the vapour pressure. Usually on the suction sides, gas bubbles are formed and these will
implode, causing them to damage the walls of the pump housing. In order to prevent this, it is
necessary to ensure that the suction height and pressure losses in the suction pipe and suction
nozzle of the pump are not too large. The permitted suction height is found with the NPSH value
specified by the manufacturer and extracted from figure 72 and 75 in the appendix.

$NPSH_{Pomp1r} = 1,3$
$NPSH_{Pomp2r} = 1,8$

The net positive suction head available can be calculated by using equation 3.5. NPSHA (net
positive suction head available) and NPSHR (net positive suction head required). NPSHA must be
equal to or greater than the NPSHR and NPSHR is mostly given by the manufacturer.

$$NPSH_a = \frac{p_{atm}}{\rho\, g} - h_s + \frac{c_{1'}^2}{2g} - \Delta h_p - \Delta h_m - \frac{p_{vap}}{\rho\, g} \qquad (4.11)$$

	Pump 1	Pump 2
p_{atm} (pa)	$1,013 \cdot 10^5$	$1,013 \cdot 10^5$
$\rho_{30°C}$ (kg/m³)	995	995
g (m/s²)	9,81	9,81
h_s (m)	0	0
$c_{1'}$ (m/s) (table 46)	2,0981	1,625
$\Delta h_p - \Delta h_m$ (table 46)	0,323	0,275
$p_{vap-30\,°C}$ (pa) [61]	$4,245 \cdot 10^3$	$4,245 \cdot 10^3$

Table 47: NPSH check pumps

Description	$NPSH_r$ (m)	$NPSH_a$ (m)	$NPSH_a > NPSH_r$?
Pump 1	1,3	9,845	OK
Pump 1	1,8	9,803	OK

We can conclude that $NPSH_a$ is many times larger than $NPSH_r$ and that there will be absolutely no
cavitation in the pumps.

4.3.6 List of materials

Table 48: List of materials

Description	Type	Quantity
Pump 1	SIHI Supernova - 050315	1
Pump 2	SIHI Supernova - 040315	1
Motor 1	SIHI Supernova – 132 M	1
Motor 2	SIHI Supernova – 112 M	1
Ball valves	Optibal – DN 100	4
Filter	5466 10 - DN 100	1
Three-way valve	Tri-CTR	2
Flow regulator	Hydromat QTR – DN 50	3
Back pressure regulator	Hydrocontrol VTR – DN 50	3
Pipe	DN 50	90 meter
Pipe	DN 100	68 meter
Reheater		1

4.3.7 Mixing water flows using three-way valve

When two water flows are mixed, the first law of thermodynamics for open systems can be used. The mass flows (kg/h) of the wastewater and the mass flow (kg/h) of the tap water can be determined from this. This can then be converted to the flow rate. The first law of thermodynamics is given in formula 4.12.

$$\Delta U = Q - W \tag{4.12}$$

ΔU is the internal energy of a closed system and is equal to the amount of heat Q supplied to the system, minus the amount of work W done by the system on its surroundings. For an open system with multiple entrances and exits, like in our example, this formula can be transformed into formula 4.13.

$$\dot{Q} - \dot{W}_t + \sum_i \dot{m}_i \left(e_{kin,i} + e_{pot,i} + h_i \right) - \sum_u \dot{m}_u \left(e_{kin,u} + e_{pot,u} + h_u \right) = 0 \tag{4.13}$$

The entrances are 1 and 2, and the exit is 3.

$$\dot{Q} - \dot{W}_t + \dot{m}_1 (e_{kin,1} + e_{pot,1} + h_1) - \dot{m}_2 \left(e_{kin,2} + e_{pot,2} + h_2 \right) - \dot{m}_3 (e_{kin,3} + e_{pot,3} + h_3) = 0 \tag{4.14}$$

We can simplify this equation to equation 4.15 since we know that $\dot{m}_1 + \dot{m}_2 = \dot{m}_3$:

$$\dot{m}_1 h_1 + \dot{m}_2 h_2 = (\dot{m}_1 + \dot{m}_2) h_3 \tag{4.15}$$

h is the enthalpy in kJ/kg and can be found by interpolating the values in the table book of thermodynamics. Since we have 2 equations and m_1 and m_2 are unknown, we can calculate the mass flow in each situation. In table 49 all the data is shown and the needed waste water flow and tap water flow in the three situations are calculated.

Table 49: data mixing water flows

			Tap water	Waste water	Cooling water
Enthalpie	h	[kJ/kg]	16,786	125,79	50,402
Temperature	T	[°C]	4	30	12
Flow rate 1	Q	[m³/h]	12,448 944	5,551056	18
Mass flow 1	m	[kg/h]	12 448,944	5551,056	18 000
		[kg/s]	3,458	1,542	5
Flow rate 2	Q	[m³/h]	24,897	11,102	36
Mass flow 2	m	[kg/h]	24 897,888	11102,112	36 000
		[kg/s]	6,916	3,084	10
Flow rate 3	Q	[m³/h]	37,346	16,653	54
Mass flow 3	m	[kg/h]	37346,832	16653,168	54 000
		[kg/s]	10,374	4,626	15

Now the waste water flows are found, we can calculate how much waste water we recuperate.

Design flow rate: situation 1

Tap water
$T_{tapw} = 4\ °C$
$Q_{tapw} = 37,35\ m^3/h$

$T_{RMM} = 30\ °C$
$Q_{RMM} = 16,65\ m^3/h$

$T_{icd} = 12\ °C$
$Q_{icd} = 54\ m^3/h$
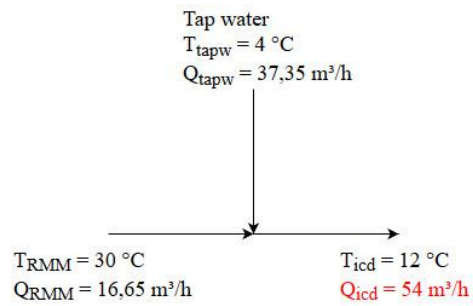
Figure 66: Flow rate situation 1

Average flow rate: situation 2

Tap water
$T_{tapw} = 4\ °C$
$Q_{tapw} = 24,9\ m^3/h$

$T_{RMM} = 30\ °C$
$Q_{RMM} = 11,10\ m^3/h$

$T_{icd} = 12\ °C$
$Q_{icd} = 36\ m^3/h$
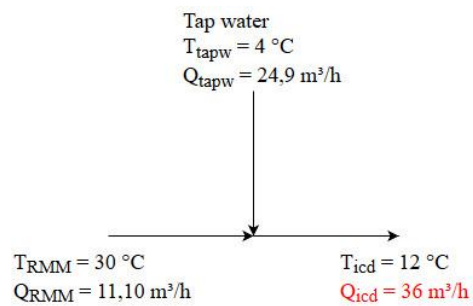
Figure 67: Flow rate situation 2

Low flow rate: situation 3

Tap water
$T_{tapw} = 4\ °C$
$Q_{tapw} = 12,45\ m^3/h$

$T_{RMM} = 30\ °C$
$Q_{RMM} = 5,55\ m^3/h$

$T_{icd} = 12\ °C$
$Q_{icd} = 18\ m^3/h$

Figure 68: Flow rate situation 3

4.4   Conclusion case B

Figure 69: Final process scheme

Each component and each pipe has their hydraulic pressure loss. The total hydraulic loss in the worst case that has to be compensated by the pumps is 27,8 m or 273 kPa. The losses can be compensated using 2 centrifugal pumps connected in parallel and will have an annual electrical cost of € 412,77.

We assume that the installation works for 60 hours at high flow (54 m³/h), 300 hours at medium flow (36 m³/h) and 700 hours at low flow (18 m³/h). When we ar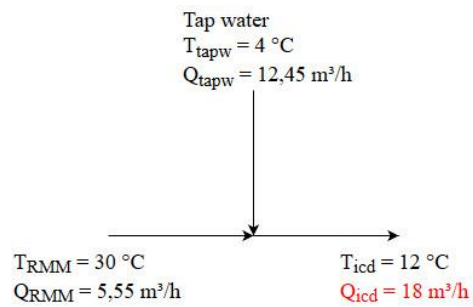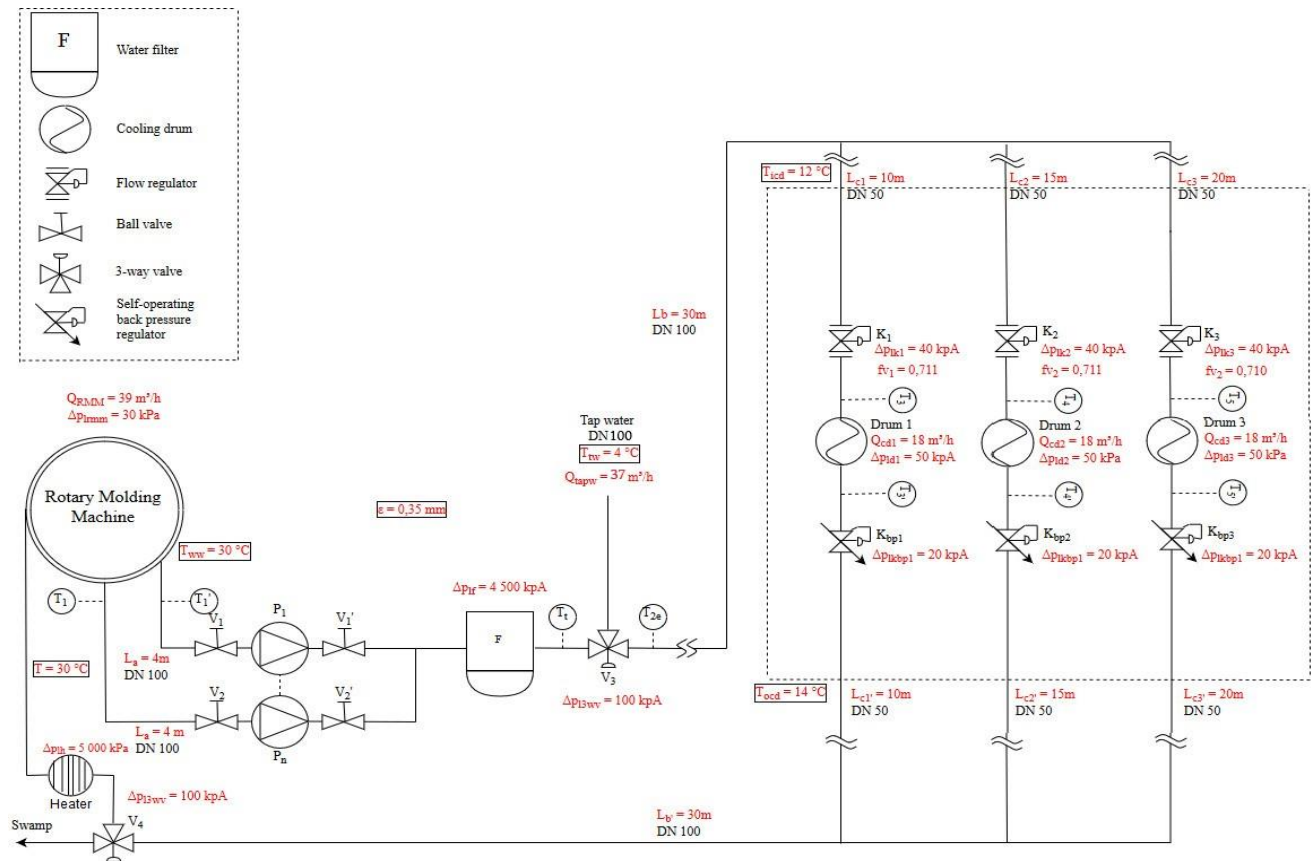e operating at high flow we recuperate 16,65 m³/h, medium flow 11,10 m³/h and low flow we recuperate 5,55 m³/h. Further on in the diagram, we see that there is another three-way valve that discharges part of the water into the river, and can recover part of it. The amount of water that can be recovered here depends on the amount of water that can be used in machine A at the same time. Since we do not know the exact water storage capacity of the rotary molding machine, we assume that 20% of this recurring water can be recovered.

Suomen Kerta has the ability to save 1 643,11 m³ of waste water each year using this method. Depending on how often both the machines are running simultaneously and if the rotary molding machine has the ability to generate 39 m³/h waste water at 30°C in the worst case. The average price for 1 m³ water in Finland is €4,48 / m³ [62], so Suomen Kerta can save up to € 7 361,14 on water costs.

5 Conclusion

STES systems will not offer a possible solution (temperature waste water only 30 °C) and the constructions for these systems will be too cost effective. ORC installation will not have a sufficiently high efficiency due to the too low temperature of the waste water. A closed hydraulic system, on the other hand, is cheaper and easier to install and can save up to 1 643,11 m³ waste water each year. This will result in water savings, money savings and less environmental pollution since the waste water is not discharged into the river anymore.

It is important to keep in mind that a calculation method has been developed in Excel for the calculation of such hydraulic systems. The values that are shown here can only be considered as guidelines. If we have more data on the situations, we can use this Excel to calculate a more accurate system than in our case. Due to lack of time and little data from the company, many estimates and assumptions have to be made, so this design can be regarded as a calculation example.

References

[1]   Häme University of Applied Sciences, "Hämeen ammattikorkeakoulu - Häme University of applied sciences," 2019. [Online]. Available: https://www.hamk.fi/?lang=en. [Accessed: 07-May-2019].

[2]   Suomen Kerta Oy, "Company | Suomen Kerta Oy," 2019. [Online]. Available: http://www.suomenkerta.fi/en/company/. [Accessed: 03-May-2019].

[3]   H. Kürschner, "Rotary molding machine RGM-1550 / 3,195 molds – Technology for candles," 2019. [Online]. Available: https://www.herrhammer.de/en/products/molding/rotary-molding-machine-rgm-1550-3195-molds/. [Accessed: 08-Apr-2019].

[4]   H. Kürschner, "Pulverisation of liquid raw material by means of spraying drums – Technology for candles," 2019. [Online]. Available: https://www.herrhammer.de/en/products/preparing/pulverisation-of-liquid-raw-material-by-means-of-spraying-drums/. [Accessed: 08-Apr-2019].

[5]   F. M. Institute, "Climate Elements." [Online]. Available: https://en.ilmatieteenlaitos.fi/climate-elements. [Accessed: 02-Apr-2019].

[6]   *Tieteessä tapahtuu*. Yliopistopaino, 2007. [Accessed: 02-Apr-2019].

[7]   J. Heier, C. Bales, and V. Martin, "Combining thermal energy storage with buildings - A review," *Renew. Sustain. Energy Rev.*, vol. 42, pp. 1305–1325, 2015. [Accessed: 02-Apr-2019].

[8]   "Mean Annual Air Temperature | MATT | Ground temperature | Renewable Energy | Interseasonal Heat Transfer | Solar Thermal Collectors | Ground Source Heat Pumps | Renewable Cooling." [Online]. Available: http://www.icax.co.uk/Mean_Annual_Air_Temperature.html. [Accessed: 04-Apr-2019].

[9]   M. YLI-HALLA and D. MOKMA, "Soil temperature regimes in Finland," *Agric. Food Sci.*, vol. 7, no. 4, pp. 507–512, 2018. [Accessed: 02-Apr-2019].

[10]   B. Nordell, "Underground Thermal Energy Storage Methods," *12th Int. Conf. Energy Storage*, pp. 1–14, 2011. [Accessed: 02-Apr-2019].

[11]   K. S. Lee, "A review on concepts, applications, and models of aquifer thermal energy storage systems," *Energies*, vol. 3, no. 6, pp. 1320–1334, 2010. [Accessed: 02-Apr-2019].

[12]   M. Bloemendal and N. Hartog, "Analysis of the impact of storage conditions on the thermal recovery efficiency of low-temperature ATES systems," *Geothermics*, vol. 71, no. November 2017, pp. 306–319, 2018. [Accessed: 02-Apr-2019].

[13]   L. Gao, J. Zhao, and Z. Tang, "A Review on Borehole Seasonal Solar Thermal Energy Storage," *Energy Procedia*, vol. 70, pp. 209–218, 2015. [Accessed: 02-Apr-2019].

[14]   D. Mangold, "Cogen Europe - Prospects of Solar Thermal and Heat Storage in DHC," 2010. [Accessed: 02-Apr-2019].

[15]   "Finland Population 2019 (Demographics, Maps, Graphs)." [Online]. Available: http://worldpopulationreview.com/countries/finland-population/. [Accessed: 02-Apr-2019].

[16]   T. Schmidt, D. Mangold, and H. Müller-Steinhagen, "Seasonal thermal energy stroage in germany," *ISES Sol. World Congr.*, pp. 1–7, 2003. [Accessed: 22-Apr-2019].

[17]   M. Lanahan and P. C. Tabares-Velasco, "Seasonal thermal-energy storage: A critical review on BTES systems, modeling, and system design for higher system efficiency," *Energies*, vol. 10, no. 6, 2017. [Accessed: 22-Apr-2019].

[18]   A. Réveillère, V. Hamm, H. Lesueur, E. Cordier, and P. Goblet, "Geothermal contribution to the energy mix of a heating network when using aquifer thermal energy storage:

Modeling and application to the paris basin," *Geothermics*, vol. 47, no. October 2017, pp. 69–79, 2013. [Accessed: 22-Apr-2019].

[19]   "Understanding and avoiding pump cavitation." [Online]. Available: https://www.flowcontrolnetwork.com/understanding-avoiding-pump-cavitation/. [Accessed: 22-Apr-2019].

[20]   M. Possemiers, M. Huysmans, and O. Batelaan, "Influence of Aquifer Thermal Energy Storage on groundwater quality: A review illustrated by seven case studies from Belgium," *J. Hydrol. Reg. Stud.*, vol. 2, pp. 20–34, Nov. 2014. [Accessed: 22-Apr-2019].

[21]   S. Homuth, W. Rühaak, K. Bär, and I. Sass, "Medium Deep High Temperature Heat Storage," *Eur. Geotherm. Congr. 2013*, vol. 2013, no. June, pp. 1–6, 2013. [Accessed: 22-Apr-2019].

[22]   D. Mangold and L. Deschaintre, "Seasonal thermal energy storage-Report on state of the art and necessary further R + D," *Task 45 Large Syst.*, pp. 1–48, 2015. [Accessed: 22-Apr-2019].

[23]   H. Hvidtfeldt Larsen and L. Sønderberg Petersen, *DTU international energy report 2013 : energy storage options for future sustainable energy systems*. 2013. [Accessed: 05-Apr-2019].

[24]   M. Krarti and M.-V. MISSING-VALUE, "Thermal Energy Storage Systems," *Energy Audit Build. Syst.*, no. November, pp. 273–290, 2018. [Accessed: 05-Apr-2019].

[25]   N. Nasrollahi and F. A. Abarghoee, "Thermal Performance of Earth-Sheltered Residential Buildings : a Case Study of Yazd Naqshejahan Thermal Performance of Earth-Sheltered Residential Buildings : a Case Study of Yazd," *Naghshejahan*, vol. 64, no. November, pp. 56–67, 2017. [Accessed: 05-Apr-2019].

[26]   "Efficient Earth-Sheltered Homes | Department of Energy." [Online]. Available: https://www.energy.gov/energysaver/types-homes/efficient-earth-sheltered-homes. [Accessed: 05-Apr-2019].

[27]   Helen Oy, "Finland's largest rock cavern heat storage planned for Helsinki | Helen," *© Helen Oy*, 2018. [Online]. Available: https://www.helen.fi/en/news/2017/rock-cavern-heat-storage-planned-for-Helsinki/. [Accessed: 01-May-2019].

[28]   P. A. J. Donkers, L. C. Sögütoglu, H. P. Huinink, H. R. Fischer, and O. C. G. Adan, "A review of salt hydrates for seasonal heat storage in domestic applications," *Appl. Energy*, vol. 199, pp. 45–68, 2017. [Accessed: 05-Apr-2019].

[29]   F. Trausel, A. De Jong, and R. Cuypers, "A Review on the Properties of Salt Hydrates for Thermochemical Storage ScienceDirect A review on the properties of salt hydrates for thermochemical storage," no. December, 2014. [Accessed: 05-Apr-2019].

[30]   "Empa - Communication - NaOH-heat-storage." [Online]. Available: https://www.empa.ch/web/s604/naoh-heat-storage. [Accessed: 05-Apr-2019].

[31]   Claire Ferchaud, "Can salt hydrates be used for domestic seasonal heat storage?," *April 19*, 2016. [Online]. Available: https://www.tue.nl/en/university/departments/mechanical-engineering/news/19-04-2016-can-salt-hydrates-be-used-for-domestic-seasonal-heat-storage/#top. [Accessed: 02-May-2019].

[32]   C. Haddad, C. Périlhon, A. Danlos, M. X. François, and G. Descombes, "Some efficient solutions to recover low and medium waste heat: Competitiveness of the thermoacoustic technology," *Energy Procedia*, vol. 50, pp. 1056–1069, 2014. [Accessed: 02-May-2019].

[33]   M. E. Mondejar, J. G. Andreasen, L. Pierobon, U. Larsen, M. Thern, and F. Haglind, "A review of the use of organic Rankine cycle power systems for maritime applications," *Renew. Sustain. Energy Rev.*, vol. 91, pp. 126–151, Aug. 2018. [Accessed: 02-May-2019].

[34]   T. Veijola, A. Thesis Supervisor Veijola, and T. M. Ruusunen, "DOMESTIC DRAIN WATER HEAT RECOVERY Process engineering Domestic drain water heat recovery," no.

March, 2016. [Accessed: 02-May-2019].

[35] "Hydraulischer_Abgleich_by-Ra_Boe-1.jpg (JPEG-afbeelding, 2580 × 2195 pixels) - Geschaald (36%)." [Online]. Available: https://upload.wikimedia.org/wikipedia/commons/c/c2/Hydraulischer_Abgleich_by-Ra_Boe-1.jpg. [Accessed: 26-Apr-2019]. [Accessed: 26-Apr-2019].

[36] O. G. & C. KG, "Valves , controls + systems Flow , pressure and temperature balancing Flow , pressure and temperature balancing," 2018. [Accessed: 26-Apr-2019].

[37] R. Bolger and P.-O.-M. V. Inc., "Pressure Regulators vs. Backpressure Regulators," *Process. Mag.*, 2008. [Accessed: 26-Apr-2019].

[38] A. I. Sheet, "Self-operated Pressure Regulators Back Pressure Valve Type 41-73 T 2518 T 2518," no. May, 1999. [Accessed: 26-Apr-2019].

[39] "Industrial Filtration." [Online]. Available: https://www.evoqua.com/en/products/filtration/Pages/industrial-filtration.aspx?stc=ppc300305&utm_term=%2Bindustrial %2Bwater%2Bfilter&utm_campaign=Products&utm_source=adwords&utm_medium=ppc& hsa_acc=3118474098&hsa_net=adwords&hsa_cam=1680031166&hsa_ad=32. [Accessed: 23-Apr-2019].

[40] A. Control *et al.*, "T 8012 EN Type 3241-1 and Type 3241-7 Pneumatic Control Valves · Type 3241 Globe Valve ANSI version," no. April, pp. 1–12, 2018. [Accessed: 23-Apr-2019].

[41] T. Themp, "Ontwerp pompinstallatie voor een proceskoelwater-installatie," pp. 1–6, 2017. [Accessed: 23-Apr-2019].

[42] Oventrop GmbH & Co. KG, "'Hydromat QTR' Flow regulator Tender specification : Technical data : Function : Advantages :," pp. 1–4, 2015. [Accessed: 26-Apr-2019].

[43] "Definition of Back Pressure Regulator | Equilibar Precision Pressure Control." [Online]. Available: https://www.equilibar.com/back-pressure-regulators/how-it-works/bpr-definition/. [Accessed: 26-Apr-2019].

[44] O. G. & C. KG, "'Hydrocontrol VTR / VPR' Bronze double regulating and commissioning valves PN 16 / PN 25," pp. 1–10, 2018. [Accessed: 26-Apr-2019].

[45] D. Dirtmag, "Materials : Performance :" [Accessed: 26-Apr-2019].

[46] D. I. N. En, T. Oventrop, G. Energy, and S. Directive, "Brass ball valves with full flow," 2018. [Accessed: 26-Apr-2019].

[47] O. Gmbh and C. Kg, "'Tri-CTR' Three-way diverting and mixing valves PN 16 Tender specification : Technical data : Function : Material : Application : Models : Performance data," pp. 1–2, 2015. [Accessed: 26-Apr-2019].

[48] EU, "EU Regulation No 641/2009 - ecodesign requirements for glandless standalone circulators and glandless circulators integrated in products," no. 641, pp. 35–41, 2009. [Accessed: 26-Apr-2019].

[49] Mc Nally Institute, "Series or parallel pump operation – Mc Nally Institute," 2019. [Online]. Available: http://www.mcnallyinstitute.com/18-html/18-1.htm. [Accessed: 04-May-2019].

[50] Engineering ToolBox, "Pumps in Parallel or Serial," 2004. [Online]. Available: https://www.engineeringtoolbox.com/pumps-parallel-serial-d_636.html. [Accessed: 04-May-2019].

[51] N. P. for Everybody, "Parallel Operation of Centrifugal Pumps," 2019. [Accessed: 04-May-2019].

[52] N. P. for Everybody, "Cavitation in Centrifugal Pumps," 2019. [Accessed: 04-May-2019].

[53] J. E. McDade, "Legionella and the Prevention of Legionellosis ," *Emerg. Infect. Dis.*, vol. 14, no. 6, pp. 1006a – 1006, 2009. [Accessed: 04-May-2019].

[54] U. of S. S Beck and R Collins, "File:Moody diagram.jpg - Wikimedia Commons," *24 July,*

2018. [Online]. Available: https://commons.wikimedia.org/wiki/File:Moody_diagram.jpg. [Accessed: 07-May-2019].

[55] water-link, "Debiet | Water link," *2019*. [Online]. Available: https://www.water-link.be/info-advies/debiet. [Accessed: 09-May-2019].

[56] Engineers Edge, "Water - Density Viscosity Specific Weight | Engineers Edge | www.engineersedge.com," *2019*. [Online]. Available: https://www.engineersedge.com/physics/water__density_viscosity_specific_weight_13146.htm. [Accessed: 10-May-2019].

[57] "What is manometric head in cetrifugal pump? - Quora," 2019. [Online]. Available: https://www.quora.com/What-is-manometric-head-in-cetrifugal-pump. [Accessed: 15-May-2019].

[58] SIHI Supernova, "SIHI SuperNova KENNLINIENÜBERSICHT 50 Hz Baureihe series," 2012. [Accessed: 15-May-2019].

[59] Flowserve, "Volute casing pumps SIHI SuperNova," vol. 2, pp. 1–8, 2015. [Accessed: 15-May-2019].

[60] Helen Oy, "Electricity products for SMEs and associations | Helen," 2019. [Online]. Available: https://www.helen.fi/en/electricity/companies/electricity-products-for-smes-and-associations2/. [Accessed: 16-May-2019].

[61] D. R. Lide, *CRC handbook of chemistry and physics : a ready-reference book of chemical and physical data*. CRC Press, 2004. [Accessed: 16-May-2019].

[62] Vercon Oy, "The price of water," 2016. [Online]. Available: https://www.verto.fi/en/services-products/information-about-water-consumption/the-price-of-water/. [Accessed: 17-May-2019].

[63] "Blog | What is Hydraulic Conductivity?" [Online]. Available: https://www.preene.com/blog/2014/07/what-is-hydraulic-conductivity. [Accessed: 01-May-2019].
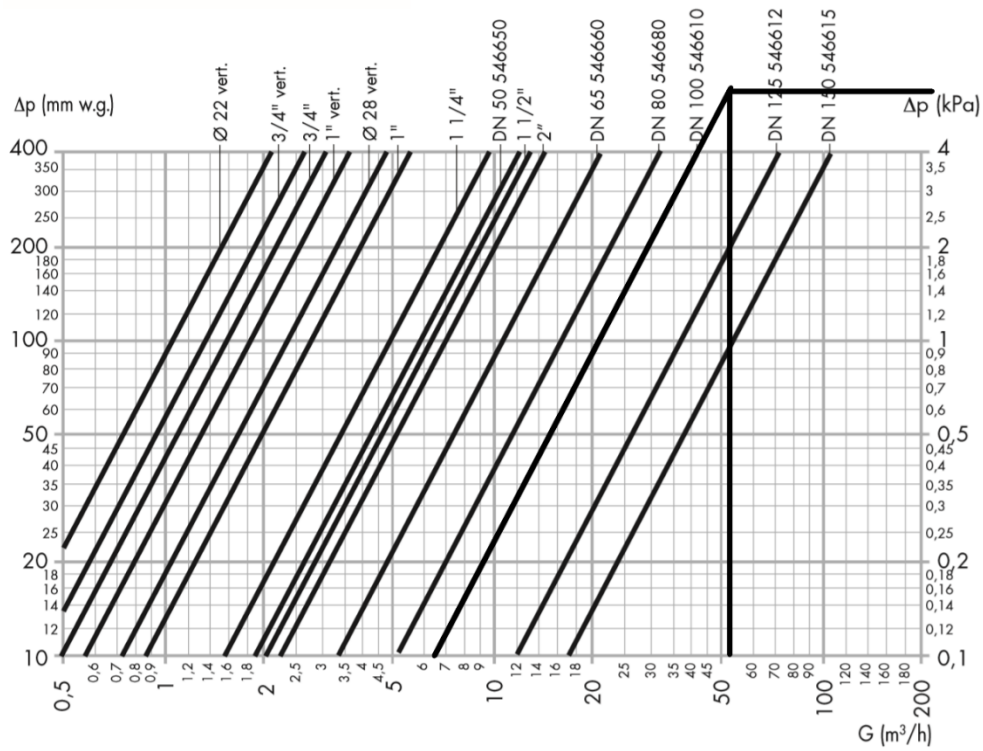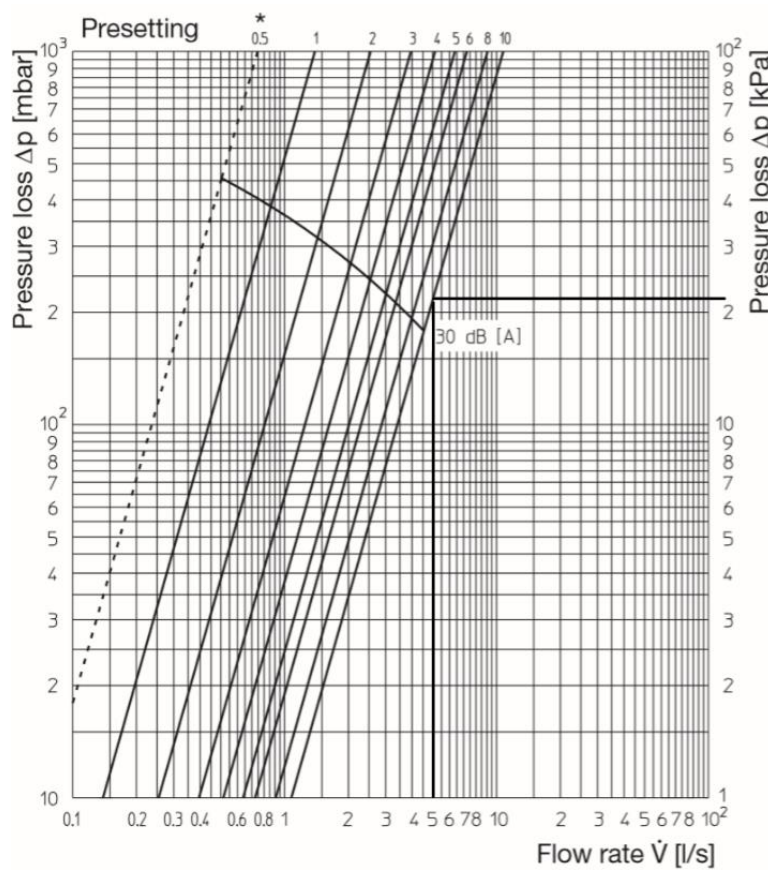
Appendix

Figure 70 - Appendix - Pressure loss filter [45]

Figure 71: Appendix - Pressure loss back pressure regulator [44]

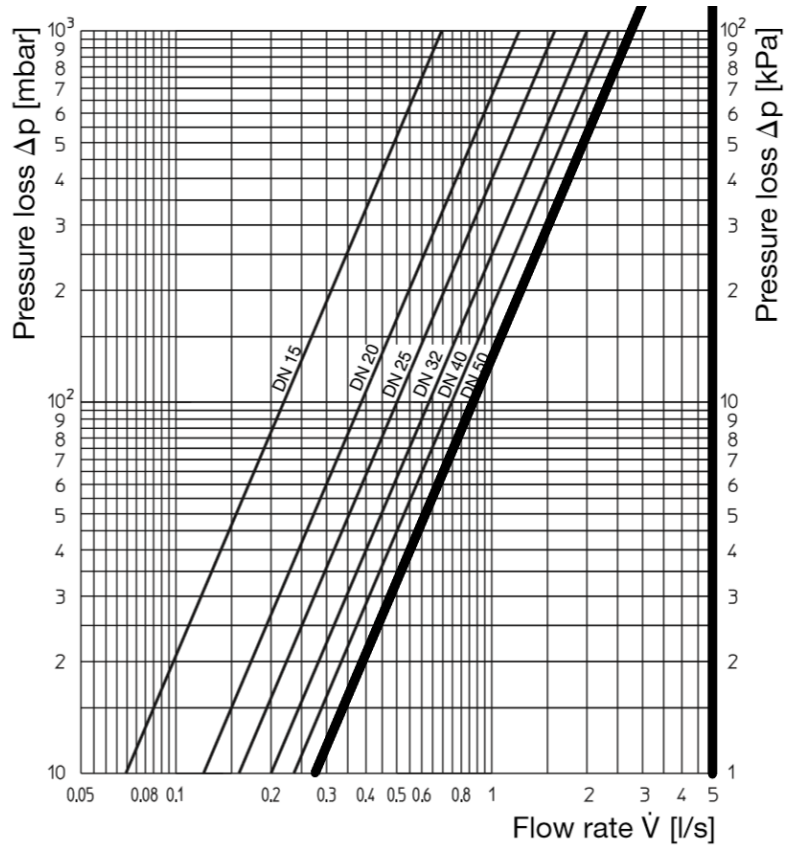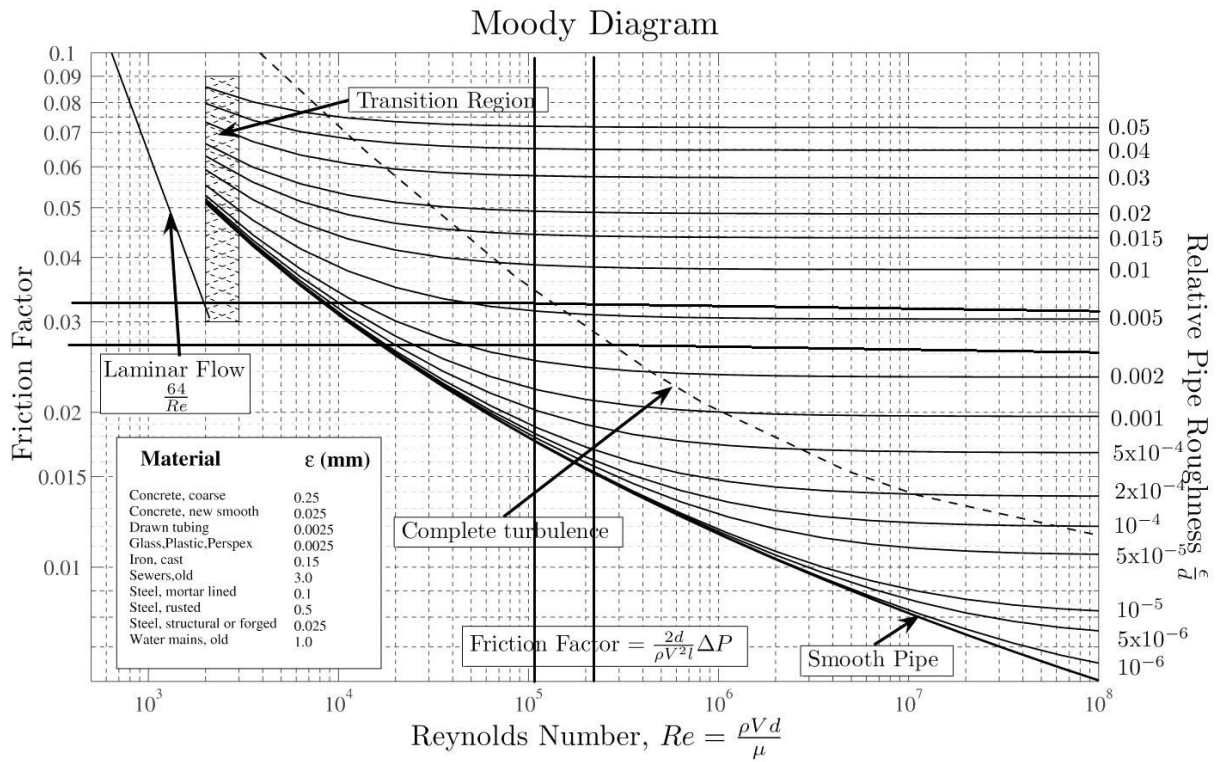*Figure 72: Appendix - Pressure loss three-way valve* [47]

Moody Diagram

Figure 73: Appendix - Friction factor pipes [54]

Figure 74: Appendix - Friction factor pipe La [54]

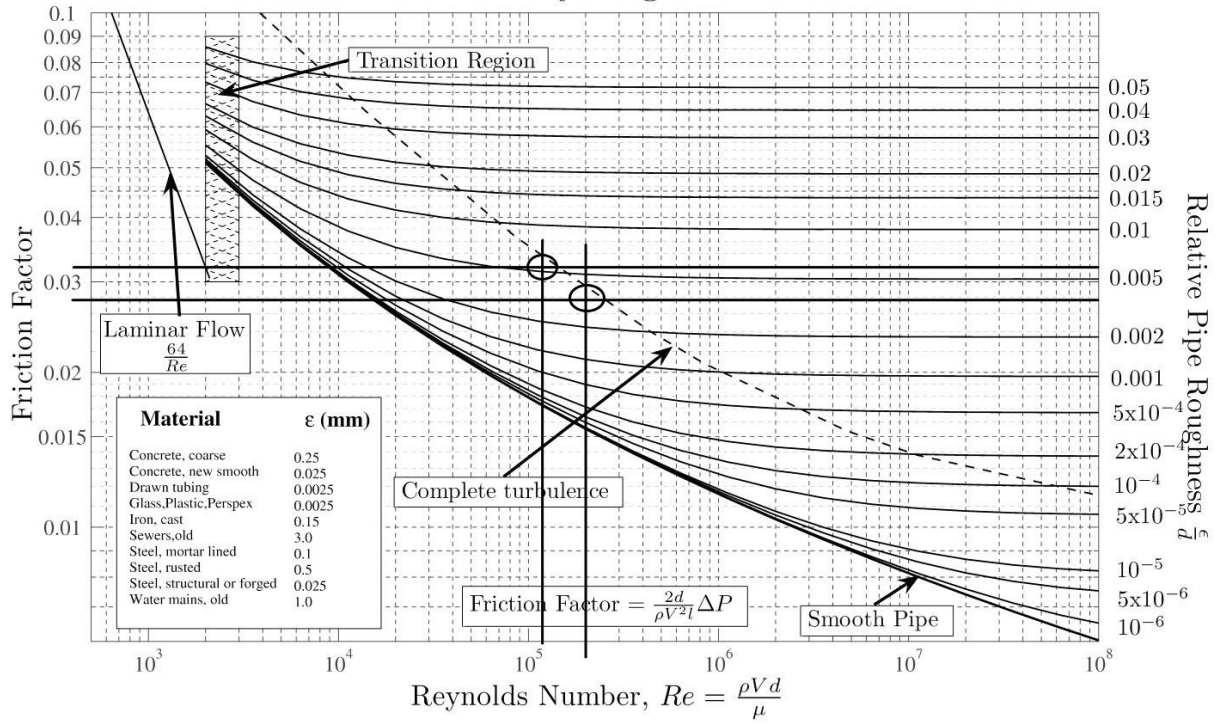**n = 1450 1/min**
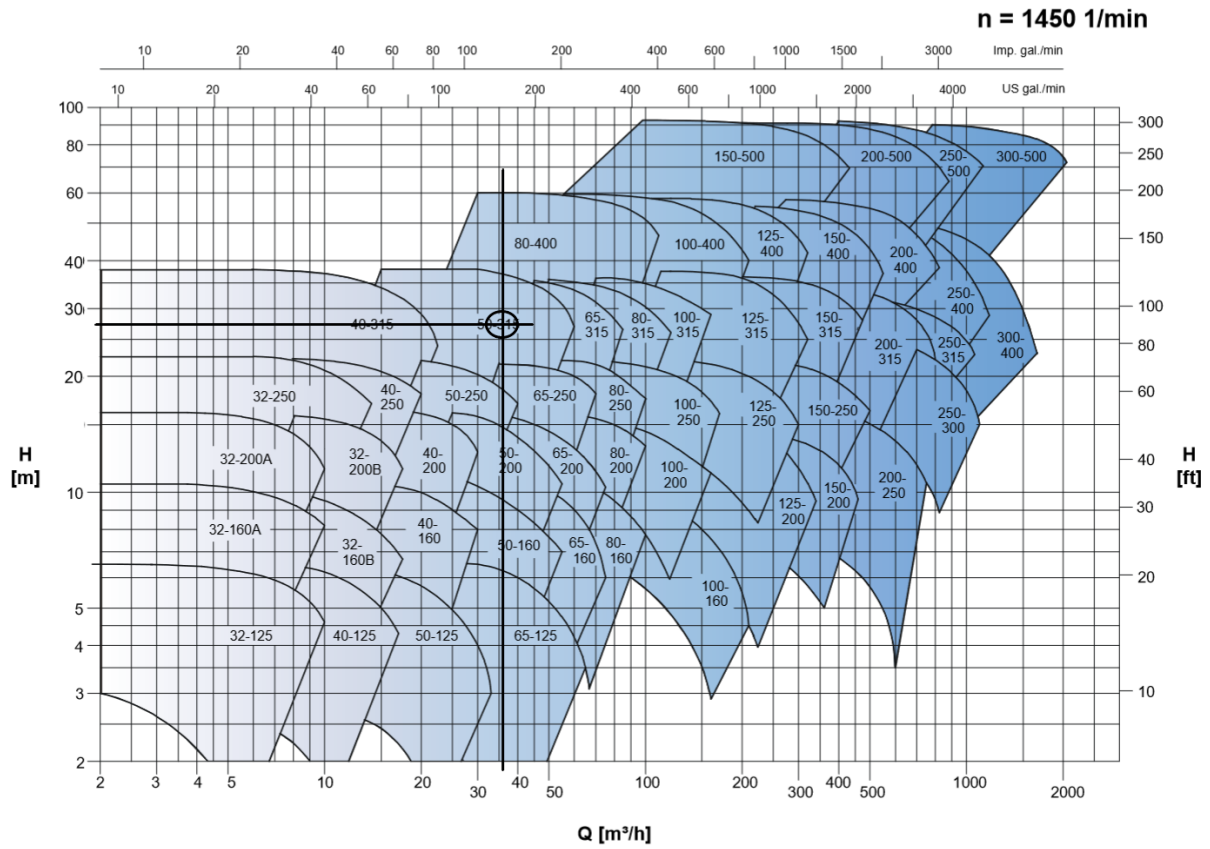

Figure 75: Appendix - Selection pump 1 [58]

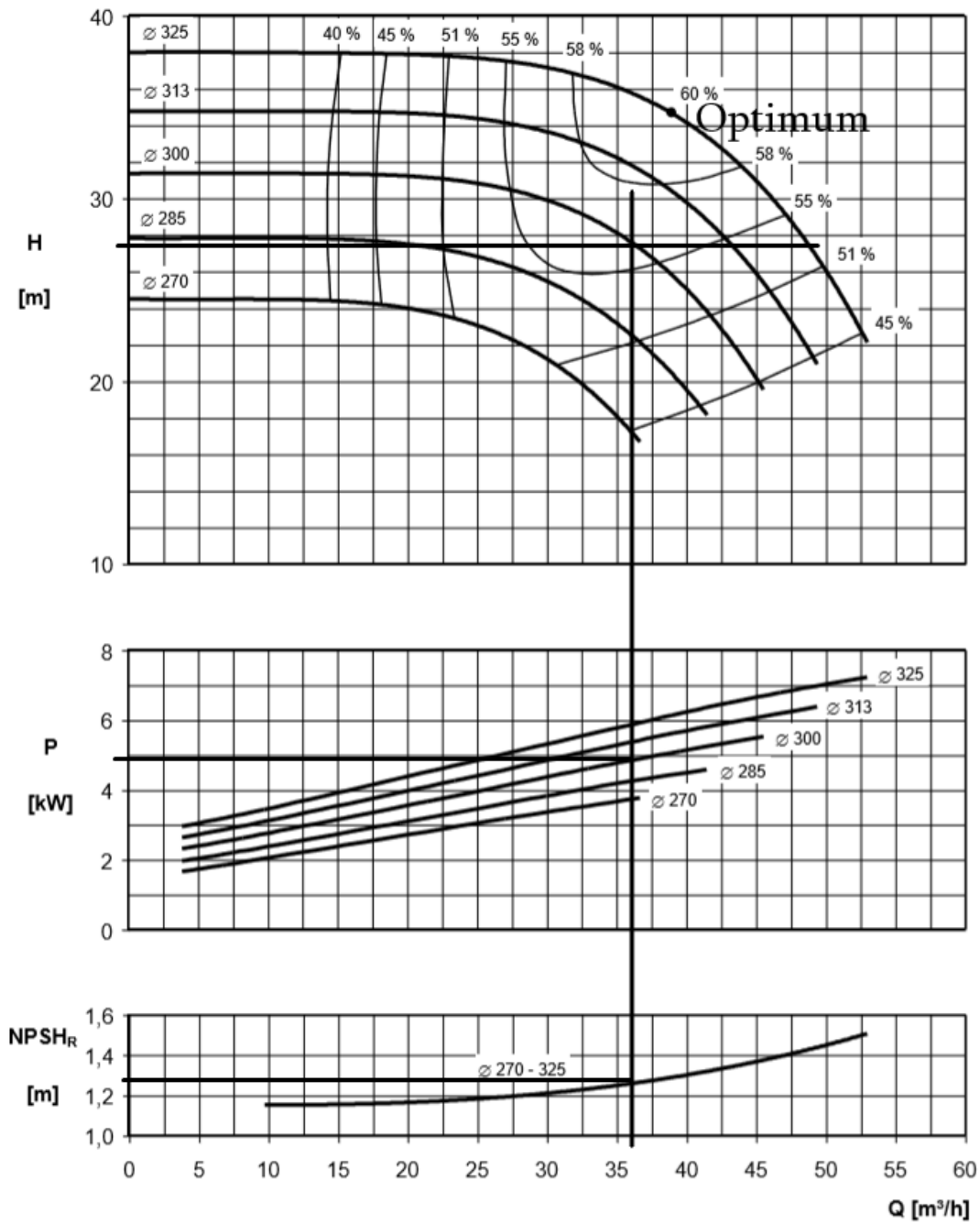*Figure 76: Appendix - Data pump 1* [58]

Motor dimensions   n = 1450 rpm

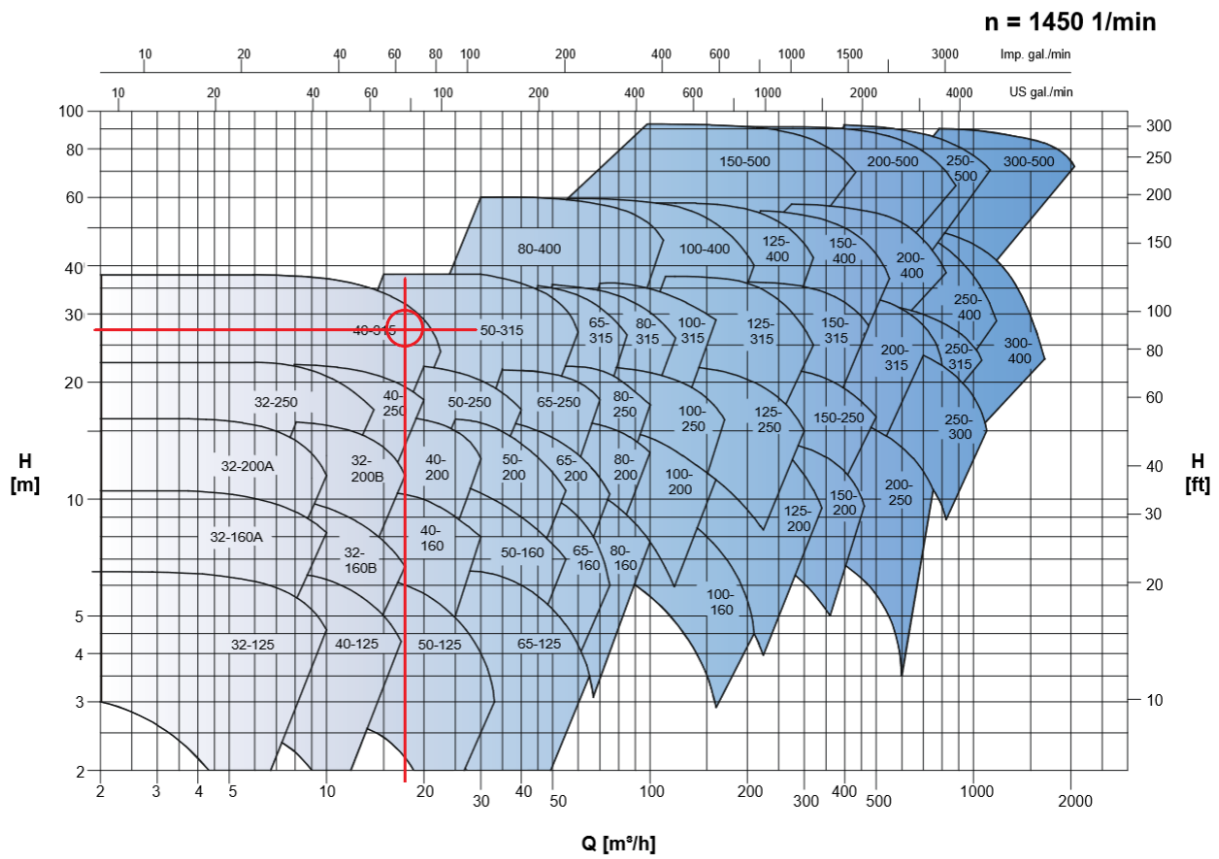| Size	kW	b₁*	c₁*	D₁	g*	h*	m*	m₃	m₄*	m₅	n₃*	n₄	o₁*	s	w*	kg
80	0,55 / 0,75	--	--	200	158	--	--	--	--	--	--	--	238	10	135	13
90S	1,1	--	--	200	178	--	--	--	--	--	--	--	255	10	150	18
90L	1,5	--	--	200	178	--	--	--	--	--	--	--	280	10	150	22
100L	2,2 / 3,0	--	--	250	198	--	--	--	--	--	--	--	316	12	160	28 / 30
112M	4,0	--	--	250	223	--	--	--	--	--	--	--	334	12	179	45
132S	5,5	--	--	300	262	--	--	--	--	--	--	--	372	12	205	56
132M	7,5	--	--	300	262	--	--	--	--	--	--	--	410	12	205	64
160M	11,0	--	--	350	312	--	--	--	--	--	--	--	485	15	248	101
160L	15,0	--	--	350	312	--	--	--	--	--	--	--	529	15	248	110
180M	18,5	80	28	350	357	180	75	121	294	241	350	279	557	15	241	174
180L	22,0	80	28	350	357	180	75	121	332	279	350	279	595	15	279	185
200L	30,0	82	30	400	397	200	85	133	332	305	385	318	619	19	267	240

Figure 77: Appendix - Data motor pump 1 [59]

Figure 78: Appendix - Selection pump 2 [58]
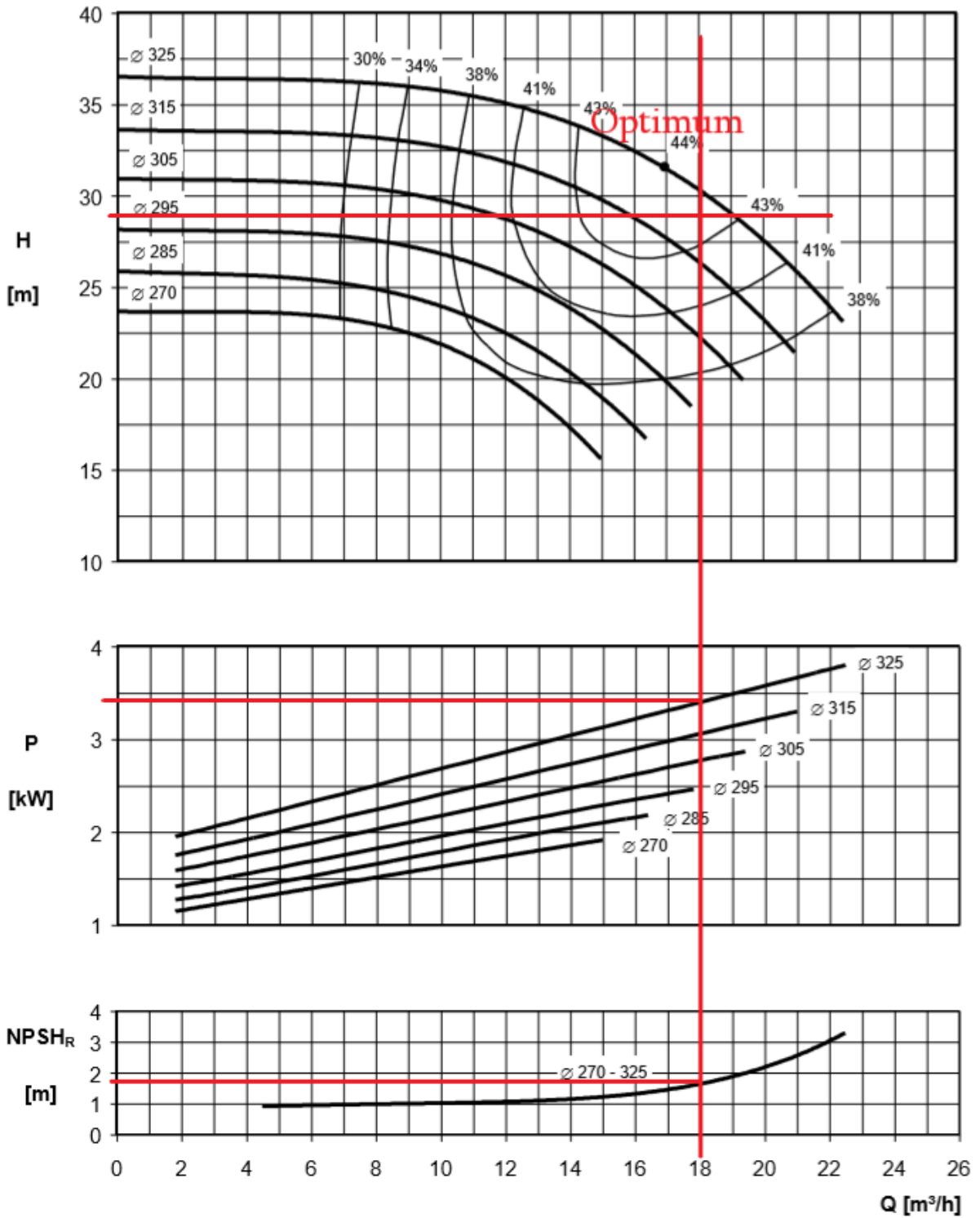
Figure 79: Appendix - Data pump 2 [58]

Motor dimensions n = 1450 rpm

Size	kW	b_1*	c_1*	D_1	g*	h*	m*	m_3	m_4*	m_5	n_3*	n_4	o_1*	s	w*	kg
80	0,55 / 0,75	--	--	200	158	--	--	--	--	--	--	--	238	10	135	13
90S	1,1	--	--	200	178	--	--	--	--	--	--	--	255	10	150	18
90L	1,5	--	--	200	178	--	--	--	--	--	--	--	280	10	150	22
100L	2,2 / 3,0	--	--	250	198	--	--	--	--	--	--	--	316	12	160	28 / 30
112M	4,0	--	--	250	223	--	--	--	--	--	--	--	334	12	179	45
132S	5,5	--	--	300	262	--	--	--	--	--	--	--	372	12	205	56
132M	7,5	--	--	300	262	--	--	--	--	--	--	--	410	12	205	64
160M	11,0	--	--	350	312	--	--	--	--	--	--	--	485	15	248	101
160L	15,0	--	--	350	312	--	--	--	--	--	--	--	529	15	248	110
180M	18,5	80	28	350	357	180	75	121	294	241	350	279	557	15	241	174
180L	22,0	80	28	350	357	180	75	121	332	279	350	279	595	15	279	185
200L	30,0	82	30	400	397	200	85	133	332	305	385	318	619	19	267	240

Figure 80: Appendix - Data motor 2 [59]

119